FRAME SYNCHRONIZATION IN OFDM SYSTEMS

A THESIS SUBMITTED TO

THE GRADUATE SCHOOL OF NATURAL AND APPLIED SCIENCES

OF

MIDDLE EAST TECHNICAL UNIVERSITY

BY

HAKAN YESARİ GÜRSAN

IN PARTIAL FULFILLMENT OF THE REQUIREMENTS

FOR

THE DEGREE OF MASTER OF SCIENCE

IN

ELECTRICAL AND ELECTRONICS ENGINEERING

JANUARY 2005

Approval of the Graduate School of Natural and Applied Sciences

_____

Prof. Dr. Canan Özgen
Director

I certify that this thesis satisfies all the requirements as a thesis for the degree of Master of Science.

_____

Prof. Dr. İsmet Erkmen
Head of Department

This is to certify that we have read this thesis and that in our opinion it is fully adequate, in scope and quality, as a thesis for the degree of Master of Science.

_____

Assoc. Prof. Dr. T. Engin Tuncer
Supervisor

Examining Committee Members

Assoc. Prof. Dr. Tolga Çiloğlu	(METU, EE)	_____
Assoc. Prof. Dr. T. Engin Tuncer	(METU, EE)	_____
Asst.Prof. Dr. Özgür Yılmaz	(METU, EE)	_____
Dr. Özgür Barış Akan	(METU, EE)	_____
Dr. Bora Dikmen	(MİKES A.Ş.)	_____

I hereby declare that all information in this document has been obtained and presented in accordance with academic rules and ethical conduct. I also declare that, as required by these rules and conduct, I have fully cited and referenced all material and results that are not original to this work.

Name, Last name : Hakan Yesari GÜRSAN

Signature :

ABSTRACT

FRAME SYNCHRONIZATION IN OFDM SYSTEMS

Gürsan, Hakan Yesari

M.S., Department of Electrical and Electronics Engineering

Supervisor: Assoc. Prof. Dr. T.Engin Tuncer

December 2004, 86 pages

In this thesis, we considered the problem of frame synchronization and channel estimation in Orthogonal Frequency Division Multiplexing (OFDM) systems. Since framing error may cause severe ISI and may disturb the orthogonality of the subcarriers, frame synchronization must be accomplished at the OFDM receiver. Furthermore, the effects of channel must be compensated to obtain the symbols accurately. We investigated several frame synchronization algorithms including a maximum likelihood (ML) synchronizer which relies on the periodicity induced in the OFDM structure, and a robust synchronizer which uses a special training symbol. These algorithms are evaluated in AWGN and Rayleigh fading multipath channels and performances are compared in terms of percentage of ISI-free synchronization, mean squared error and symbol error rate. The IEEE 802.11a framework is used to compare these algorithms with the standard system which utilizes training symbols dedicated for synchronization. It is shown that an adjustment for the frame start estimates must be done to avoid the effects of the channel delay spread. It is also pointed that ideal synchronization is not necessary unless symbol boundaries are detected inside an ISI-free region and the error aroused in ISI-free synchronization can be compensated by applying channel estimation and equalization regarding the same symbol boundaries.

Keywords: OFDM, symbol synchronization, 802.11a, channel estimation

ÖZ

OFDM SİSTEMLERİNDE ÇERÇEVE EŞZAMANLAMASI

Gürsan, Hakan Yesari

Yüksek Lisans, Elektrik ve Elektronik Mühendisliği Bölümü

Tez Yöneticisi: Doç. Dr. T.Engin Tuncer

Aralık 2004, 86 sayfa

Bu tezde, Dikgen Frekans Bölüşümlü Çoklama (OFDM) sistemlerindeki çerçeve eşzamanlaması ve kanal kestirimi problemini inceledik. Çerçeveleme hatası simgeler arasında ciddi karışmaya yol açacağından ve alt taşıyıcılar arasındaki dikgenliği bozacağından OFDM alıcısında çerçeve eşzamanlılığı başarılmalıdır. Ayrıca, kanal etkileri doğru sembolleri elde etmek için telafi edilmelidir. OFDM yapısı içindeki dönemliliğe dayanan en büyük olabilirlik eşzamanlayıcısı ve özel bir eğitme simgesi kullanan sağlam eşzamanlayıcı dahil olmak üzere çeşitli çerçeve eşzamanlama algoritmalarını inceledik. Bu algoritmalar toplanır beyaz Gauss gürültülü (AWGN) ve Rayleigh sönümlü çok-yollu kanallarda değerlendirilerek performansları simgeler arası karışmasız eşzamanlama yüzdesi, ortalama karesel hata ve simge hata oranı üzerinden karşılaştırılmıştır. Bu algoritmaları eşzamanlama için ayrılmış eğitme sembollerinden faydalanan standart sistemle karşılaştırmak için IEEE 802.11a çerçeve yapısı kullanılmıştır. Kanal gecikme yayılmasının etkilerinden kaçınmak amacıyla çerçeve başlatma kestirimlerinde ayar yapılması gerektiği gösterilmiştir. Simge sınırları, simgeler arası karışma olmayacak şekilde seçildikçe ideal eşzamanlamanın gerekmediği ve simgeler arası karışmasız eşzamanlamanın getirdiği hataların aynı sembol sınırlarına dayanarak yapılan kanal kestirimi ve denkleştirme ile telafi edilebileceği vurgulanmıştır.

Anahtar kelimeler: OFDM, sembol eşzamanlaması, 802.11a, kanal kestirimi

ACKNOWLEDGEMENTS

I would like to thank Assoc. Prof. Dr. T. Engin Tuncer, for his help, professional advice and valuable supervision during the development of this thesis. This thesis would not be completed without his guidance and support.

Special thanks to my family and my friend Metin Aktaş for their great encouragement and continuous moral support.

TABLE OF CONTENTS

LIST OF FIGURES

LIST OF TABLES

LIST OF ABBREVIATIONS

ADC	Analog-to Digital Converter
ADSL	Asymmetric Digital Subscribers Line
AGC	Automatic Gain Control
AWGN	Additive White Gaussian Noise
BER	Bit Error Rate
BPSK	Binary Phase Shift Keying
CP	Cyclic-Prefix
DAB	Digital Audio Broadcasting
DAC	Digital-to-Analog Converter
dB	Decibel (ratio in log scale)
DFT	Discrete Fourier Transform
DSP	Digital Signal Processing
DSSS	Direct Sequence Spread Spectrum
DVB	Digital Video Broadcasting
FFT	Fast Fourier Transform
FHSS	Frequency Hopping Spread Spectrum
GHz	Giga Hertz
GI	Guard Interval
HIPERLAN	High Performance Radio Local Area Network

ICI	Inter-Carrier Interference
IDFT	Inverse Discrete Fourier Transform
IEEE	The Institute of Electrical and Electronics Engineers
IFFT	Inverse Fast Fourier Transform
IQ	In-phase and Quadrature
ISI	Inter-Symbol Interference
LAN	Local Area Network
Mbps	Megabits per second
ML	Maximum Likelihood
MSE	Mean Squared Error
OFDM	Orthogonal Frequency Division Multiplexing
P/S	Parallel-to-Serial Conversion
PN	Pseudo-noise
PSK	Phase Shift Keying
QAM	Quadrature Amplitude Modulation
QPSK	Quaternary Phase Shift Keying
RF	Radio Frequency
S/P	Serial-to-Parallel Conversion
SC	The method of Schmidl & Cox
SER	Symbol Error Rate
SL	The method using short and long symbols in 802.11a frame
SNR	Signal-to-Noise Ratio
Sync.	Synchronization
WLAN	Wireless Local Area Network

CHAPTER 1

INTRODUCTION

In today's world, wireless communications has gained great importance and the information that must be transmitted between two points needs for higher data rates. However, high speed data transmission suffers from band-limited channels. The channel must be properly estimated and equalized to effectively use the available bandwidth. Also, the delay introduced in the channel results in the loss of synchronization between the transmitter and receiver. This is an important problem when the data is processed at the receiver block by block. Due to lack of synchronization, the receiver cannot estimate the exact block boundaries and this may result in severe errors.

The Orthogonal Frequency Division Multiplexing (OFDM) is a multi-carrier modulation scheme operating on data blocks. Thus, the block synchronization is important in these systems. However, in OFDM, the estimation and equalization of channel are simple since the convolutional channel is converted into many, parallel single-tap channels.

OFDM has gained great interest in the recent years [1] and is widely used in wireless telecommunication networks such as IEEE 802.11a [2] which is a Wireless Local Area Network (WLAN) standard in the U.S. and in HIPERLAN/2 [3], a counterpart of 802.11a in Europe. OFDM is also adopted for Digital Audio Broadcasting (DAB) [4] and for Digital Video Broadcasting (DVB) [5] in Europe for digital radio and television systems. Certainly, the reasons why OFDM became so popular are hidden in the advantages it brings with its modulation scheme.

OFDM may operate under channels with non-flat frequency response such as multipath fading channels. Due to reflections in the transmission, channel frequency response may not be flat and deep fades or nulls may be observed which causes

cancellation of some frequencies at the receiver leading to the loss of the signal. However, if the subcarrier frequencies are designed such that the channel zeros are avoided then, the signal arrives at the receiver without any cancellation [6].

Another important aspect of the OFDM is its immunity to Inter-Symbol-Interference (ISI) which is a major problem when multipath fading channels are under concern. This is achieved by inserting a guard interval that is long enough to clear the channel memory from previous symbols. The guard interval, as a cyclic extension or zero padding of the symbols, together with the orthogonality of the carriers prevents the received signal from the Inter-Carrier-Interference (ICI) [7].

The use of cyclic-prefix and orthogonal subcarriers convert the convolutional channel to low bit-rate, flat-fading, parallel subchannels. The idea of transforming a high bit rate but dispersive environment to low bit rate but non-dispersive parallel channels is first proposed by Chang [8] in 1966. However, the practical implementation had to wait for the efficient Fast Fourier Transform (FFT) techniques and the chips to perform such operations.

The simplicity of channel estimation and equalization in OFDM is another attractive property. Estimation is performed by sending known data on the subcarriers. Since the channel is separated into many single coefficient channels, equalization can be performed by dividing each subcarrier by the inverse of the flat-fading coefficient on that subcarrier [9].

Despite these advantages, OFDM has some drawbacks such as sensitivity to carrier frequency offset and framing errors. An offset in the carrier frequency or a phase error causes the loss of orthogonality of the subcarriers, resulting in ICI. Framing error creates an ambiguity about the alignment point of the OFDM symbols. This is mainly caused by the delay spread of the multipath channel. The misalignment of the FFT window at the receiver may cause ISI in OFDM symbols and hence result in severe bit error rate (BER) degradation.

To combat with such disadvantages, many methods have been proposed. Mainly, they may be grouped into two. Some methods utilize training signals and pilot subcarriers to extract the frame timing information and to estimate the carrier frequency offset and phase error ([10] - [13]). Generally, these procedures dedicate

one or more OFDM symbols for training the receiver. The receiver tunes its Automatic Gain Control (AGC) block to maximize the Signal-to-Noise Ratio (SNR) in the received signal by considering the power level of the known symbols. The dedicated and known symbols are searched in the frame of received OFDM symbols by means of correlation. The symbol where the correlation is maximized is the first OFDM symbol of the frame.

Inserting known symbols into the OFDM frame decreases the efficiency since no information data is transmitted at the synchronization symbols. Sometimes the dedicated symbols are not known by value but some properties are imposed onto the synchronization symbols such as impulse-like correlation [14] or symmetry [15] property. The receiver searches for the special symbol in the frame. The method of [15], which will be discussed in further chapters, also saves some bandwidth utilizing half of the carriers as both for data and for synchronization.

On the other hand, there are several methods that reject the necessity of pilots and use the information already inherent in the OFDM signal ([16] - [21]). Because of cyclic-prefix, an OFDM symbol has two copies of some samples and the separation of these copies is the FFT size, a design parameter of OFDM system. A correlative search of these copies yields the start of the OFDM symbol.

In this thesis, we will deal with the problem of frame synchronization in OFDM systems. Our assumption is that the carrier frequency and phase are perfectly synchronized with that of the transmitter. We will focus on both the data-aided and non-data-aided frame synchronization techniques in the presence of Rayleigh fading channel and additive white Gaussian noise (AWGN) in the background. As a data-aided solution, we will mention the approach in [15] and as a non-data-aided solution we will refer to [21]. Our aim is to compare the performances of these methods and to exhibit the effect of the channel on the synchronization algorithms. These methods are designed for AWGN channels need some adjustment in their output in the Rayleigh fading channel case. We will point out that the frame synchronization and channel estimation may be performed jointly without any degradation in the performance. In this way, ideal synchronization, which is hard to achieve due to channel, is not necessary and ISI-free synchronization is possible.

As an application of the OFDM, we implemented IEEE 802.11a standard frame structure. Although a synchronization procedure in 802.11a is not given in the specifications [2], it is based on detecting dedicated symbols supplied in the frame structure. These symbols are used for frame detection, timing and frequency synchronization and channel estimation. We will show how frame synchronization can be carried out using those symbols. We will apply the mentioned frame synchronization techniques and using their outputs together with the known training symbols, we will estimate the channel.

The organization of the thesis is as follows: Chapter 2 summarizes the frame synchronization problem and techniques used in single carrier systems. In Chapter 3, the mathematical model of the OFDM system is given and the performance in ideal conditions is illustrated. In Chapter 4, the effect of frame synchronization errors and both a non-data-aided and a data-aided frame synchronization algorithm are given. The rationale behind joint frame synchronization and channel estimation is explained. In Chapter 5, IEEE 802.11a frame structure is introduced and the previously mentioned techniques are applied. Finally we will conclude our discussion in Chapter 6.

CHAPTER 2

FRAME SYNCHRONIZATION TECHNIQUES

In a typical communication system, the information data is sent as a sequence of bits. The bit stream is divided into data words, and a collection of sequential data words constitute a frame. The problem is to detect a frame in series of bits transmitted for further processing, such as block processing or coding, in the presence of noise and non-ideal channel conditions.

If noise is present, it can reveal itself in at least three ways [22]: 1) detect a 0 instead of a 1 and vice versa; 2) skip a clock tick and lose a bit; 3) insert an extra clock tick and create an extra data bit.

Going through the effects above, the properties of a good frame synchronization system are listed below [22]:

1. Rapid initial frame acquisition
2. Rapid detection of timing anomalies and frame synchronization recovery
3. Reliability of the lock indication
4. Simplicity of the clock synchronization algorithm
5. Minimal insertion of redundancy in the data bit stream for frame synchronization purposes

Some transmission schemes utilize markers in their frame synchronization algorithms. Marker is a word indicating the receiver that a new frame is started. Marker may be an element of the alphabet of the communication scheme or a collection of the elements of the alphabet but the most important property of the marker is that it is known by the receiver.

There are some assumptions in the design of markers: The data is assumed to be random, the channel errors are assumed to be random and the bit clock is assumed to be stable. With these assumptions, marker design includes some considerations. Marker may be selected from the communication alphabet but the data symbols never use the same symbol. This means that a transmitter should guarantee that the marker symbol never be duplicated in the data part. This approach limits the transmission efficiency since the size of the alphabet used by data symbols is decreased by one symbol.

When full alphabet is available for data, the marker usually consists of a fixed sequence of symbols which is less probable than any other data sequence in a message. This again reduces the transmission efficiency.

Given a message sequence, the search for a marker sequence involves a correlation calculation or minimization of the Hamming distance of symbols to the marker. Massey [23] has shown that the coherent frame-sync acquisition system shown in Figure 1 is optimal for detecting the marker in a received sequence under the presence of AWGN.

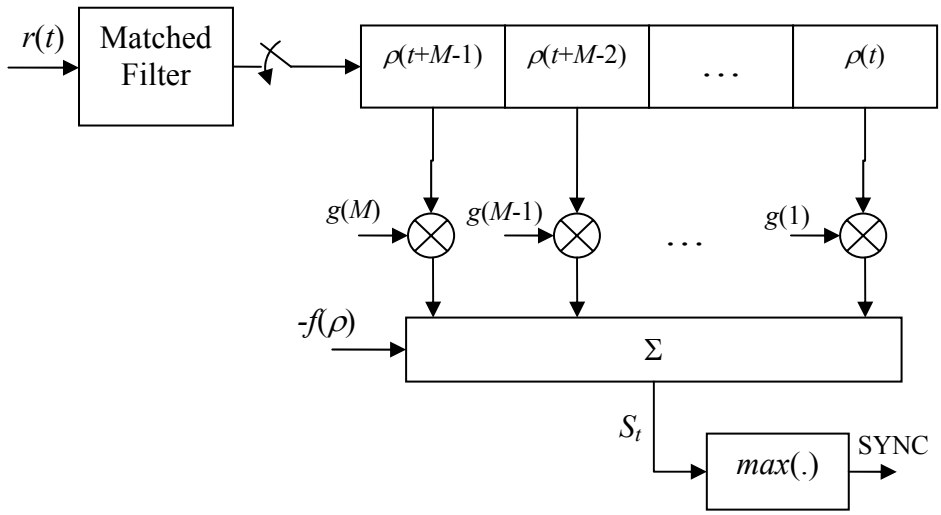

Figure 1 – A coherent frame-sync acquisition system [22].

The detected samples $\rho(t)$ are filtered with the marker sequence $g(t)$ and that filter output is passed through a known nonlinear function $f(.)$ which is a function of its argument and the SNR. The measure is given as

$$S_t = \left(\sum_{j=1}^{M} g(j)\rho\left((t+j-1)_M\right) \right) - \left(\sum_{j=1}^{M} f\left(\rho\left((t+j-1)_M\right)\right) \right) \quad (1)$$

where the first term is the correlation of received samples with the known marker and the second term is a correction term to compensate for the random data surrounding the marker. The function $f(.)$ is needed because due to random noise, samples with high amplitudes may yield high outputs even though the signals are uncorrelated. Usually, this is a measure for the power of the correlated window which is used to prevent spurious maxima. Maximization is performed among $M+D$ observations, where M is the length of the marker and D is the number of samples between two markers in a sequence and $(.)_M$ denotes an operation in modulo M. The subscript of the maxima is the estimated location of the marker.

An example of the function $f(\rho)$ is given by Nielsen [24]. He suggests using $|\rho|$ at high SNR environments without degrading the performance. This prevents from misdetection of the frame start due to excessive noise.

Markers are efficient especially when used with large frames where the ratio of the marker size to the number of samples in the frame is extremely low. Additionally, marker synchronization is simple to implement and supported by various modulation schemes and coding techniques.

Another method used for framing the transmitted data is to leave gaps between frames as shown in Figure 2. The gaps may be constructed by inserting zeros, thus somewhere between frames, the transmission power is minimized. The receiver knows the number of inserted zeros, M_Z and searches for the minimum power in a sliding window of length M_Z. An application utilizing gaps for synchronization is given for OFDM systems as inserting a null symbol in [25]. However, this method may be problematic in that an ambiguity arises due to random noise; especially at low SNRs. Noise may hide the gap and mislead the detector which is searching for the minimum power. Also, when a burst mode transmission is

used instead of a continuous transmission, there is no way to distinguish between the gap and the idle period between the bursts.

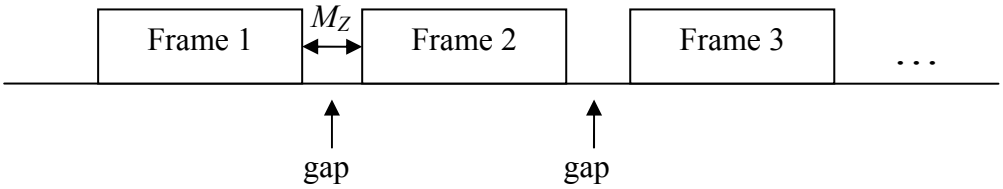

Figure 2 – Leaving gaps between the frames

A method neither utilizing known samples nor using null symbols is shown in Figure 3. In this scheme, a portion at the end of the frame is transmitted also at the beginning of the frame. The receiver is not forced to know the marker sequence. It performs a correlation between two windows which are D samples apart where D is the length of the useful portion of a frame. This is inherently used in OFDM systems as cyclic-prefixing to avoid also the inter-block interference and we will refer to this method in more detail in Chapter 4.

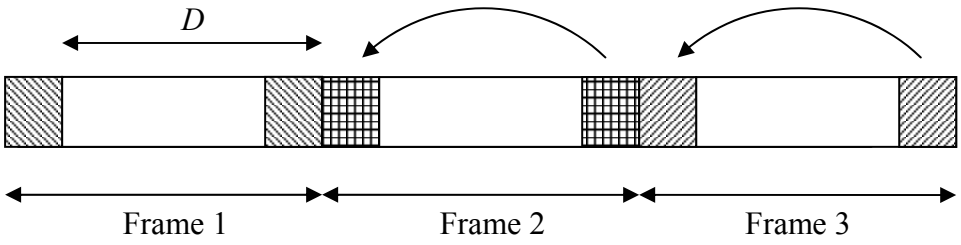

Figure 3 – Prefixing with the data from the end of the frame

As it can be seen from these methods, some of the transmission time is spent for sending known or repetitive samples. This decreases the transmission efficiency especially when the frame lengths are short. However, this is the price paid for accurate synchronization.

CHAPTER 3

OFDM SYSTEM OVERVIEW

OFDM is a popular multi-carrier modulation technique currently used in DVB, DAB, WLAN (IEEE 802.11a) and ADSL systems.

OFDM brings bandwidth efficiency, overcomes ISI and ICI improving the performance of the system under frequency selective multi-path channels.

3.1 Multi-carrier System Model

The low-pass equivalent OFDM signal is represented as [26]

$$X(t) = \sum_{n} X_n \left(t - nT\right) \tag{2}$$

$$X_n\left(t\right) = \sum_{k=0}^{N-1} X_{n,k}\phi_k\left(t\right), \qquad 0 \le t < T$$

$$\phi_k(t) = \begin{cases} e^{j2\pi f_k t} & 0 \le t < T \\ 0 & \text{elsewhere} \end{cases} \tag{3}$$

where T is the symbol period, N is the number of subcarriers, ϕ_k is the k^{th} subcarrier with frequency f_k and $X_n(t)$ is the n^{th} OFDM symbol.

To maintain the orthogonality of the subcarriers, the following orthogonality condition must be satisfied:

$$\int_0^T \phi_k\left(t\right)\phi_l^*\left(t\right)dt = a\delta\left(k-l\right) \tag{4}$$

In order to satisfy the orthogonality condition in (4), the subcarrier frequencies must be separated by the integer multiples of the inverse of the symbol period as

$$f_k = f_0 + \frac{k}{T}, \quad k = 0,1,...,N-1 \tag{5}$$

where f_0 is the frequency of the first subcarrier.

The orthogonality conditions in (4) and (5) are essential for OFDM and this is the key point on how OFDM removes the ICI. The importance of orthogonality is also depicted in Figure 4. Here, since the subcarriers are windowed by a rectangular window of duration *T*, the subcarrier spectrum exhibits a sinc function. As it is seen from Figure 4, when the demodulator's frequency is tuned to the k^{th} subcarrier, the contribution of subcarriers *k*+1 and *k*-1 are both zero, verifying (4).

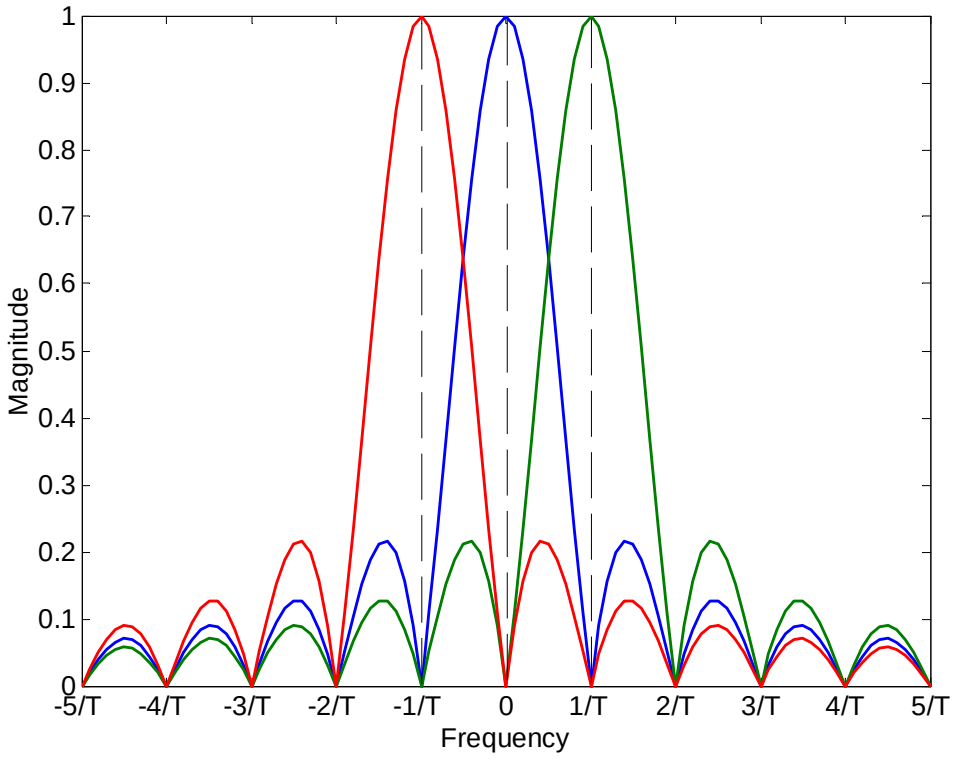

Figure 4 – The spectrum of orthogonal subcarriers

On the other hand, the spectrum of non-orthogonal carriers (violation of (5)) is shown in Figure 5. When subcarrier k is demodulated, the subcarriers k-1 and k+1 will contribute to the result, introducing ICI.

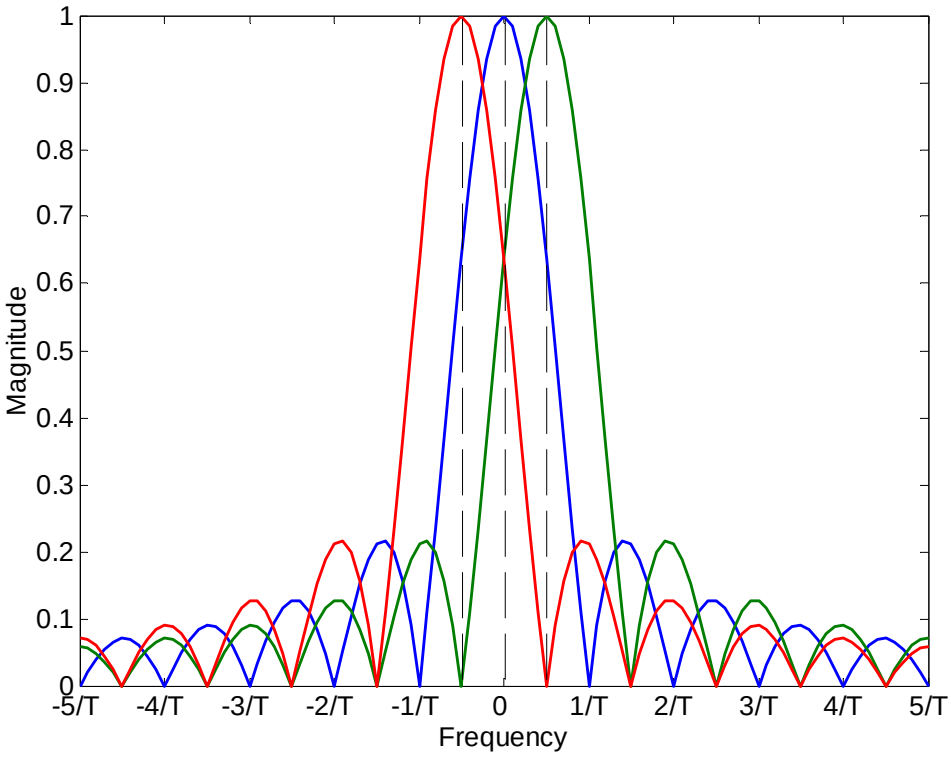

Figure 5 – The spectrum of non-orthogonal subcarriers

After ensuring the orthogonality, the OFDM modulator and demodulator can be implemented as shown in Figure 6 and Figure 7, respectively. Here, X_n's are complex samples from the modulation map of a constellation such as Binary Phase Shift Keying (BPSK), Quaternary Phase Shift Keying (QPSK) or Quadrature Amplitude Modulation (QAM).

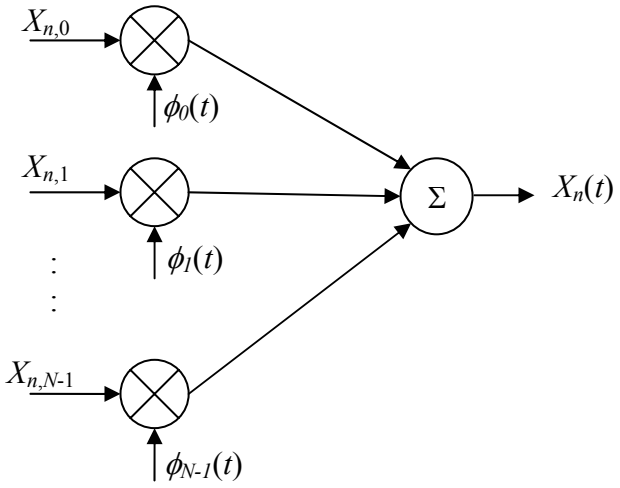

Figure 6 – The OFDM modulator

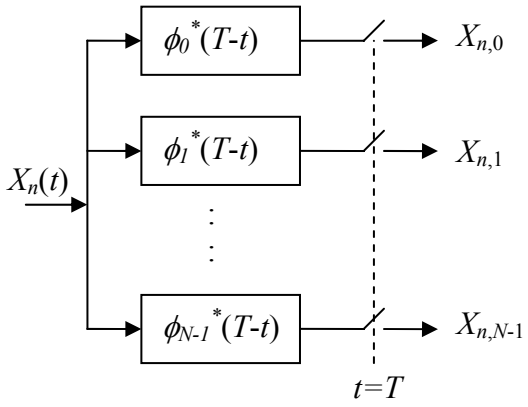

Figure 7 – The OFDM demodulator

Instead of using many mixers and filters, the OFDM modulation and demodulation may be implemented using Discrete Fourier Transform (DFT). The forward and inverse DFT of a discrete-time signal $x(n)$ is as given in (6) and (7), respectively.

$$X(k) = \frac{1}{\sqrt{N}} \sum_{n=0}^{N-1} x(n) e^{-j\frac{2\pi nk}{N}}, \quad 0 \le k < N \tag{6}$$

$$x(n) = \frac{1}{\sqrt{N}} \sum_{k=0}^{N-1} X(k) e^{j\frac{2\pi nk}{N}}, \quad 0 \le n < N \tag{7}$$

These equations can be given also in the matrix form [9] as

$$\mathbf{v} = \mathbf{F}\mathbf{u} \tag{8}$$

$$\mathbf{u} = \mathbf{F}^H \mathbf{v} \tag{9}$$

where $\mathbf{u} = [x(0), x(1), ..., x(N-1)]^T$, $\mathbf{v} = [X(0), X(1), ..., X(N-1)]^T$ and $\mathbf{F}$ is the N-by-N DFT matrix, $\mathbf{F}(m,n) = \frac{1}{\sqrt{N}} e^{-j\frac{2\pi mn}{N}}$ with $(\,)^T$ being the transpose and $(\,)^H$ being conjugate transpose or Hermitian transpose.

Note that the kernels of these transforms also obey the orthogonality constraint given in (4). This gives us an efficient method in implementing the OFDM modulation and demodulation using the forward and inverse FFT. Instead of the modulator in Figure 6 and the demodulator in Figure 7, the DSP implementations in Figure 8 and Figure 9 can be used, respectively. Here, the data samples are modulated onto the subcarriers in the frequency domain. The frequency domain data is transformed into the time domain by IFFT performed on sample blocks yielding an *OFDM symbol*. Thus, each OFDM symbol contains a number of complex samples. *Frames* are created by appending each OFDM symbol one another. At the receiver side, the received time domain samples are transformed back to the frequency domain with an FFT operation and the data on each subcarrier is detected.

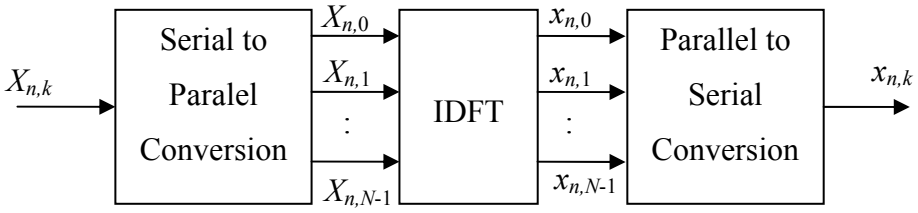

Figure 8 – The DSP implementation of the OFDM modulator

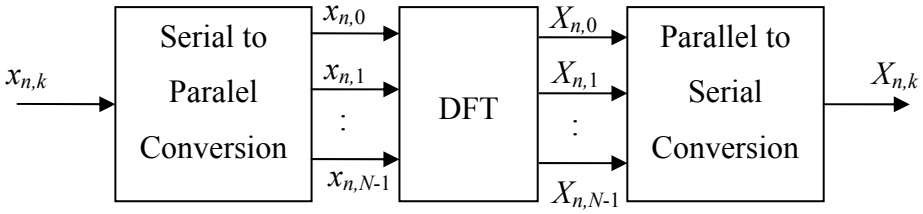

Figure 9 – The DSP implementation of the OFDM demodulator

3.2 The Cyclic Prefix

Usually, there are two main factors affecting the transmitted signal in telecommunication systems. The first one is the noise which is inevitable due to thermal effects in components and the environment. The second one is the multipath effect due to the objects in the path of transmission.

The multipath effect may be modeled as a filter whose frequency characteristics is non-ideal. Thus, the relation between a signal input to the medium and the output of the medium may be given as

$$y(n) = \sum_{i=0}^{L} h(i)x(n-i) + \eta(n) \tag{10}$$

where $h(n)$ is the channel impulse response, $x(n)$ is the input signal and $\eta(n)$ is the AWGN. As it can be seen from (10), the output is affected not only by the current input but also the previous inputs. This problem is severe for OFDM systems in which a block processing of data is performed at the receiver. Due to channel impulse response, a sample from another OFDM symbol may interfere with the current OFDM symbol.

To combat with this inter-block interference, the OFDM symbol is extended with a guard interval such as a cyclic-prefix (CP). The last M samples of the IFFT output are copied and placed before the first sample. Thus the block now holds $M+N$ samples where M is the cyclic prefix length and N is the number of subcarriers. This operation is illustrated in Figure 10.

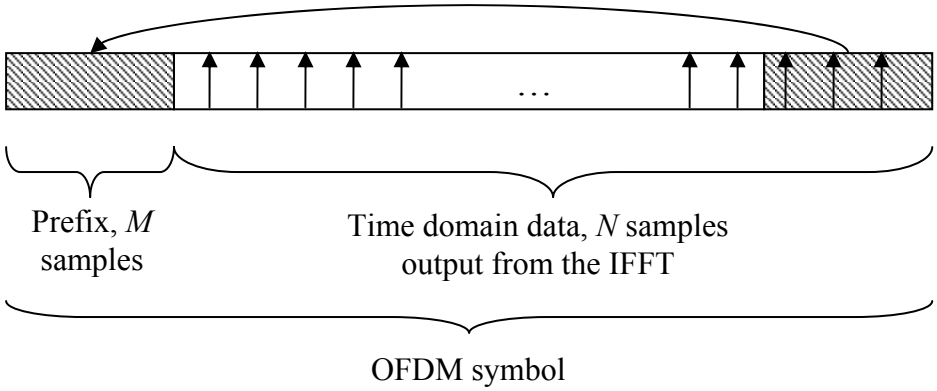

Figure 10 – The structure of an OFDM symbol

The constraint on the cyclic-prefix is that its length must be longer than the order of the channel. This is done in order to avoid the effects of the channel memory. During the convolution of the channel with the cyclically extended OFDM symbol, taps of the channel filter are filled with the samples in the cyclic-prefix. Thus, ISI only affects the CP part and does not interfere with the previous data part.

The reason for a cyclic guard interval is to match the channel eigenvectors to the DFT basis vectors. As the CP is added at the transmitter and removed at the receiver, the equivalent channel has the DFT coefficients as the eigenvalues and the DFT basis vectors as the eigenvectors.

The structure of the OFDM transmitter at the baseband is given in Figure 11.

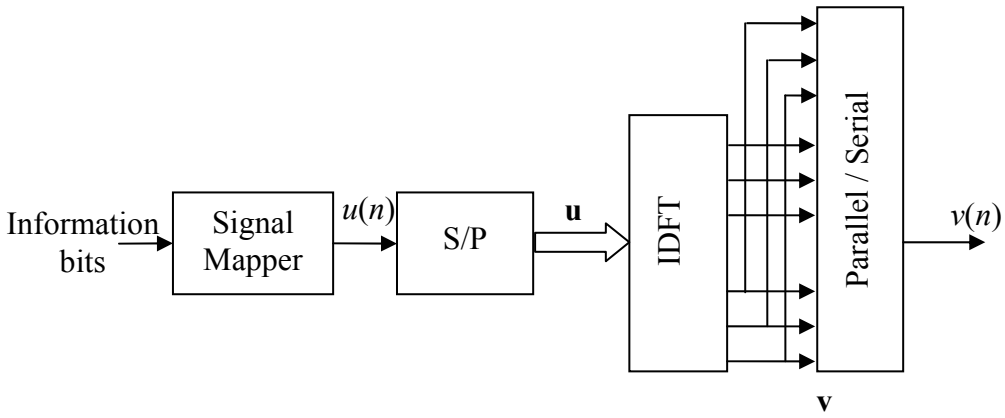

Figure 11 – The OFDM transmitter

The information bits are grouped and each group is mapped to a sample in a constellation forming $u(n)$. Then, the serial samples are converted to parallel constituting the vector at time p $\mathbf{u}(p) = [u(pN), \quad u(pN+1), \quad \ldots \quad u(pN+N-1)]^T$. The vector **u** is the frequency domain data modulated onto the subcarriers. Then, this frequency domain data is converted to the time domain by IDFT and the cyclic prefix is inserted to the time domain data yielding the vector **v** in (11)

$$\mathbf{v}(p) = \mathbf{T}\mathbf{F}^H \mathbf{u}(p) \tag{11}$$

where **T** is the (N+M)-by-N transmit-matrix $\mathbf{T} = [\mathbf{I}_{CP}{}^T, \mathbf{I}_N{}^T]^T$, $\mathbf{I}_{CP}$ being the last M rows of the N-by-N identity matrix $\mathbf{I}_N$. After the CP is inserted to the beginning of the IDFT output, vector **v** is converted to serial as $v(n)$ and given to an IQ modulator as shown in Figure 12. The real part of $v(n)$ constitutes the in-phase component and the imaginary part forms the quadrature component. The discrete time signal is converted to analog and after anti-aliasing low-pass filters the in-phase and quadrature components are modulated with two carriers having 90^o phase shift. The analog signal is then pulse-shaped and given to the channel.

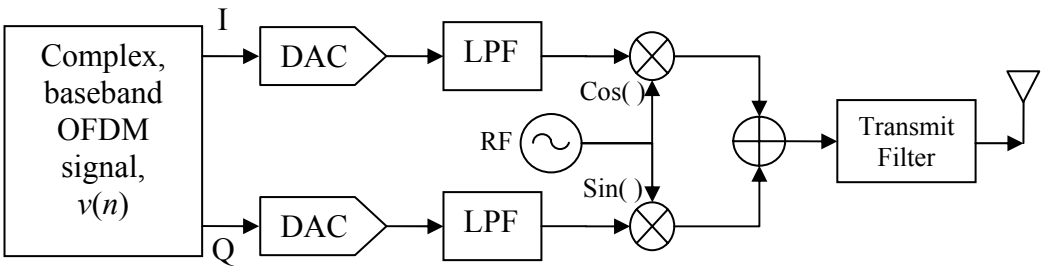

Figure 12 – RF transmitter

The RF receiver is shown in Figure 13. The received signal is separated into in-phase and quadrature components and digitized to form the complex baseband samples $x(n)$.

Assuming perfect RF modulation and demodulation, the received signal may be modeled in the baseband as shown in Figure 14.

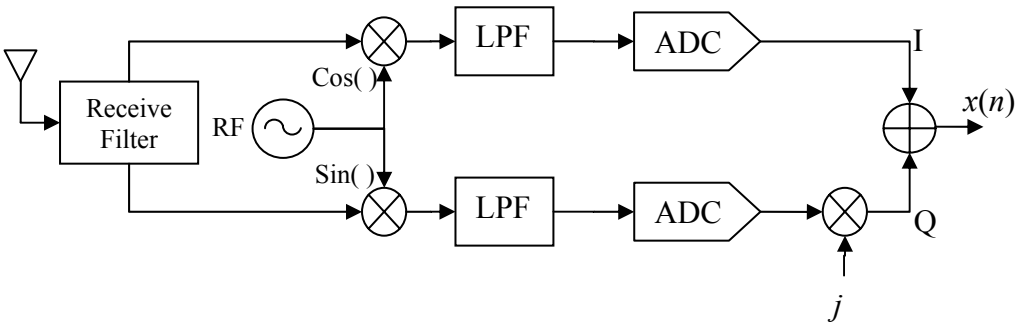

Figure 13 – RF receiver

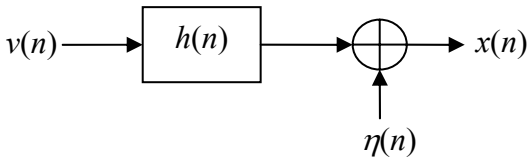

Figure 14 – The channel structure

In Figure 14, $v(n)$'s are the complex baseband samples output from the OFDM transmitter, $h(n)$ is the channel impulse response, $\eta(n)$ is the additive white Gaussian noise and $x(n)$'s are the samples output from the RF receiver.

In Figure 15, the block diagram of the OFDM receiver is shown.

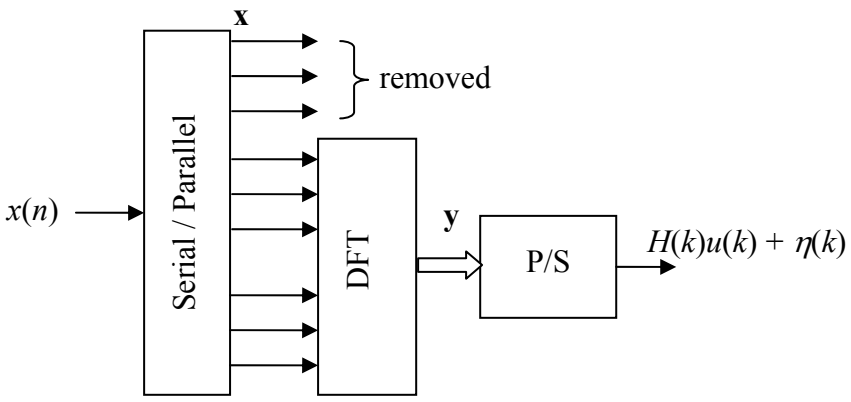

Figure 15 – The OFDM receiver

At the OFDM receiver, first, the received samples are converted from the serial to parallel as $\mathbf{x}(p) = [x(p(M+N)),\ \ x(p(M+N)+1),\ \ \ldots\ \ x((p+1)(M+N)-1)]^T$. Assuming perfect frame and symbol timing, the p^{th} received OFDM symbol at the receiver can be written as [9]

$$\mathbf{x}(p) = \mathbf{H_0}\mathbf{v}(p) + \mathbf{H_1}\mathbf{v}(p-1) + \boldsymbol{\eta}(p) \tag{12}$$

where $\mathbf{H_0}$ is an (M+N)-by-(M+N) lower triangular Toeplitz matrix with first column being $[h(0),...,h(L),0,...,0]^T$ and $\mathbf{H_1}$ is an (M+N)-by-(M+N) upper triangular Toeplitz matrix with first row $[0,...,0,h(L),...,h(1)]^T$.

In (12), $\mathbf{H_0}$ denotes the effect of the channel to the current OFDM symbol and $\mathbf{H_1}$ is the inter-OFDM symbol interference originating from the previous OFDM symbol.

At the receiver, the linear shift caused by the channel on the data part is converted into a cyclic shift and thus the received OFDM symbol is turned out to be the cyclic convolution of the channel impulse response with the transmitted OFDM symbol. The removal of cyclic prefix can be written as

$$\mathbf{y} = \mathbf{FRx} \tag{13}$$

where $\mathbf{R} = [\mathbf{0}_{M\times N}, \mathbf{I}_N]$ is the receive-matrix. If we expand (13), we obtain the decomposition of the received OFDM symbol as

$$\begin{aligned}
\mathbf{y}(p) &= \mathbf{FRH_0}\mathbf{v}(p) + \mathbf{FR}\boldsymbol{\eta}(p) \\
\mathbf{y}(p) &= \mathbf{FRH_0}\mathbf{T}\mathbf{F}^H\mathbf{u}(p) + \mathbf{FR}\boldsymbol{\eta}(p) \\
\mathbf{y}(p) &= \mathbf{FHF}^H\mathbf{u}(p) + \bar{\boldsymbol{\eta}}(p)
\end{aligned} \tag{14}$$

where $\bar{\boldsymbol{\eta}}(p) = \mathbf{FR}\boldsymbol{\eta}(p)$ is the filtered noise vector and $\mathbf{H} = \mathbf{RH_0T}$ is the resultant channel matrix. Note that the received OFDM symbol does not contain any interference from the previous OFDM symbol in (14). Since the CP length is greater than the channel order, the receive-matrix cancels the interference of previous symbol as $\mathbf{RH_1} = \mathbf{0}$.

It can be shown that **H** is a circulant matrix and, (14) becomes [27]

$$\mathbf{y}(p) = \mathbf{D}\mathbf{u}(p) + \bar{\boldsymbol{\eta}}(p) \tag{15}$$

where $\mathbf{D} = diag\left[H(0), H(1), ..., H(N-1)\right]$ with $H(k)$ being the DFT of $h(n)$ in (6) with only the $\frac{1}{\sqrt{N}}$ scale factor difference.

Because of the CP and the DFT operations for orthogonality, the convolving, frequency selective multipath channel is transformed into N parallel, flat-fading subchannels as shown in Figure 16.

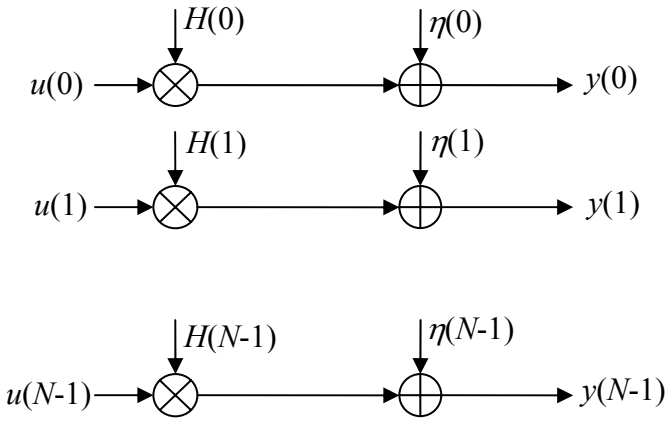

Figure 16 – Equivalent model with parallel flat-fading subchannels

3.3 Equalization

The input signal can be recovered by simply dividing the received sample on a subcarrier by the channel's frequency response on the same subcarrier if the channel is known apriori (16). With this simple operation the need for an extra equalizer is eliminated.

$$y_k = H_k u_k + \overline{\eta_k}$$
$$\frac{y_k}{H_k} = u_k + \frac{\overline{\eta_k}}{H_k} \tag{16}$$

On the other hand, when the channel frequency response has deep fades or nulls, the sample on the corresponding subcarriers may be lost. If the channel is known, then the number of subcarriers may be selected such that to avoid these nulls as shown in Figure 17. However, this may need to change the symbol size and also the channel may change in time so a pre-design may not be a good solution.

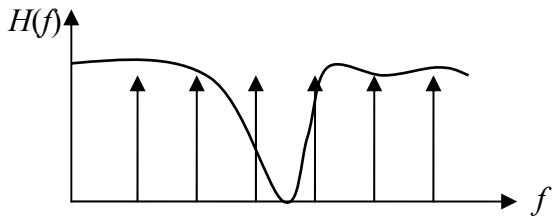

Figure 17 – Avoiding channel nulls by designing subcarrier spacing

Additionally, if the channel frequency response at a subcarrier is small, then in the recovery, noise is amplified with respect to the original symbol and this may increase the MSE and SER of the symbols. To avoid this, usually error control coding is used in standards ([2] - [5]) applying OFDM as the modulation scheme.

3.4 Performance of OFDM

In this part, the performance of the OFDM system will be shown using the simulation results. The simulations are performed under AWGN and Rayleigh fading frequency selective channels. We will make comparisons in terms of Mean-Squared Error (MSE) in the received signal and the Symbol Error Rate (SER) in the detected output under changing SNR conditions. It is assumed that at the receiver side, perfect frame synchronization is done and the channel is known.

The list of OFDM simulation parameters are given in Table 1. In these simulations SNR is calculated as the ratio of signal power to the noise power, $\sigma_v^2 / \sigma_\eta^2$ in Figure 14. For each SNR, a total of 256000 BPSK, QPSK or 16-QAM symbols are sent to calculate the SER.

In the signal mapping, Gray coding is used to minimize BER and the symbols are detected considering the minimum distance criterion.

Table 1 – OFDM simulation parameters

Parameter	***Value***
Number of subcarriers	128
Length of cyclic-prefix	15
Number of OFDM symbols used	10
Constellation	BPSK, QPSK and 16-QAM with Gray coding
Number of trials for each SNR	200

3.4.1 Performance under AWGN Channel

When the OFDM signal is perfectly equalized, each subcarrier seems to be modulated independently as if in a single carrier scheme. Thus, the error probability of OFDM is the same with the error probability of a single carrier scheme which uses the same modulation map.

The MSE performance of OFDM under AWGN channel is shown in Figure 18 and the corresponding SER performance is given in Figure 19.

As in a single carrier scheme, BPSK and QPSK have better performance than 16-QAM. The SER is very low after 10 dB SNR for BPSK and 12 dB SNR for QPSK, whereas the limit for such a low SER is 20 dB when 16-QAM is employed. This behavior is inherited from the single carrier schemes.

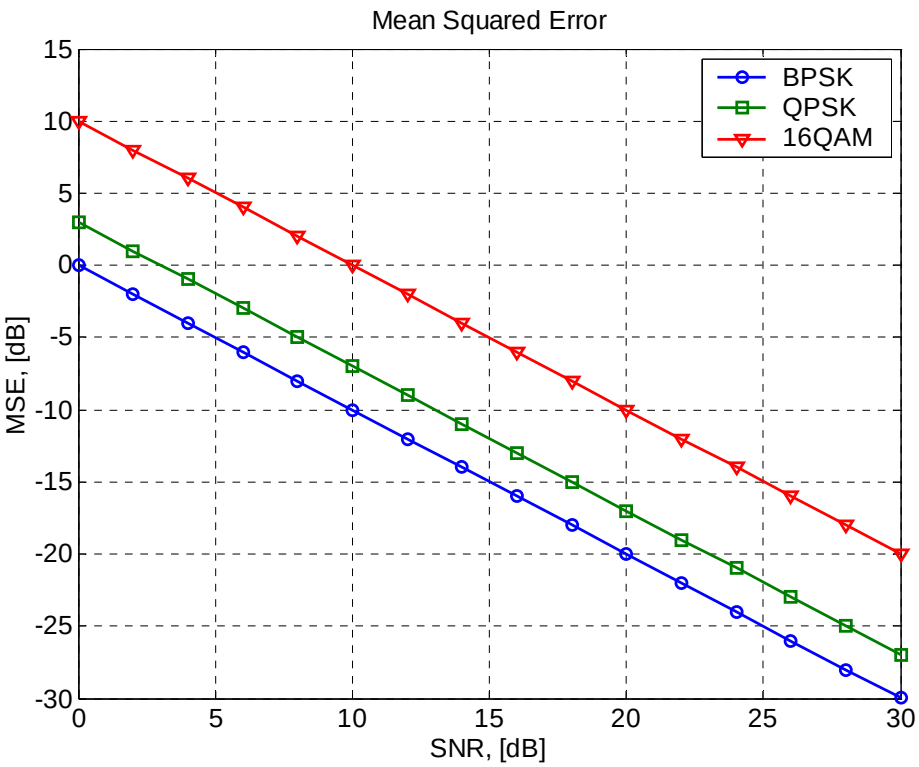

Figure 18 – MSE performance of OFDM under AWGN channel

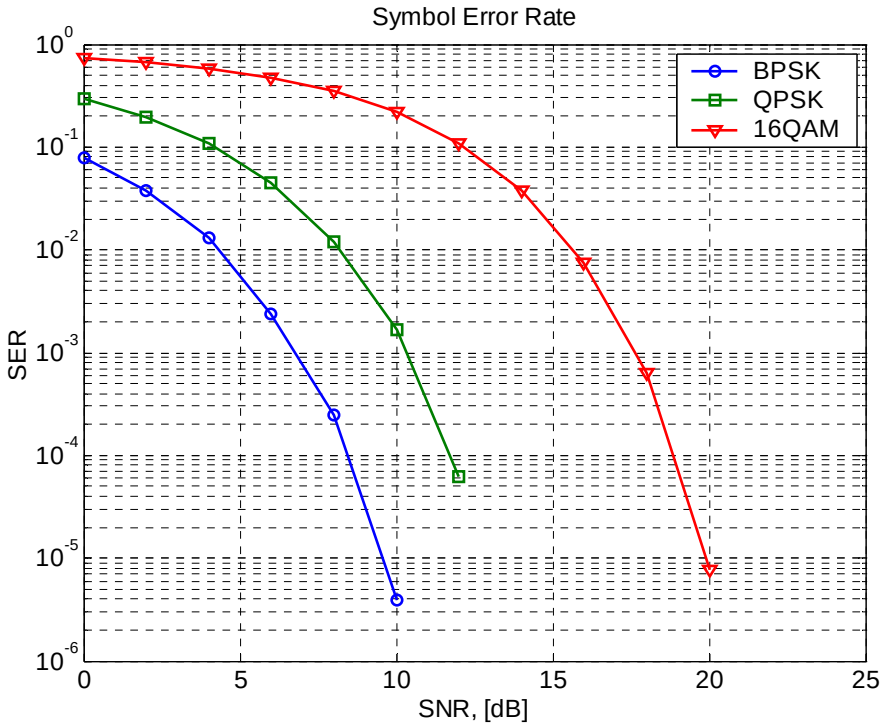

Figure 19 – Symbol error performance of OFDM under AWGN channel

3.4.2 Performance under Rayleigh Fading Channel

A Rayleigh fading channel is generated by selecting the real and imaginary parts of the channel from a Gaussian distribution to make the envelope of the channel have a Rayleigh distribution. Then, the channel vector is normalized to unit norm for fair comparison. Monte-Carlo simulation is performed by changing the channel, data and noise at each trial.

The performance under Rayleigh channel is illustrated for MSE in Figure 20 and for SER in Figure 21. The MSE is higher in received signal than that in the AWGN case because of the flat-fading equalization. When the amplitude of a channel subcarrier is small, then the division of the received sample to the channel coefficient increases the noise power as given by (16). The SER performance under Rayleigh fading multipath channel is consistent with the one given in [28] (pp. 786-787).

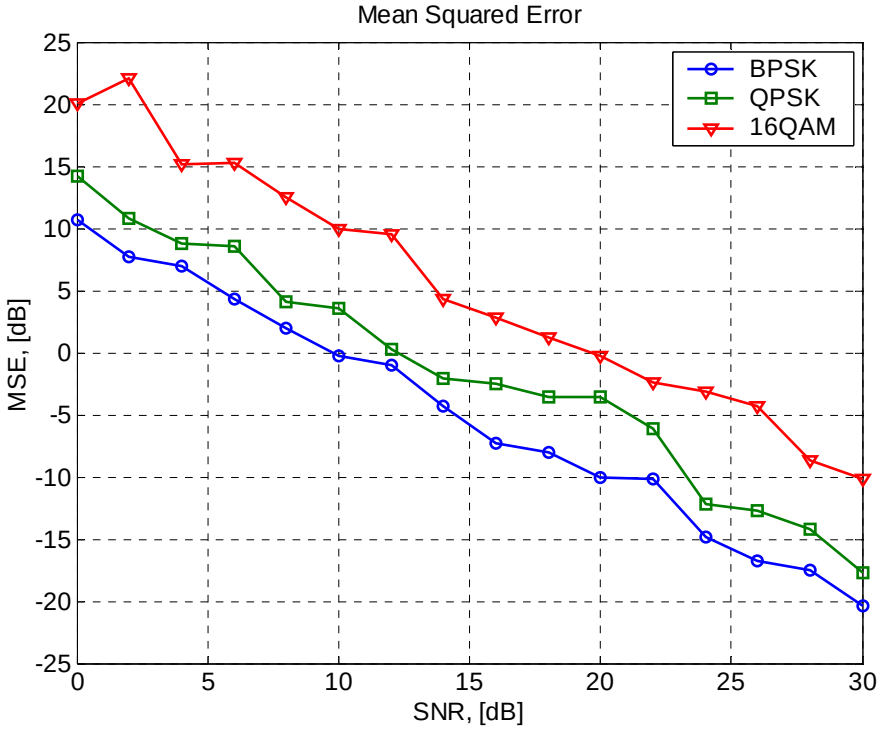

Figure 20 – MSE performance of OFDM under 6th order Rayleigh fading channel

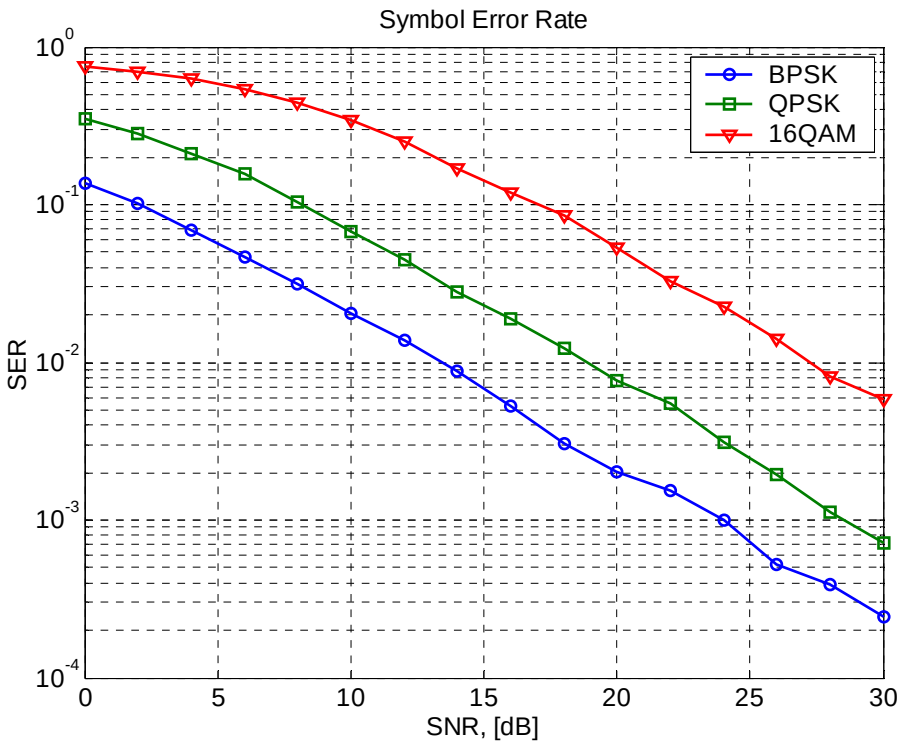

Figure 21 – Symbol error performance of OFDM under 6th order Rayleigh fading channel

In this section we would also like to illustrate the effect of a channel null. For this purpose, the generated channels are adjusted so that at least one subcarrier coincides with a channel null as shown in Figure 22. The SER performance of the system for this case can be observed in Figure 23. As observed from Figure 23, the channel null at $z = j$, the subcarrier 32 is completely lost, and noise power at the receiver blows up for that subcarrier. This is also reflected in the symbol error rate. When compared to Figure 21, the SER level 10^{-2} is never reached, even for high SNR.

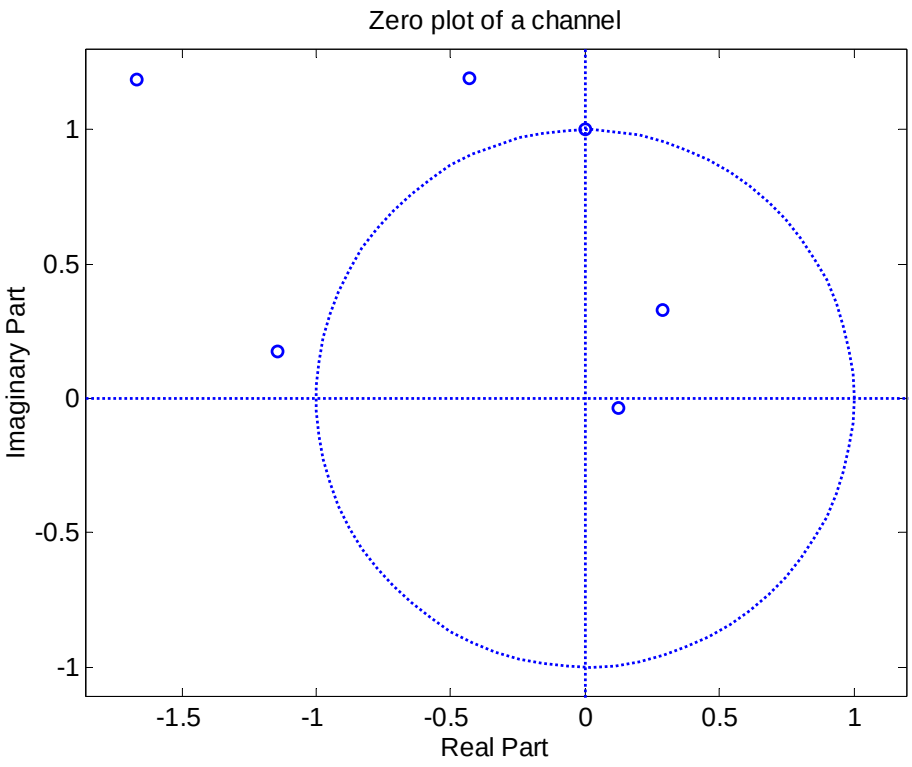

Figure 22 – Zero plot of a channel with a null on a subcarrier

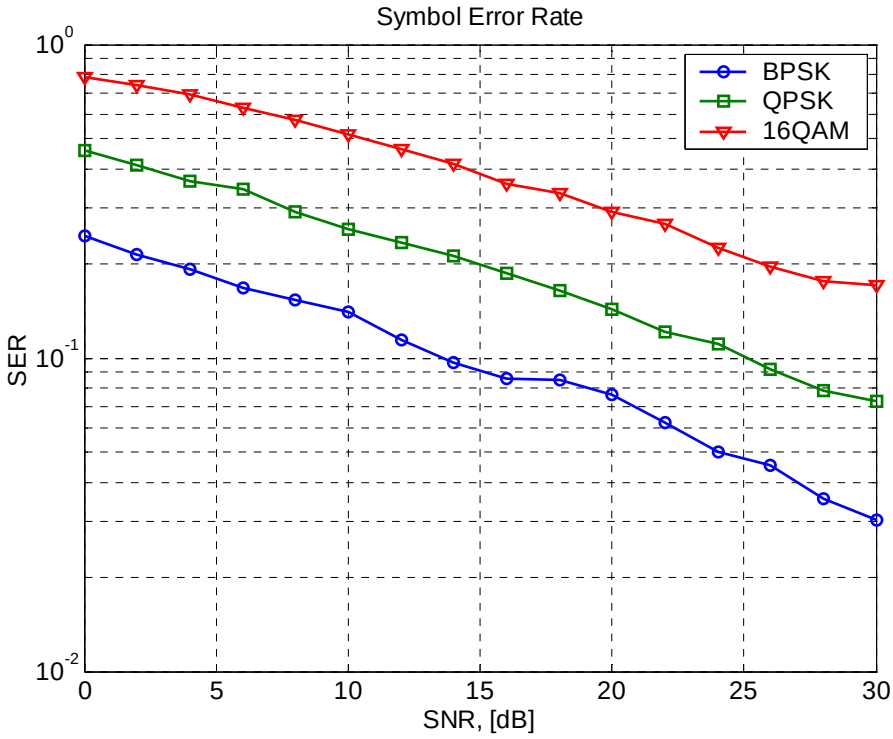

Figure 23 – Symbol error rate when the channel has at least one null

CHAPTER 4

FRAME SYNCHRONIZATION AND CHANNEL ESTIMATION IN OFDM

In chapter 3, an ideal receiver structure is considered, such that the channel is known apriori and ideal frame synchronization is performed. In this chapter, we will discuss the details of the OFDM receiver and the sensitivity of OFDM to synchronization errors will be investigated.

There are two types of synchronization that an OFDM receiver must achieve. The first one is the synchronization of the carriers of receiver and the transmitter. This is important for the orthogonality between subcarriers, which is essential to avoid ICI. We will assume that the carrier frequency and phase synchronization is achieved, and concentrate on the symbol timing and hence frame synchronization of OFDM system.

The second synchronization task is to align the FFT window at the correct received sample. If this is not achieved then, the samples from the adjacent OFDM symbol can be included in the FFT block, resulting in ISI. We will discuss especially two timing synchronization algorithms proposed in [21] and [15].

In addition, we will discuss the channel estimation which is done jointly with frame synchronization. This operation is necessary if there is no perfect synchronizer and the channel is unknown at the receiver.

In Figure 24, the OFDM receiver structure with synchronization and channel estimation blocks is given. Typically, the frame synchronizer operates on the data in the time domain and its output is used as an alignment point in serial to parallel conversion. The frequency synchronizer also operates on the time domain data and the carrier frequency error is cancelled together with the equalization. Channel estimation usually depends on frequency domain data. It uses pilot subcarriers or

dedicated symbols to estimate the channel frequency response on the subcarriers. Then the estimated channel is equalized by dividing the received subcarriers to the channel subcarriers

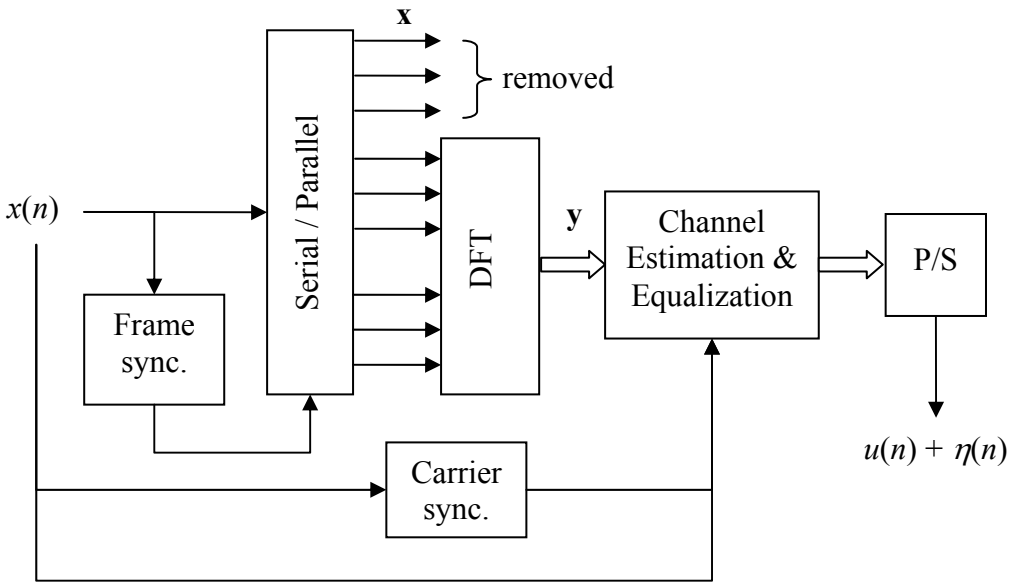

Figure 24 – OFDM receiver structure with frame synchronizer, carrier synchronizer and channel estimation blocks

4.1 Effect of Synchronization Errors

It is important to identify the synchronization problem clearly. The problem statement is as follows: *"Given a frame of OFDM symbols, find a sample in the OFDM symbol to locate the beginning of the FFT window in order to avoid ISI."*

In Figure 25, we present the complete structure of an OFDM symbol with CP in order to show the channel effects. In this figure, channel placement during convolution operation and ideal FFT window is shown.

If we can find the beginning of the ideal FFT window, then we would have the desired equation

$$y(k) = H(k)u(k) + \eta(k) \tag{17}$$

where each transmitted subcarrier is multiplied with a channel subcarrier in the presence of noise.

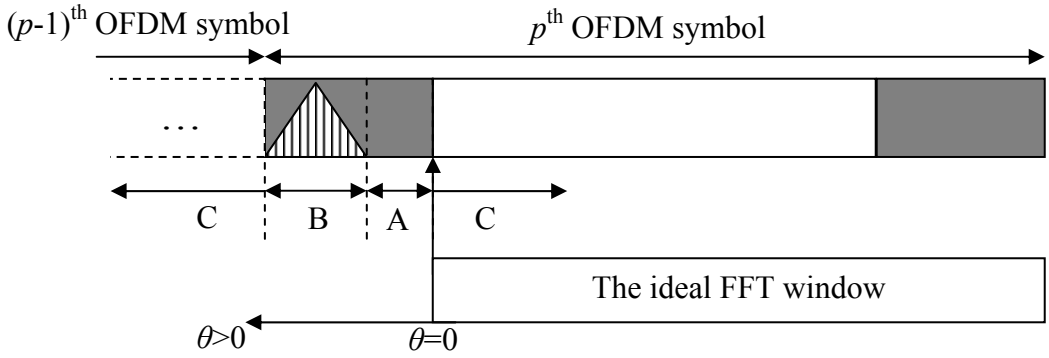

Figure 25 – Principle of frame synchronization

However, due to channel delay spread, noise and mismatch between transmitter and receiver oscillators, the ideal FFT window may not be found. Instead, a sample in one of the three regions, A, B, C, shown in Figure 25 is found.

If the FFT window starts in a point in region A, then we do not lose any data but the only effect is the rotation of data in the FFT window. Since this is a circular shift, the only effect in this case is a change in phase that increases with the subcarrier index according to [29]. This is given in (18)

$$y(k) = u(k)H(k)e^{-j2\pi k\frac{\theta}{N}} + \eta(k) \tag{18}$$

where θ is the shift from the ideal FFT window position in samples. This phase effect is indistinguishable from the channel frequency response and hence its compensation may be done with the compensation of the channel. Since there is no ISI induced in this region, it is called the ISI-free region.

If the FFT window starts from a sample in region B or C, the FFT window now contains samples from the adjacent OFDM symbols and the received symbols are described by [29],

$$y(k) = u(k)\frac{N-\theta}{N}H(k)e^{-j2\pi k\frac{\theta}{N}} + \eta(k) + \omega(k) \tag{19}$$

Due to ISI introduced by the channel, the symbol is not only rotated but also attenuated and extra noise $\omega(k)$ is injected since the orthogonality is disturbed. An approximation for the power of the extra noise is given in [29] as

$$\sigma_\omega \approx \sum_{i<\theta} |h(i)|^2 \, E\left\{|u(k)|^2\right\} \frac{2N+(\theta-i)}{N^2}(\theta-i), \quad \theta > 0 \tag{20}$$

In regions B and C, not only ISI is created but also ICI is created because the orthogonality is disturbed. Hence, our aim is to locate the start of the FFT window at the ISI-free region, namely, the region A. In this case, the elimination of the exponential term in (18) may be left to the channel estimator and equalizer.

4.2 Frame Synchronization Techniques in OFDM Systems

In this section we will review some frame synchronization techniques in the literature. They may also be referred as OFDM symbol synchronization because an OFDM symbol may be viewed as a frame of many complex samples. Also a frame of OFDM symbols is synchronized when the first OFDM symbol is correctly synchronized since the same reference may be used in the other OFDM symbols in that frame.

In [14], an m-sequence (maximal length shift register sequence) based synchronization is given. The idea behind this is to use the m-sequence as a marker to synchronize with the frame of OFDM symbols. At the transmitter, an m-sequence known by the receiver is summed up with the first OFDM symbol of the frame. At the receiver, the OFDM symbols and AWGN is treated as random data against known m-sequences due to the sharp correlation property of the m-sequence. The receiver correlates the received samples with the m-sequence and finds a sharp peak. The position of the peak gives the frame position. The advantage of this method is that it does not cause overhead provided that the receiver knows the right m-

sequence however, the power of the added m-sequence must be selected carefully not to distort the original OFDM symbol.

In [18], joint symbol frame synchronization and carrier frequency estimation are performed by investigating the loss of orthogonality between the subcarriers as a new trial for the frame start point is taken. A cost function which is minimized when the orthogonality condition is met is derived and a search for frame start point is done to minimize this cost. The location of the minima gives the frame start estimate and then the carrier offset is found. Although this method does not need any overhead, it is computationally demanding.

In [29], a method utilizing some pilot subcarriers to estimate the channel by interpolation is given. A cost function depending on the estimate of channel using an interpolation filter is derived and a search to find the minimum of this cost function is performed.

The methods above either need some special pilots assigned for synchronization, or suffer from high complexity or both the transmitter and receiver need to have the value of some sequences.

In the next two sections, we will introduce two methods which are widely referenced and need minimum amount of information about the environment or sequences.

4.2.1 The Maximum Likelihood (ML) Timing and Frequency Synchronization

In [21], ML estimation procedure for joint time and frequency synchronization is given for AWGN channels. The concept depends on the cyclic structure of the OFDM symbol and does not need any extra overhead.

Assuming that the channel is non-dispersive, the received symbol may be written as

$$y(k) = u(k-\theta)e^{j2\pi\varepsilon k/N} + \eta(k) \tag{21}$$

where θ is the sampling time offset and ε is the carrier frequency offset with AWGN at the background. Considering an observation interval of $2N+M$ samples of an OFDM frame, there are two parts I and I', that are different with only a noise factor as shown in Figure 26.

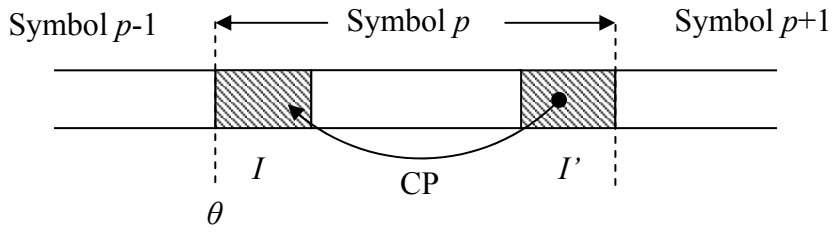

Figure 26 – The copies constituting the CP [21]

Since the noise is assumed to be AWGN, then we have the following relation after correlating the received samples

$$\forall k \in I: \quad E\left\{y(k)y^*(k+m)\right\} = \begin{cases} \sigma_y{}^2 + \sigma_\eta{}^2, & m = 0 \\ \sigma_y{}^2 e^{-j2\pi\varepsilon}, & m = N \\ 0, & \text{otherwise} \end{cases} \tag{22}$$

A log-likelihood function $\Lambda(\theta, \varepsilon)$ for θ and ε, is derived [21] to be as follows:

$$\Lambda(\theta,\varepsilon) = \left|\gamma(\theta)\right| \cos\left(2\pi\varepsilon + \angle\gamma(\theta)\right) - \rho\Phi(\theta) \tag{23}$$

where, $\angle$ represents the argument of a complex number and

$$\gamma(m) = \sum_{k=m}^{m+M-1} y(k)\, y^*(k+N) \tag{24}$$

$$\Phi(m) = \frac{1}{2} \sum_{k=m}^{m+M-1} \left|y(k)\right|^2 + \left|y(k+N)\right|^2 \tag{25}$$

$$\rho = \left| \frac{E\left\{ y(k)\, y^{*}(k+N) \right\}}{\sqrt{E\left\{ \left| y(k) \right|^{2} \right\} E\left\{ \left| y(k+N) \right|^{2} \right\}}} \right| = \frac{\sigma_{y}^{2}}{\sigma_{y}^{2} + \sigma_{\eta}^{2}} = \frac{\mathrm{SNR}}{\mathrm{SNR}+1} \tag{26}$$

Note that the metric to be maximized in (23) is composed of two parts, one being the correlation of samples $y(k) \in (I \cup I')$ and the second one is the energy of the correlated parts weighted by an SNR factor. The maximization of the metric in (23) for θ and ε gives the estimated timing offset and carrier frequency offset, respectively. When the maximization with respect to the frequency offset is done, we have

$$\hat{\varepsilon}_{ML}(\theta) = -\frac{1}{2} \angle \gamma(\theta) \tag{27}$$

At the optimum frequency offset, the metric turns out to be

$$\Lambda\left(\theta, \hat{\varepsilon}_{ML}(\theta)\right) = \left|\gamma(\theta)\right| - \rho \Phi(\theta) \tag{28}$$

and the optimum time and frequency offsets are found to be as

$$\hat{\theta}_{ML} = \arg\max_{\theta} \left\{ \left|\gamma(\theta)\right| - \rho \Phi(\theta) \right\} \tag{29}$$

$$\hat{\varepsilon}_{ML} = -\frac{1}{2} \angle \gamma\left(\hat{\theta}_{ML}\right) \tag{30}$$

The steps involved in ML synchronization algorithm are as follows:

1) Choose an observation interval to include at least one OFDM symbol.
2) Take the first *M*-sample window beginning from a sample in the observation interval.
3) Take the second *M*-sample window which starts from *N* samples away from the beginning of the first window.
4) Calculate the metric in (28)
5) Repeat steps 2, 3 and 4 for all the points in the observation interval.

6) Find the position of the maxima of the metric; this is the estimated symbol boundary.

A quantized metric to lower the complexity is given in [17] as

$$\Lambda_Q = \sum_{k=M}^{m+M-1} c(k)c^*(k+N) \tag{31}$$

where

$$c(k) = \mathrm{sgn}\left(\mathrm{Re}\{y(k)\}\right) + j\,\mathrm{sgn}\left(\mathrm{Im}\{y(k)\}\right) \tag{32}$$

Since the signs of the real and imaginary parts of the complex samples are used, the multiplications turn out to addition and subtractions.

Additionally, since CP is sent in all OFDM symbols throughout the frame, a metric averaging may be performed. In this way, the effect of noise variations is minimized but this needs a longer observation interval.

Simulations utilizing the ML timing synchronization procedure are performed with the parameters in Table 1 under both AWGN and Rayleigh fading channels assuming correct frequency synchronization. The correlation metrics for an AWGN channel are plotted in Figure 27, Figure 28 and Figure 29 for 0, 5 and 20 dB SNR, respectively.

The ML metric outputs a peak every time it finds a CP which is matched to the original copy in the observation interval. When the noise is added at the same power level with the signal, the metric may lead to wrong estimates. The difference between 0 dB metric and 5 dB metric is clear. In the 0 dB metric, the first and the third OFDM symbols are detected but the second OFDM symbol is missed. However, when the noise power is decreased, the correlation between the CP and the original part overcomes due to the uncorrelatedness of white noise samples. This can be clearly seen in Figure 29 where each OFDM symbol can easily be detected.

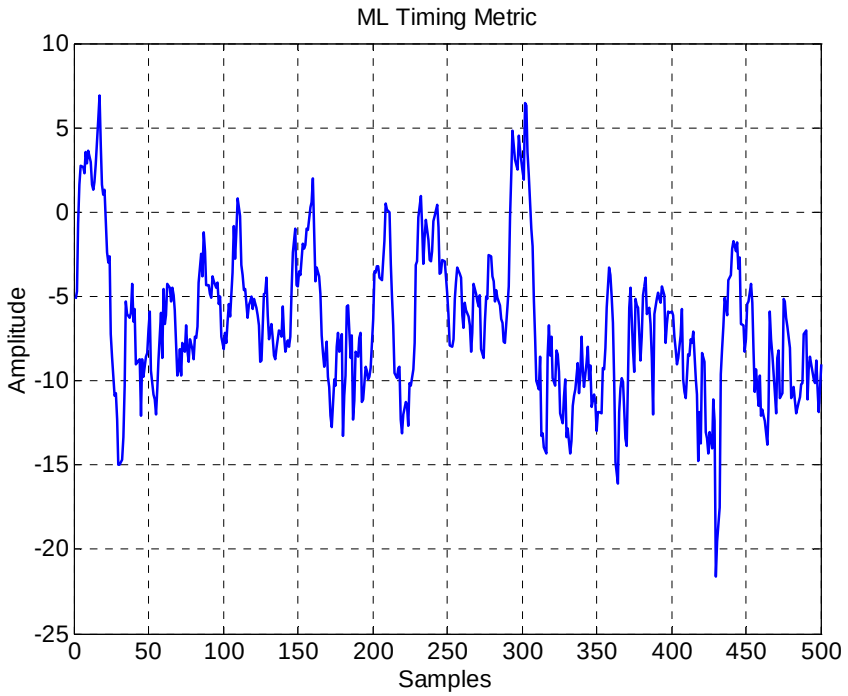

Figure 27 – ML timing metric under AWGN channel at 0 dB SNR

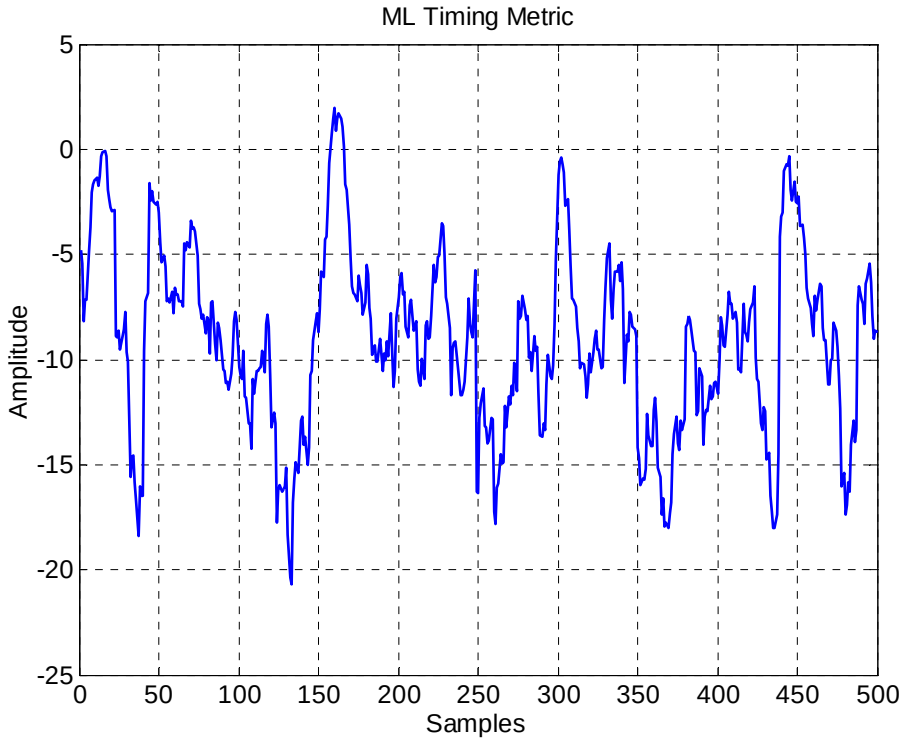

Figure 28 – ML timing metric under AWGN channel at 5 dB SNR

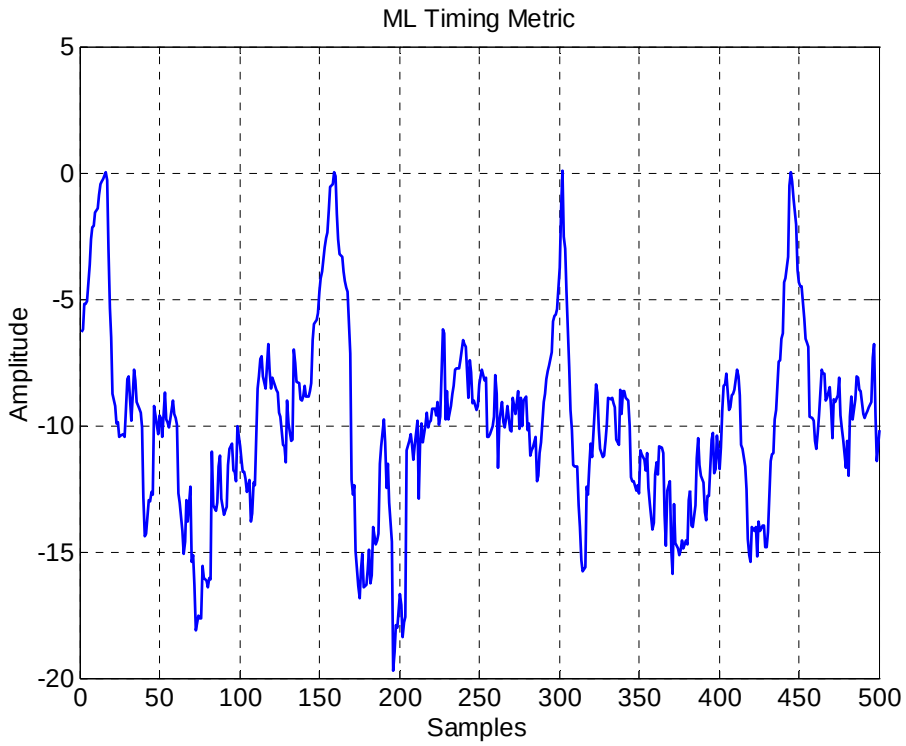

Figure 29 – ML timing metric under AWGN channel at 20 dB SNR

The peak amplitude of the metric at 20 dB SNR is about zero. This is because the correlation term in (24) is at the same time the average of the window energies which are calculated in (25) and ρ in (26) tends to 1. This is not the case for lower SNR, because the noise variations affect the metric so the correlation is not fully cancelled with the window energies.

Histogram of frame start estimates are shown in for 0 dB SNR in Figure 30, for 5 dB SNR in Figure 31 and for 20 dB SNR in Figure 32. As it can be seen from Figure 30, nearly 50 % of the trials resulted in success but it is worth noting that at the end of the OFDM symbol, the next symbol's CP and its match misleads the synchronizer and makes it skip the first symbol. As the noise power is lowered, the percentage of success increases and at 20 dB SNR, reaches nearly 100 %.

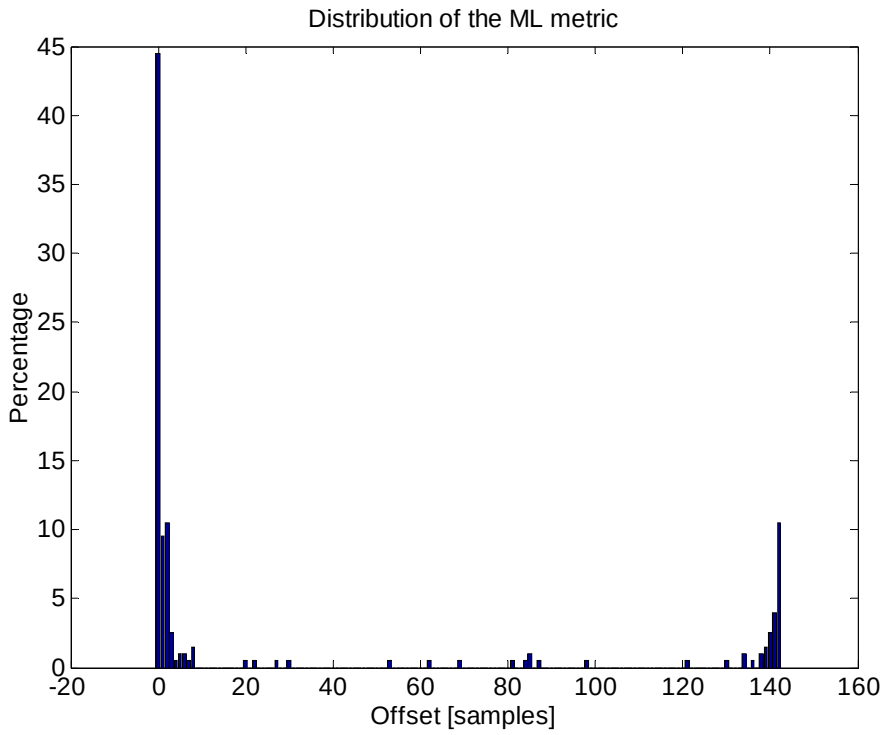

Figure 30 – Distribution of ML metric under AWGN channel at 0 dB SNR

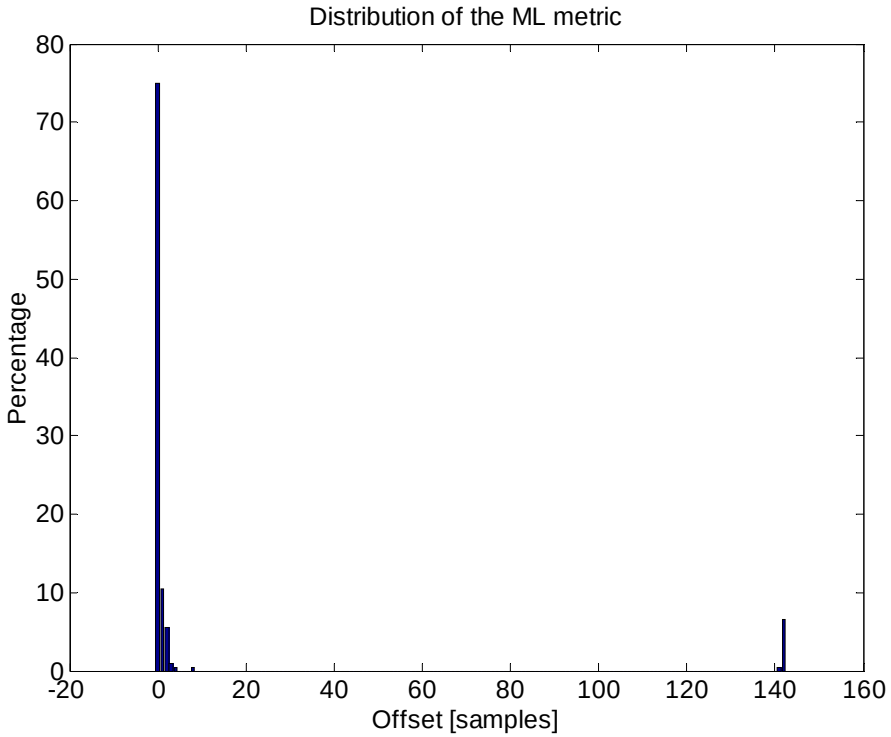

Figure 31 - Distribution of ML metric under AWGN channel at 5 dB SNR

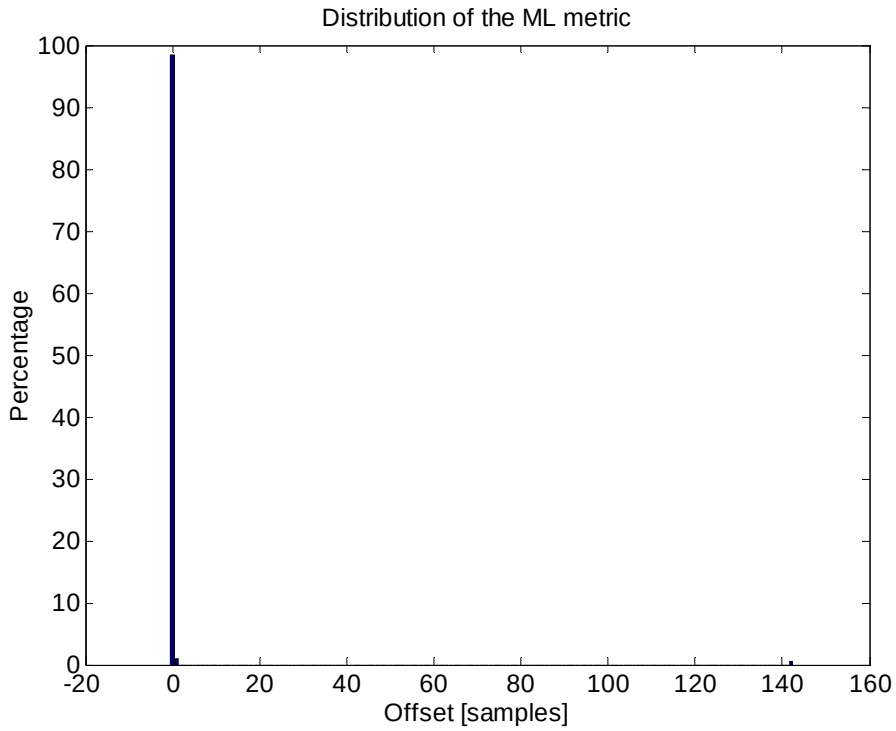

Figure 32 – Distribution of ML metric under AWGN channel at 20 dB SNR

The ML metric under 6th order Rayleigh fading channel are shown in Figure 33, Figure 34 and Figure 35 for 0, 5 and 20 dB SNR. The common characteristics of these figures are that the peaks are not sharp as they were in the AWGN case. Also, in the AWGN case the only correlated parts were the regions *I* and *I'* in Figure 26, however, the channel convolution relates one sample to the next *L* samples, *L* being the channel order, so the correlation property in (22) is disturbed. Especially, at 0 dB SNR, the symbol boundaries are insignificant. At 5 dB, boundaries are clearer but the peaks are not sharp. The maximum may be positioned anywhere in the channel impulse response residing at the cyclic prefix. At 20 dB, we see that the effective factor is not the noise but channel delay spread. A robust decision is hard, as the maximum may be positioned at a sample in region B shown in Figure 25.

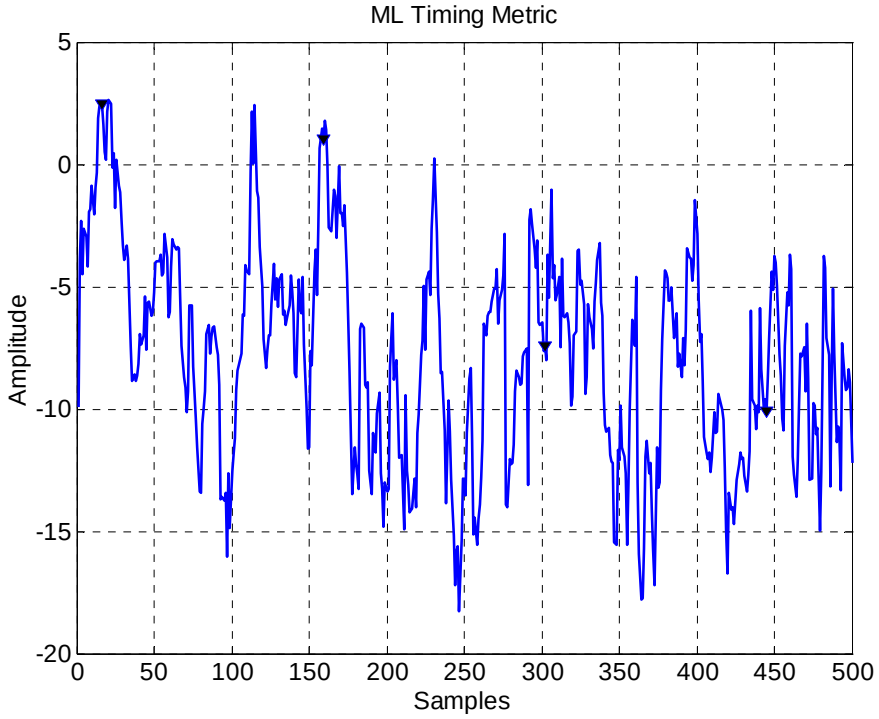

Figure 33 – ML timing metric under 6th order Rayleigh fading channel at 0 dB SNR. The triangle markers indicate the OFDM symbol boundaries.

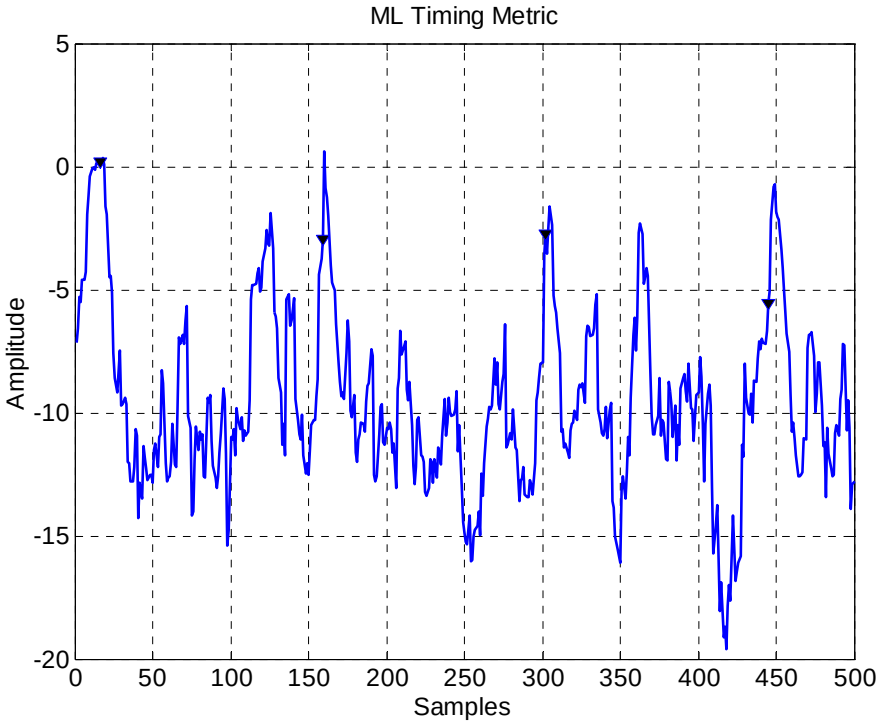

Figure 34 – ML timing metric under 6th order Rayleigh fading channel at 5 dB SNR. The triangle markers indicate the OFDM symbol boundaries.

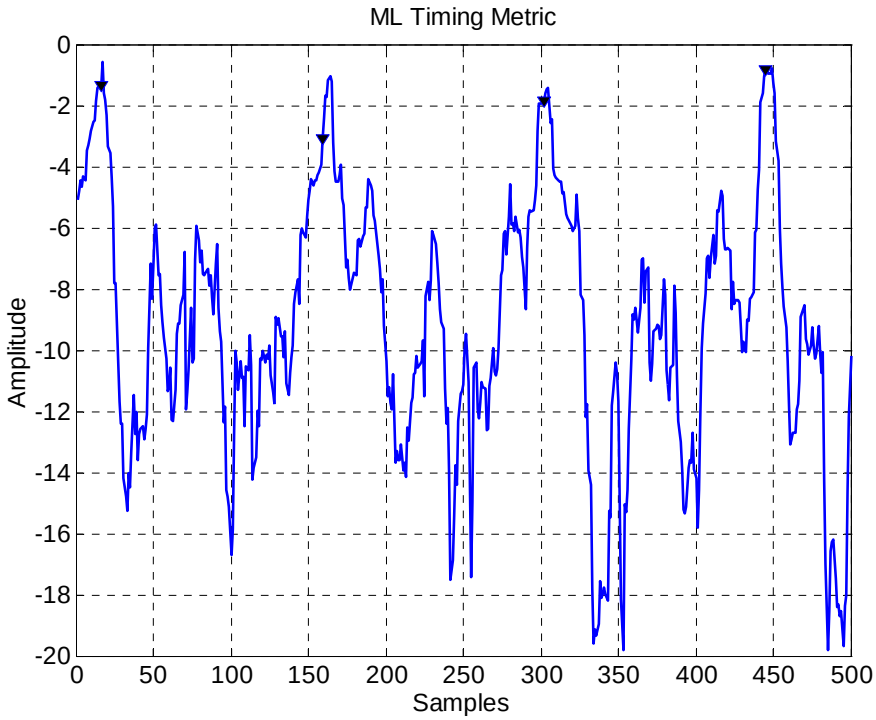

Figure 35 – ML timing metric under 6th order Rayleigh fading channel at 20 dB SNR. The triangle markers indicate the OFDM symbol boundaries.

The distribution of the ML metric for 0, 5 and 20 dB SNR under 6th order Rayleigh fading channel are shown in Figure 36, Figure 37 and Figure 38, respectively. In Figure 36, the effect of noise is clear with the variations in frame start estimates. As the SNR is increased, the variations are not so much but the channel affects the synchronizer by spreading the estimates. This is normal, since the metric gives peaks anywhere in region B. At 20 dB, the estimates are piled up into the region B. Thus, we can say that the ML estimator does not find the symbol boundary in the ISI-free region; however it locates the boundaries always in a portion of CP occupied by the channel, this corresponds to region B in Figure 25. So, if the channel length information is available, then the ML estimate may be shifted by the length of the channel to guarantee the ISI-free region. If channel length is unavailable or CP is not so long, then a fine synchronization using some training symbols must be done.

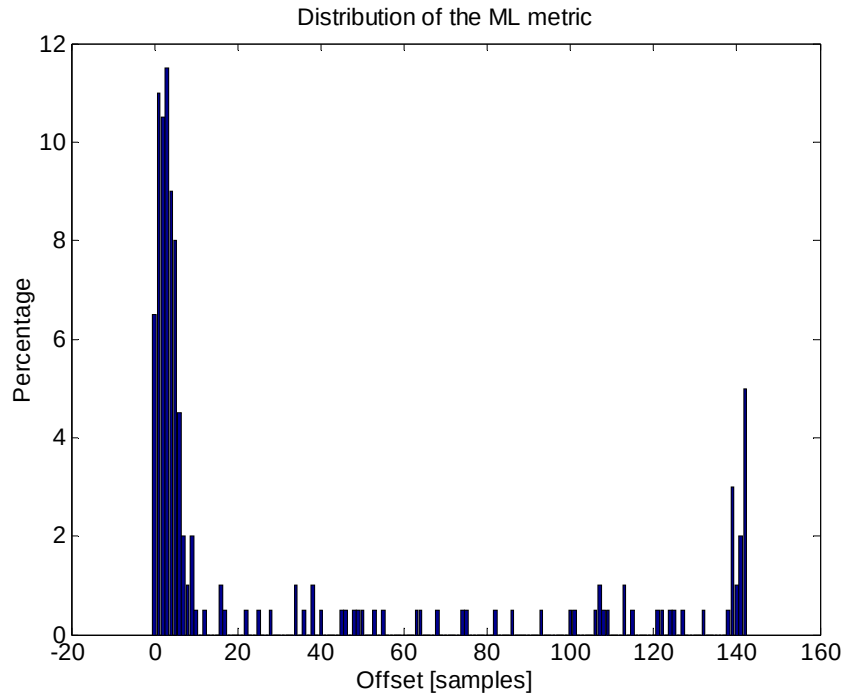

Figure 36 – Distribution of ML metric under 6th order Rayleigh fading channel at 0 dB SNR

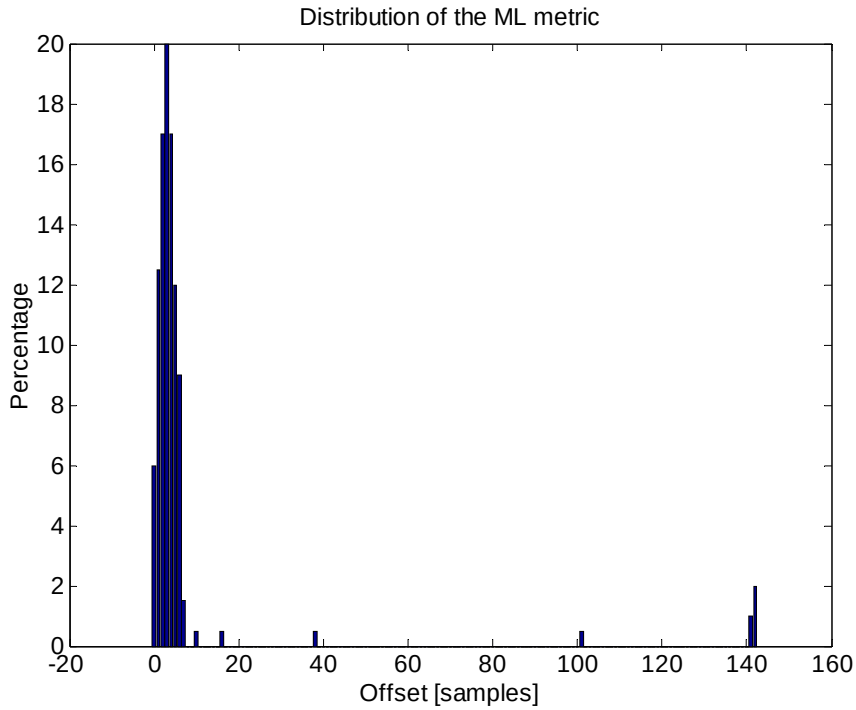

Figure 37 – Distribution of ML metric under 6th order Rayleigh fading channel at 5 dB SNR

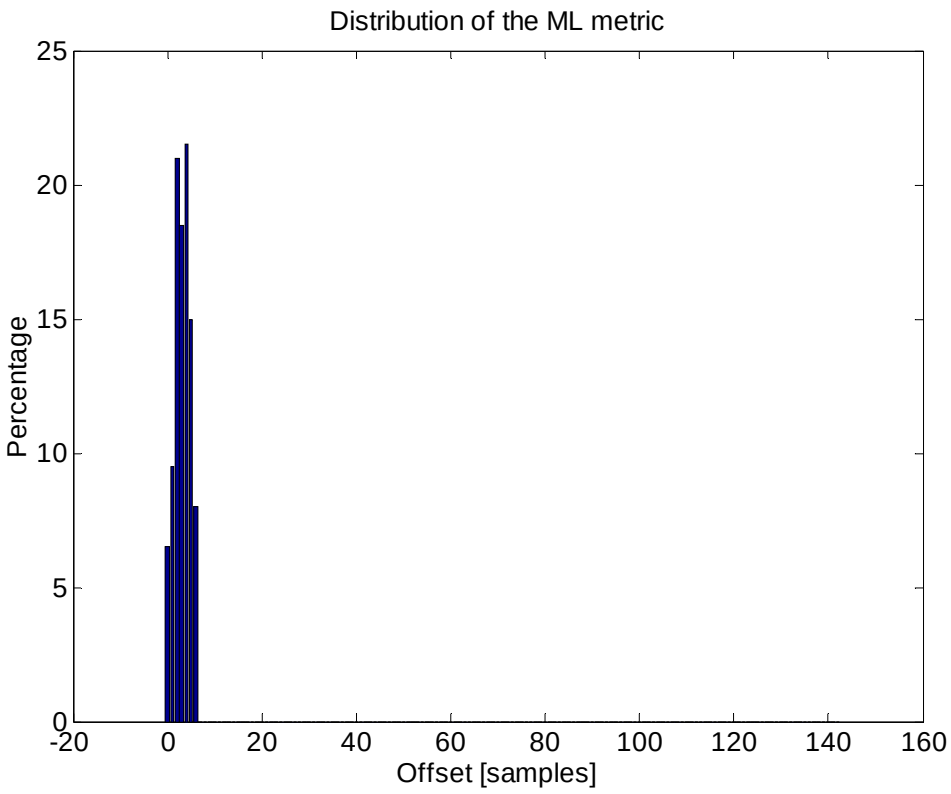

Figure 38 – Distribution of ML metric under 6th order Rayleigh fading channel at 20 dB SNR

The mean and variance of the ML synchronizer are given in Figure 39 and Figure 40, respectively. We see that the mean of the ML timing offset is constant after 10 dB SNR for the Rayleigh channel. When we look at the histograms given in Figure 36, Figure 37 and Figure 38 under multipath environment, we see that the estimator decides on samples that are within the channel impulse response and the amount of offset is determined by the channel delay spread [30]. Thus, we must be aware that the ML estimator, when used in dispersive channels, points to a sample which is not ISI-free. Hence, one can use this estimator for coarse symbol synchronization and may utilize some more operations for fine synchronization. There are many papers where this idea is considered ([11], [13], [16], [19], [29]). Usually some pilots or training sequences, in either time or frequency domains, are used to fine tune the synchronizer.

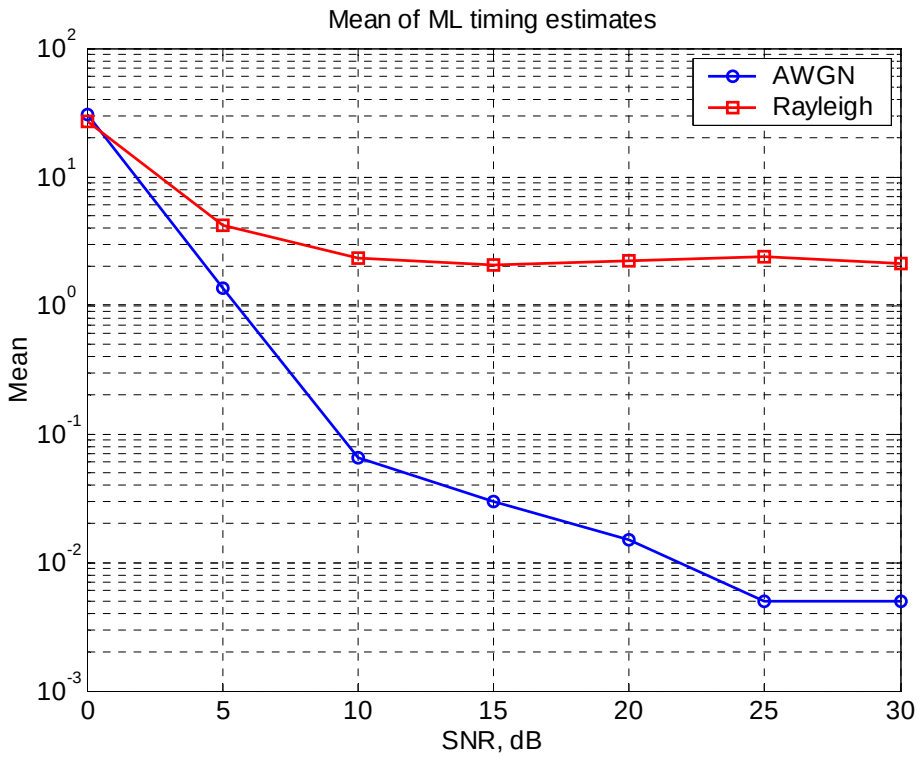

Figure 39 – Mean of ML timing offset

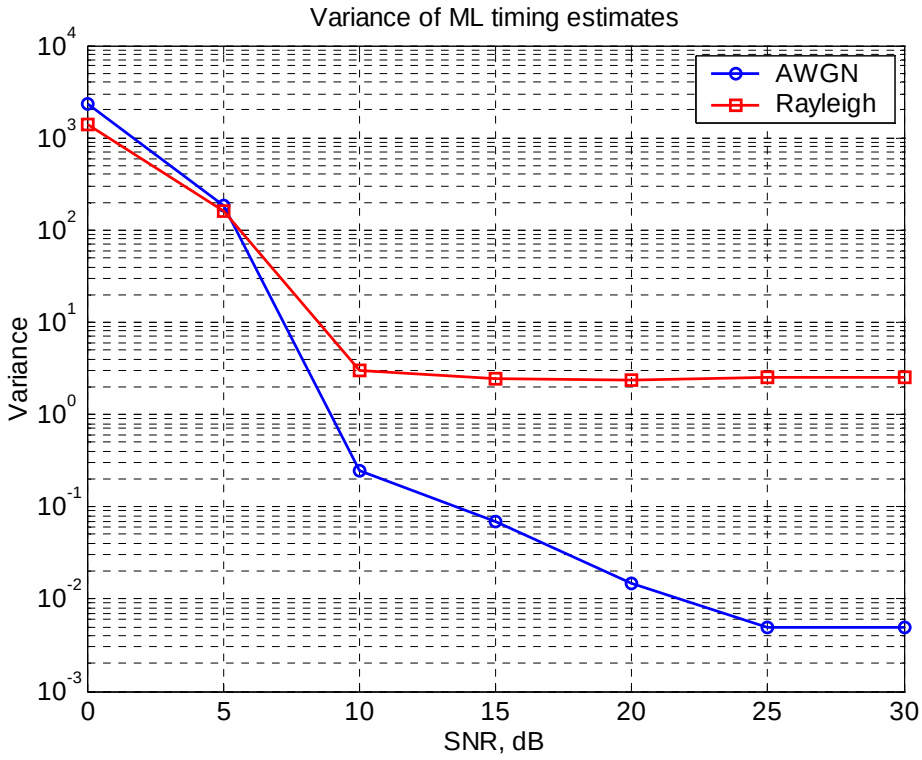

Figure 40 – Variance of ML timing offset

4.2.2 Robust Timing Synchronization

In [15], Schmidl and Cox proposes a robust timing synchronizer (hereafter called as *SC*) encouraging the use of an OFDM symbol for time synchronization. The idea in [15] relies on transmitting a special symbol which contains two identical halves shown in Figure 41.

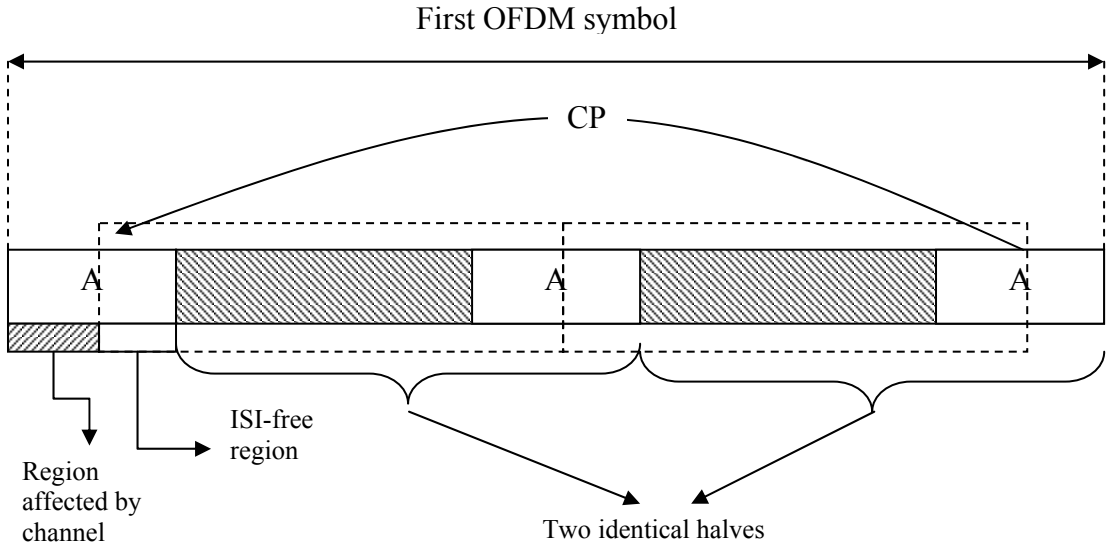

Figure 41 – Symbol used in [15] for time synchronization

The generation of a symbol with two identical halves may be achieved by transmitting a pseudonoise (PN) on even numbered subcarriers and to send zero on the odd subcarriers [15]. Since data may be assumed random, then even subcarriers may hold data, thus only half of the subcarriers are left unutilized. Then, as the normal OFDM procedure, CP is inserted and applied to the channel.

At the receiver, two consecutive windows of length *K*, half of the number of subcarriers, are correlated (33) and the energy of the second window is calculated (34) to be used in a timing metric given in (35).

$$P(d) = \sum_{m=0}^{K-1} y_{d+m}^{*} y_{d+m+K} \tag{33}$$

$$R(d) = \sum_{m=0}^{K-1} \left| y_{d+m+K} \right|^2 \tag{34}$$

$$M(d) = \frac{\left| P(d) \right|^2}{\left(R(d) \right)^2} \tag{35}$$

A noise free SC timing metric is shown in Figure 42 where the vertical lines enclose the ISI-free region. The position of the dashed rectangles in Figure 41 yields the metric value at the beginning of the ISI-free region, shown as the line at the left in Figure 42. As the windows slide synchronously to the end of CP, the metric remains constant at 1. This is due that, as long as the samples are free from ISI and noise, the numerator and the denominator in (35) are the same.

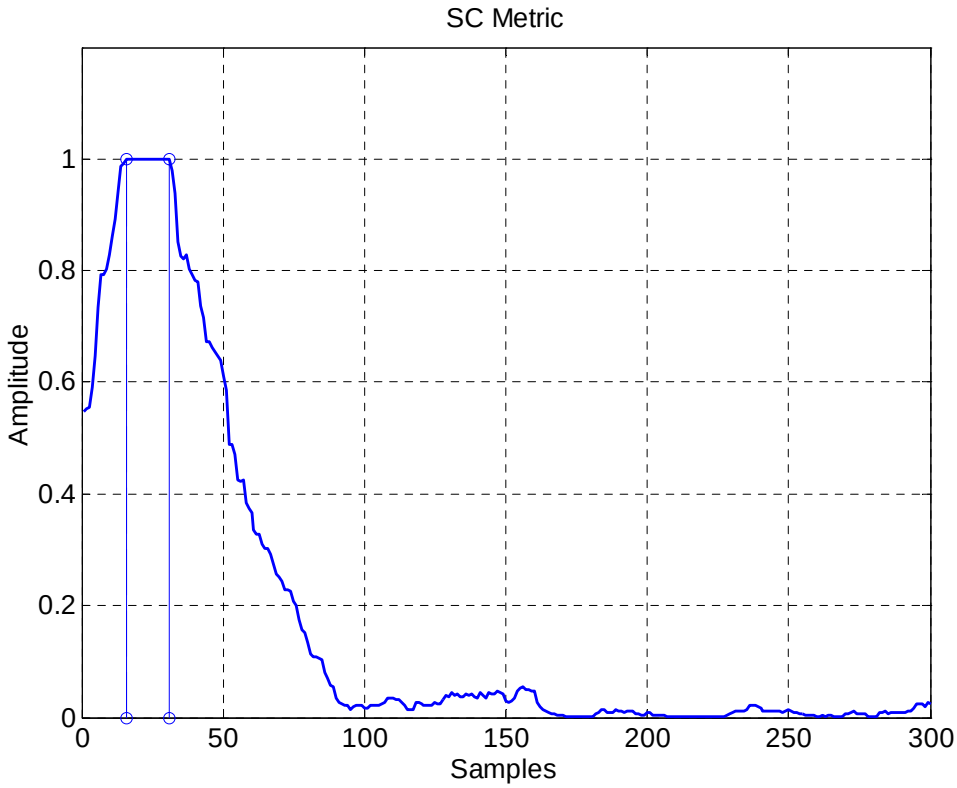

Figure 42 – Noise free SC timing metric

To summarize, the SC synchronization algorithm is given as follows:

1) At the transmitter, even numbered subcarriers are modulated with a PN sequence whereas the odd numbered subcarriers are left as zero.

2) At the receiver, an observation interval including one complete OFDM symbol is selected

3) Starting from a sample d in the observation interval, two adjacent windows with length $K = N / 2$ with N being the size of FFT are taken

4) Windows are cross-correlated to calculate the $P(d)$ in (33).

5) The energy of the second window $R(d)$ is calculated as in (34).

6) The metric $M(d)$ is calculated as in (35).

7) The windows are shifted by one sample and steps 3, 4, 5 and 6 are repeated for all samples in the selected observation interval.

8) The flat part of the metric is found as the ISI-free region and a sample from this region is selected as the symbol boundary.

The SC timing metrics for AWGN channel are shown in Figure 43, Figure 44 and Figure 45 for 0, 5 and 20 dB SNR.

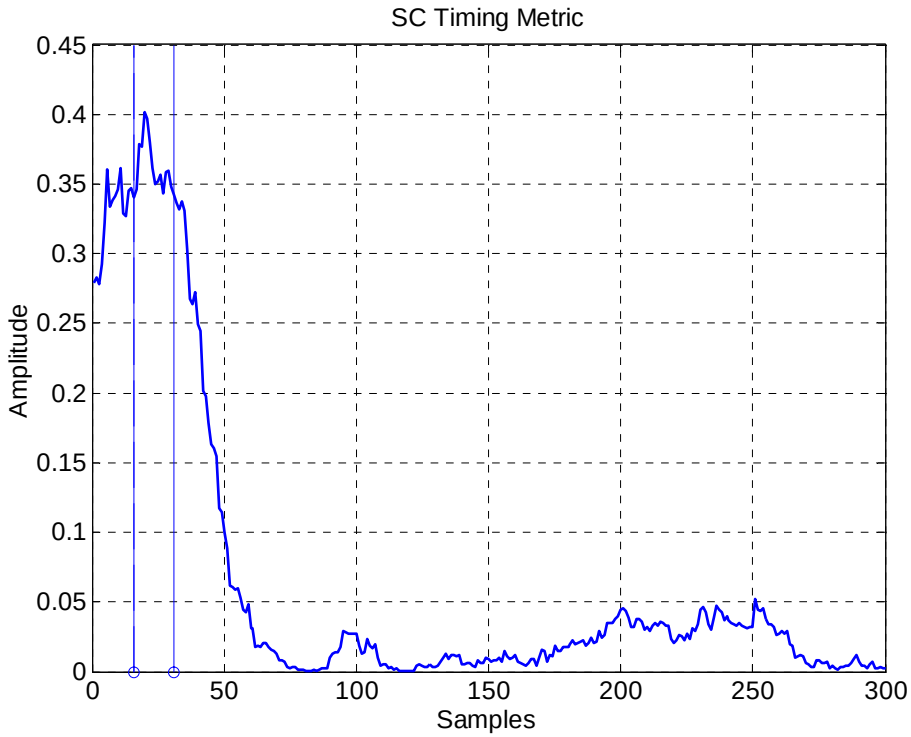

Figure 43 – SC timing metric under AWGN channel at 0 dB SNR.

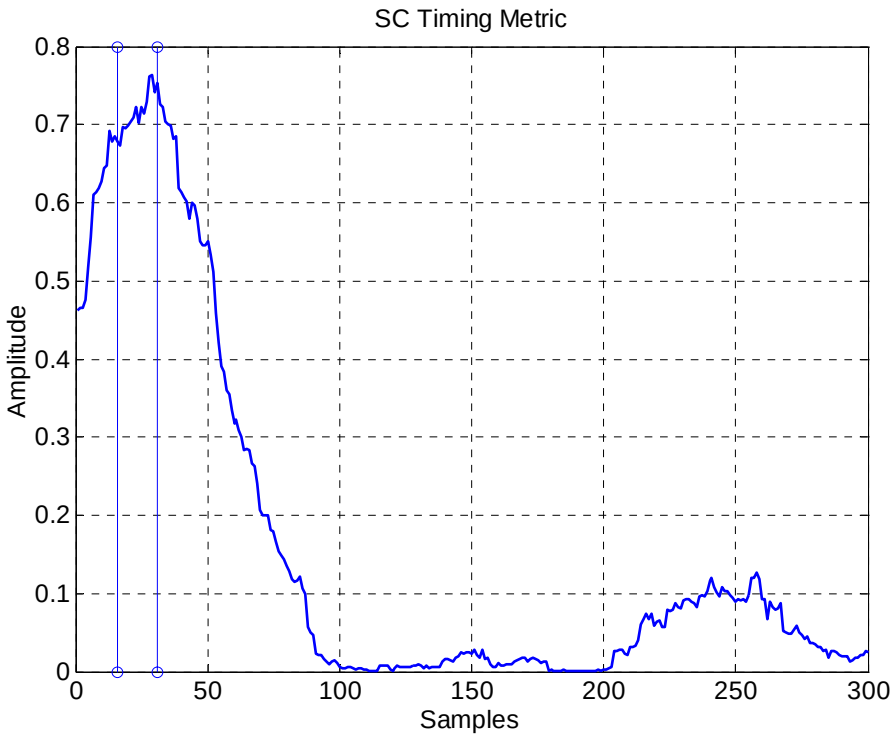

Figure 44 – SC timing metric under AWGN channel at 5 dB SNR.

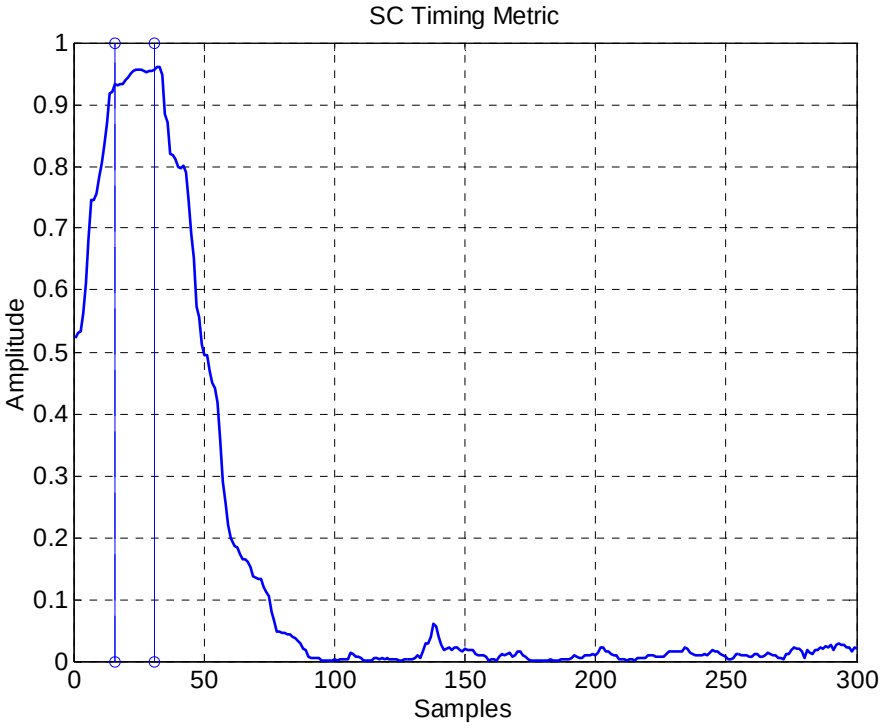

Figure 45 – SC timing metric under AWGN channel at 20 dB SNR

As it can be seen from Figure 43 and Figure 44 due to noise variations, the plateau is not obtained. At low SNR, a decision on a sample in the ISI-free region may be misleading and may cause to fall into regions B and C of Figure 25. However at high SNR, to locate a sample in ISI-free region is easier since the metric variation in this region is less and the metric value is higher than any other part of the metric.

The distribution of the SC metric is given in Figure 46, Figure 47 and Figure 48 under AWGN channel at 0, 5 and 20 dB SNR, respectively.

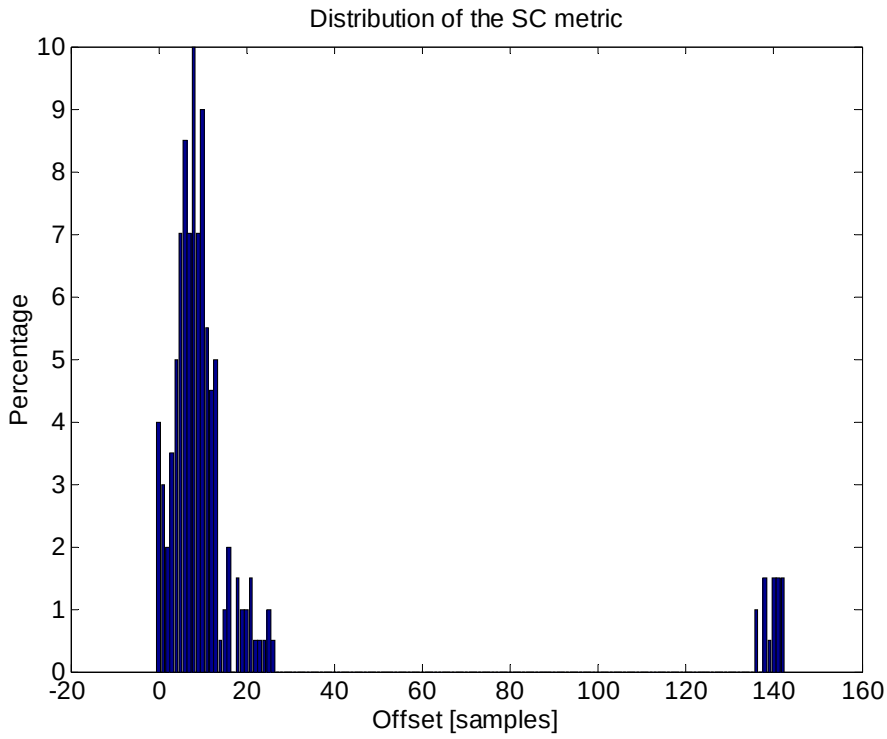

Figure 46 – Distribution of the SC metric under AWGN channel at 0 dB SNR

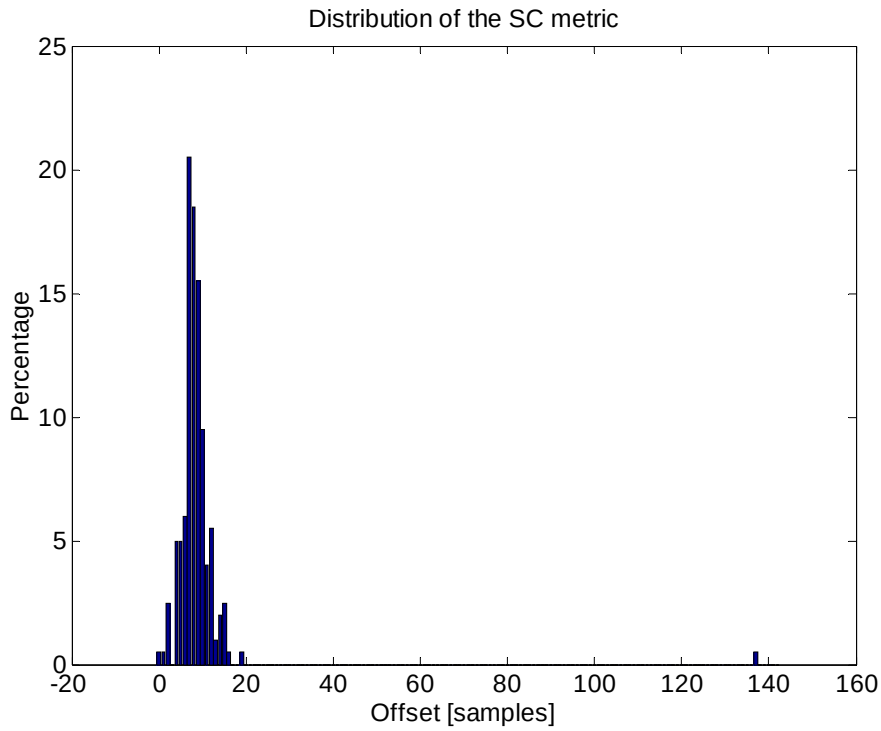

Figure 47 – Distribution of the SC metric under AWGN channel at 5 dB SNR

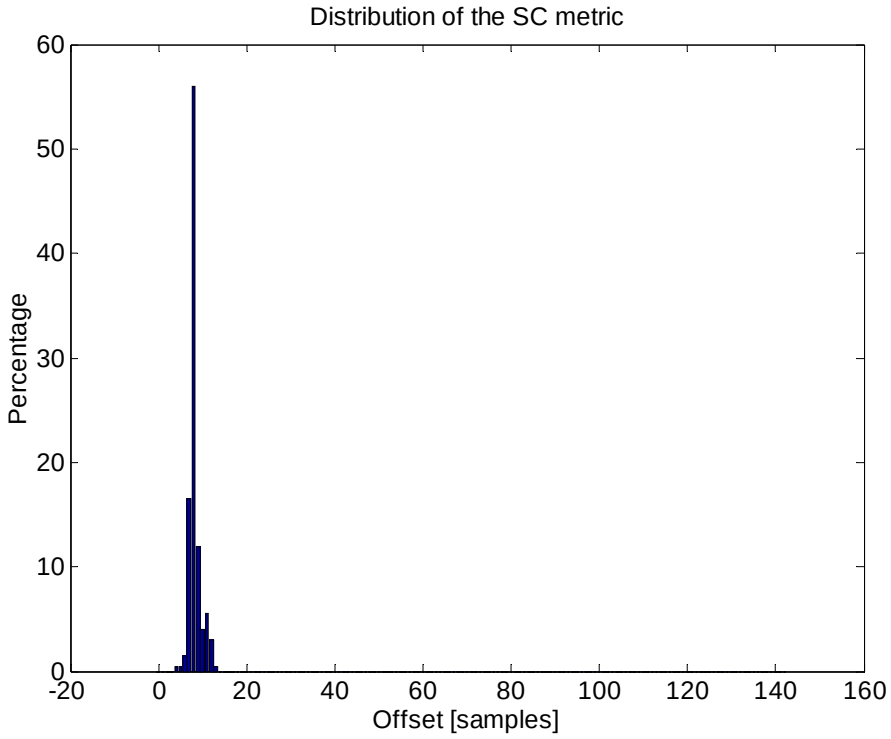

Figure 48 – Distribution of the SC metric under AWGN channel at 20 dB SNR

In Figure 46, variety of frame start estimates are observed. The noise has the same power with the signal and by misleading the estimator causes ISI. Note that the samples at the end of the symbol are also selected as frame start. If the second OFDM symbol's CP is included in the first window and the end of the second symbol is included in the second window, regarding the noise, such estimates occur. As the noise power is decreased, the estimates are located in the CP with higher percentage. However, the detection in the ISI-free region is fully accomplished at 20 dB SNR. Table 2 lists the histogram given in Figure 48 and we see from the table that all the estimates are found in the ISI-free region.

Next, Figure 49, Figure 50 and Figure 51 show the SC metric in the Rayleigh fading channel.

Table 2 – Listing of Figure 48

	ISI-free region														Data							
Offset	0	1	2	3	4	5	6	7	8	9	10	11	12	13	14	15	16	17	18	19	20	21	22
#	0	0	0	0	1	1	3	33	112	24	8	11	6	1	0	0	0	0	0	0	0	0	0

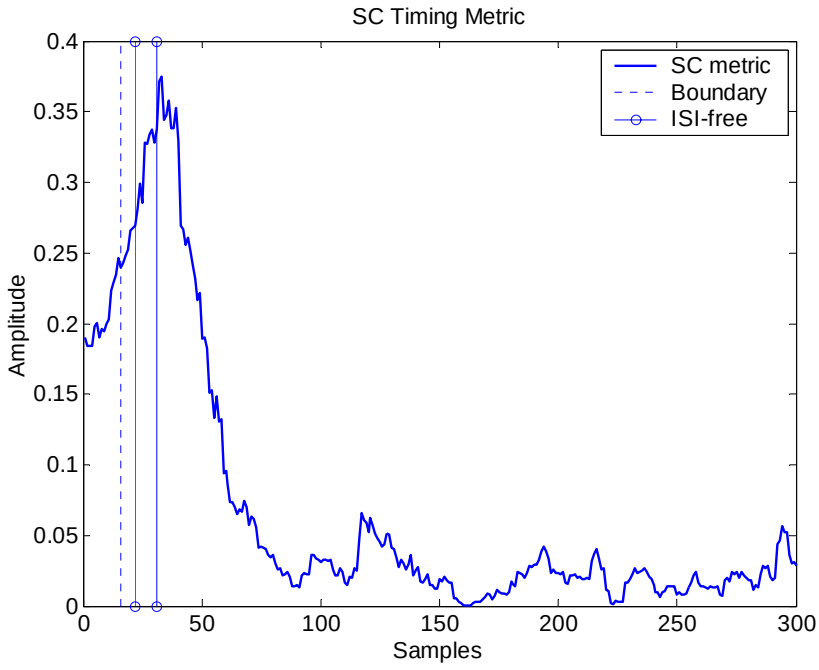

Figure 49 – SC timing metric under 6th order Rayleigh fading channel at 0 dB SNR

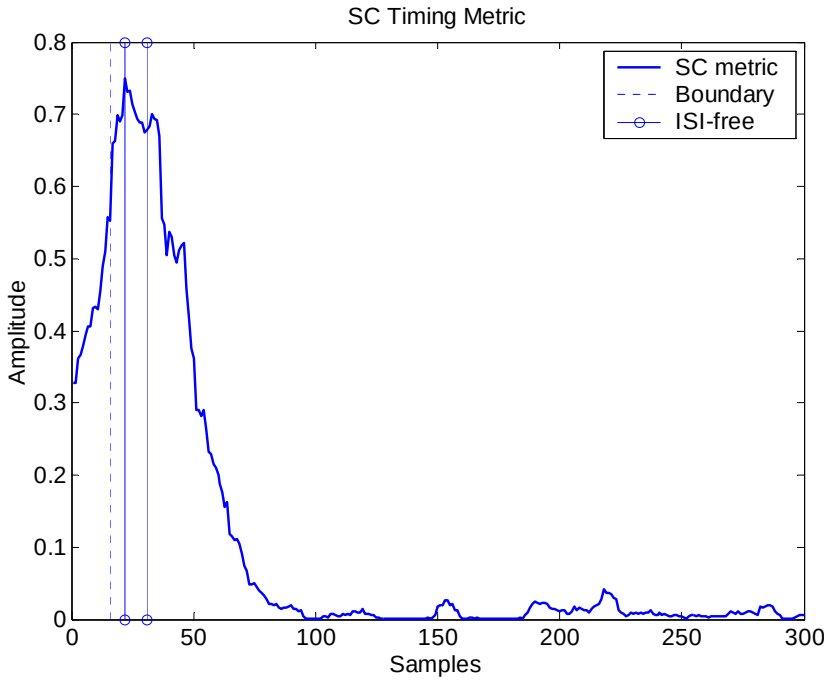

Figure 50 – SC timing metric under 6th order Rayleigh fading channel at 5 dB SNR

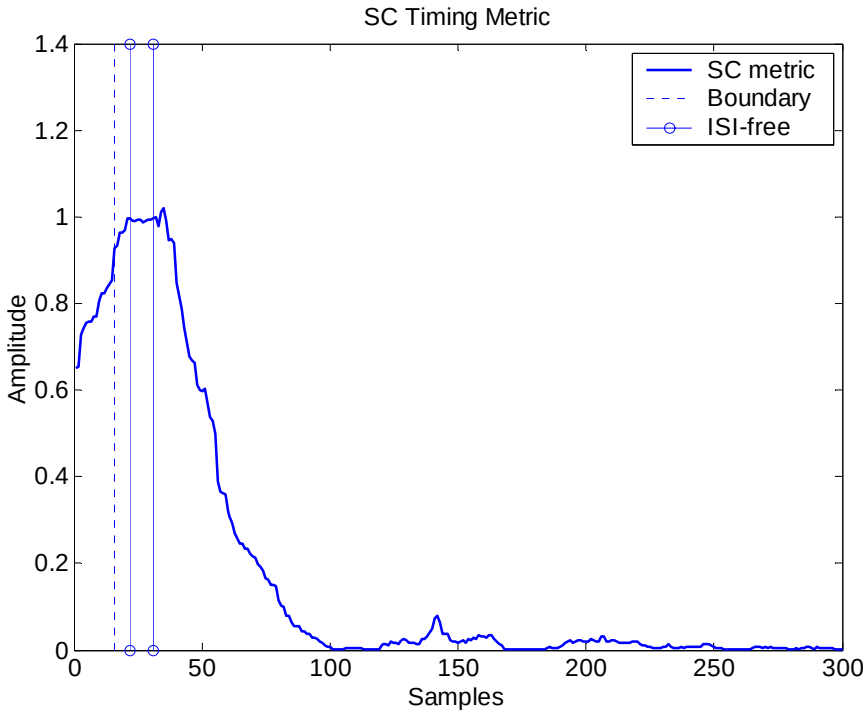

Figure 51 – SC timing metric under 6th order Rayleigh fading channel at 20 dB SNR

It seen from Figure 49 and Figure 50 that noise degrades the performance by inserting too much variation on the metric, but in the high SNR case shown in Figure 51, the SC metric stays constant in the ISI-free region. However, due to channel's spread, a peak is observed at the end of the ISI-free region which may lead to wrong estimates.

The distribution of the SC timing metric under 6th order Rayleigh fading channel is shown in Figure 52, Figure 53 and Figure 54 for 0, 5 and 20 dB SNR.

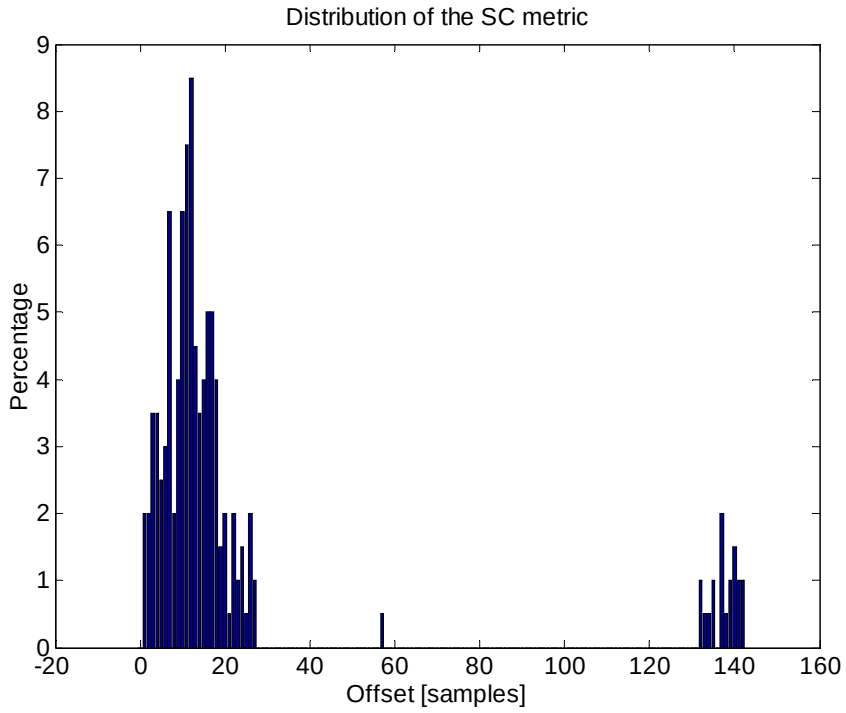

Figure 52 – Distribution of SC metric under 6th order Rayleigh fading channel at 0 dB SNR

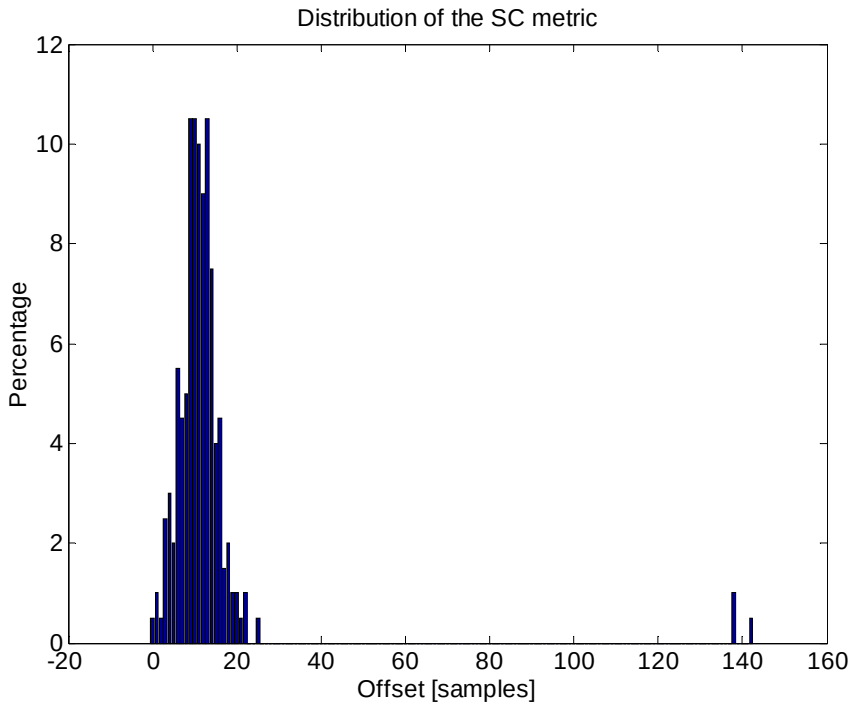

Figure 53 – Distribution of SC metric under 6th order Rayleigh fading channel at 5 dB SNR

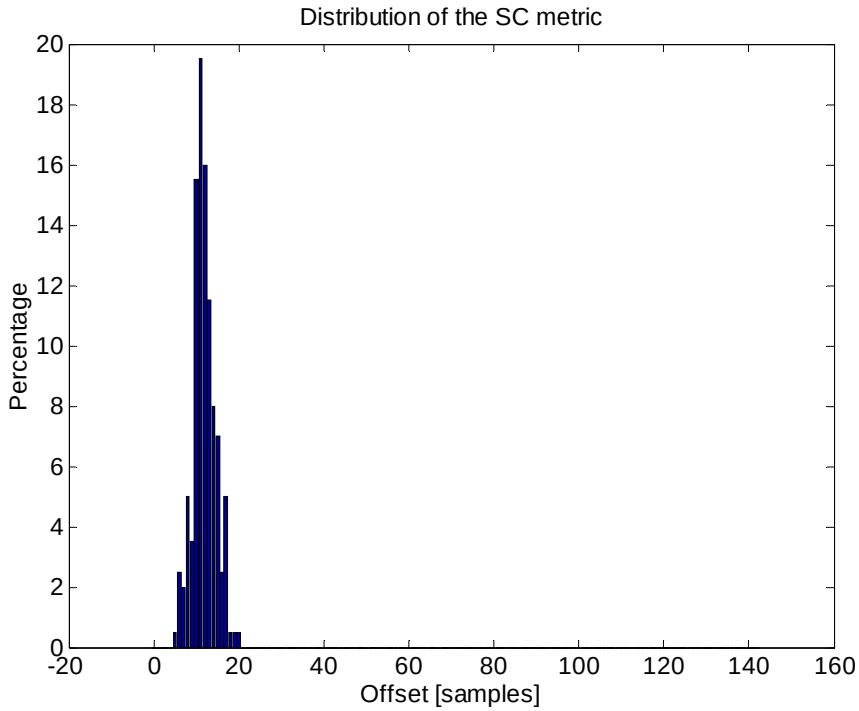

Figure 54 – Distribution of SC metric under 6th order Rayleigh fading channel at 20 dB SNR

In Figure 52 and Figure 53, it is seen that samples in the second OFDM symbol are also detected as the frame start as in the case of AWGN channel. In Figure 54, we see that all estimates are grouped at the start of frame but some estimates are found out of the ISI-free region as shown in Table 3. Channel's spread causes the estimation of frame start out of the ISI-free region in which data from the second symbol interfere with the first symbol.

Table 3 – Listing of Figure 54

	Occupied by channel memory						ISI-free region									Data							
Offset	0	1	2	3	4	5	6	7	8	9	10	11	12	13	14	15	16	17	18	19	20	21	22
#	0	0	0	0	0	1	5	4	10	7	31	39	32	23	16	14	5	10	1	1	1	0	0

When we compare the ML and SC methods, we see that ML method does not need any extra symbol for synchronization, whereas the SC method needs a special symbol at the beginning of the frame. This means that ML method is more efficient in transmission time. Additionally, since ML method uses the periodicity in the OFDM symbol, one can average the ML metric over a number of symbols for better performance especially in noisy and multipath channels. On the other hand, with the SC metric, averaging is not possible since the synchronization symbol is sent only once in a frame.

A good point in SC metric is that the metric finds a region rather than a peak as in the case with the ML estimator and we are sure that any point in that region leads us to an ISI-free solution. Thus no offset or fine check is needed. However, noise makes the detection of that region harder, but the peaks can easily be detected even in a noisy environment. This is the reason why ML estimator outperforms the SC estimator.

As the channel length is increased, the peaks of ML estimator become wider whereas the ISI-free region of the SC metric becomes narrower. Thus, the metric optimization in SC estimation turns out to finding maxima instead of searching for a flat region. In this case, maximization of SC metric is easier.

However, in both methods, the channel length information is necessary. ML estimation points to a sample which is in the delay spread of channel so shifting the estimate is needed. For the SC case, the length of the flat region and thus the correct optimization depends on the channel length.

4.3 Channel Estimation

We have previously pointed that, the effect of channel at the output of the system is to scale the input with a complex factor. Hence, if we know the information on the subcarriers sent, we can estimate the channel frequency response by observing the receiver output after the FFT demodulation. In case of perfect synchronization, this can be formulated as

$$\begin{aligned} y(k) &= H(k)b(k) + \eta(k), \\ \frac{y(k)}{b(k)} &= H(k) + \frac{\eta(k)}{b(k)} \end{aligned} \tag{36}$$

where, $b(k)$ are the known data on the subcarriers. Usually $b(k)$ are selected from the set $B = \{-1, +1\}$ not to amplify the noise while estimating the channel [2]. Moreover, some standards boost these pilots for more accurate estimations [5]. However, this must be done carefully not to cause distortion in the signal [30].

Note that (36) is valid under perfect synchronization. In this case, the frame synchronization algorithm has found the start of OFDM symbol and after removal of the CP; the FFT window is free from ISI. In the non-ideal case, the synchronization algorithms usually find a point inside the CP. As long as this point resides at the ISI-free region, namely region A in Figure 25, the CP may be removed from the end of the symbol and again an ISI-free FFT window is obtained. In this case, the relation between the input and the output of the system is given as (18) and the channel estimate $\hat{H}(k)$ which is found using the p^{th} OFDM symbol is given as

$$y_p(k) = H(k)e^{-j2\pi k\frac{\theta}{N}}b(k) + \eta_p(k)$$
$$\frac{y_p(k)}{b(k)} = H(k)e^{-j2\pi k\frac{\theta}{N}} + \frac{\eta_p(k)}{b(k)} = \hat{H}(k) \tag{37}$$

where θ is the time offset in samples from the start of the ideal FFT window. From (37), we see that the estimate of the channel frequency response is the rotated version of the original channel plus the channel estimation error which is the scaled version of the noise on the known OFDM symbol, $\zeta(k) = \eta_p(k)/b(k)$. The rotation effect is unimportant, since all the symbols, hence the frame will be aligned with the same time offset and any subcarrier in the symbol will suffer the same exponential coefficient. In this case, the received samples on the subcarriers of the q^{th} OFDM symbol can be written as

$$y_q(k) = H(k)e^{-j2\pi k\frac{\theta}{N}}u_q(k) + \eta_q(k) \tag{38}$$

If we divide each sample on the subcarriers with the corresponding estimate for the channel frequency response, we have

$$\hat{u}_q(k) = \frac{H(k)e^{-j2\pi k\frac{\theta}{N}}u_q(k) + \eta_q(k)}{H(k)e^{-j2\pi k\frac{\theta}{N}} + \zeta(k)} \tag{39}$$

where $\eta_q(k)$ and $\zeta(k)$ are from different realizations.

To see the error on the subcarriers clearly we add and subtract $u_q(k)\zeta(k)$ term to the numerator of (39) and rearrange to obtain

$$\hat{u}_q(k) = \frac{H(k)e^{-j2\pi k\frac{\theta}{N}}u_q(k) + u_q(k)\zeta(k) - u_q(k)\zeta(k) + \eta_q(k)}{H(k)e^{-j2\pi k\frac{\theta}{N}} + \zeta(k)}$$

$$\hat{u}_q(k) = u_q(k) + \frac{\eta_q(k) - u_q(k)\zeta(k)}{H(k)e^{-j2\pi k\frac{\theta}{N}} + \zeta(k)} \tag{40}$$

The second term in (40) is the noise introduced when the estimated channel frequency response is used for equalization. Thus, we can conclude that: 1) The error on each subcarrier depends on the observation noise, the transmitted samples on the

subcarriers, the channel frequency response and channel estimation error. 2) Even the channel is perfectly known, if the coefficients of the channel frequency response are smaller than 1, the noise is amplified at the receiver.

We will show the simulations on channel estimation in the next chapter where we have used the training symbols of the IEEE 802.11a frame structure.

CHAPTER 5

SYNCHRONIZATION APPLICATIONS IN THE IEEE 802.11a STANDARD

802.11 is a collection of standards for WLANs developed by a working group of the IEEE. It applies to WLANs and provides 1 or 2 Mbps transmission in the 2.4 GHz band using either frequency hopping spread spectrum (FHSS) or direct sequence spread spectrum (DSSS) [31].

IEEE 802.11a [2] is an extension of the 802.11 and provides up to 54 Mbps data rate in the 5 GHz band. Unlike 802.11, 802.11a uses OFDM as the modulation scheme. The counterpart of this standard is the HIPERLAN/2 [3] which is used in Europe.

In this chapter, we will first introduce the IEEE 802.11a standard. The frame structure of the OFDM symbols and timing parameters will be given. Then the synchronization technique of 802.11a is given and at the last part, comparison of the previously mentioned techniques with the technique used in 802.11a is done.

5.1 The 802.11a Standard

The 802.11a standard supports a variety of bit-rates by employing different combinations of constellations and coding rates. Table 4 lists the needed constellation and coding rate to achieve a given data rate.

An 802.11a frame consists of a variable number of OFDM symbols. The frame includes a PREAMBLE field, which contains the synchronization and channel estimation headers, a SIGNAL field, which carriers the information about the data rate and the length of the frame, and the DATA field in which the information symbols are sent. In the preamble 10 short and 2 long symbols are transmitted. These

symbols are predefined and also known by the receiver. The signal field is a single OFDM symbol defining the data rate and the number of data octets in transmission. The data field contains variable number of OFDM symbols. The frame structure is given in Table 5.

Table 4 – Achievable data rates

Data rate (Mbps)	**Modulation**	**Coding rate**	**Data bits per OFDM symbol**
6	BPSK	1/2	24
9	BPSK	3/4	36
12	QPSK	1/2	48
18	QPSK	3/4	72
24	16-QAM	1/2	96
36	16-QAM	3/4	144
48	64-QAM	2/3	192
54	64-QAM	3/4	216

Table 5 - The 802.11a frame structure

802.11a frame		
PREAMBLE	SIGNAL	DATA
12 symbols (10 short, 2 long symbols)	One OFDM symbol	Variable number of symbols
Fixed data	BPSK modulated, r = ½	Rate and number of symbols are indicated in SIGNAL

In an OFDM symbol, 52 subcarriers are employed. 48 of them are used for data and 4 of them are used as pilots. The subcarriers are numbered from -26 to 26. The 0^{th} subcarrier is sent as zero and the subcarriers -21, -7, 7 and 21 are used as pilots. The timing parameters are listed in Table 6.

Table 6 – Timing parameters [2]

Parameter	***Value***
Δ_F: Subcarrier frequency spacing	0.3125 MHz (=20 MHz/64)
T_{FFT}: IFFT / FFT period	3.2 μs ($1 / \Delta_F$)
$T_{PREAMBLE}$: Preamble duration	16 μs ($T_{SHORT} + T_{LONG}$)
T_{SIGNAL}: Duration of the SIGNAL BPSK-OFDM symbol	4 μs ($T_{GI} + T_{FFT}$)
T_{GI}: Guard interval duration	0.8 μs ($T_{FFT} / 4$)
T_{GI2}: Training symbol guard interval duration	1.6 μs ($T_{FFT} / 2$)
T_{SYM}: Symbol interval	4 μs ($T_{GI} + T_{FFT}$)
T_{SHORT}: Short training sequence duration	8 μs ($10 \times T_{FFT} / 4$)
T_{LONG}: Long training sequence duration	8 μs ($T_{GI2} + 2 \times T_{FFT}$)

From Table 6, the parameters of the OFDM symbols in terms of subcarriers and samples are derived in Table 7.

Table 7 – OFDM symbol parameters

Parameter	***Value***
Number of data subcarriers in an OFDM symbol	48
Number of pilot subcarriers in an OFDM symbol	4
Number of total subcarriers in an OFDM symbol	52
Size of FFT window, *N*	64
Length of Cyclic-Prefix, *M*	16

The fields in a frame are shown in Figure 55 with timings and their usage is listed in Table 8.

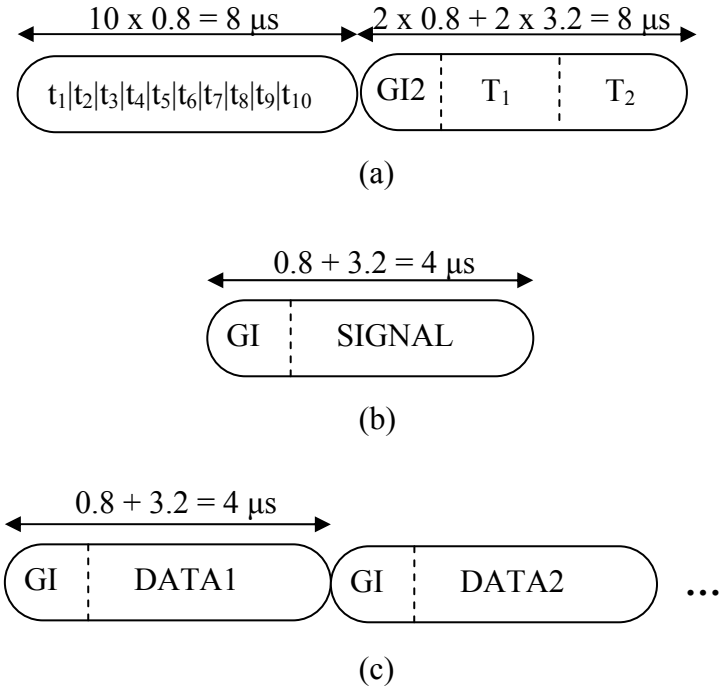

Figure 55 – The fields in the 802.11a frame structure; a) Preamble, b) Signal, c) Data

Table 8 – Usage of fields in 802.11a frame

Field	***Usage***
Short symbols $t_1 - t_7$	Signal detection and AGC
Short symbols $t_8 - t_{10}$	Coarse frequency offset estimation and timing synchronization
T_1 and T_2 (long symbols)	Channel and fine frequency offset estimation
SIGNAL	Data rate and length of frame
DATA1	Scrambler initialization and data
DATAn	Data
GI	Guard interval (cyclic-prefix) in SIGNAL and DATA symbols
GI2	Guard interval (cyclic-prefix) in long training symbols

The subcarriers of the short symbol (S) and the long symbol (L) are given in (41) and (42). Since only 12 of 52 subcarriers are used in short symbols, (41), the factor $\sqrt{13/6}$ is used to transmit the OFDM symbol in the same power with the other OFDM symbols.

$$S_{[-26,\,26]} = \sqrt{13/6} \times \{0, 0, 1+j, 0, 0, 0, -1-j, 0, 0, 0, 1+j, 0, 0, 0, -1-j, 0, 0, 0, -1-j, 0, 0, 0, 1+j, 0, 0, 0, 0, 0, 0, 0, 0, -1-j, 0, 0, 0, -1-j, 0, 0, 0, 1+j, 0, 0, 0, 1+j, 0, 0, 0, 1+j, 0, 0, 0, 1+j, 0, 0\} \quad (41)$$

$$L_{[-26,\,26]} = \{1, 1, -1, -1, 1, 1, -1, 1, -1, 1, 1, 1, 1, 1, 1, -1, -1, 1, 1, -1, 1, -1, 1, 1, 1, 1, 0, 1, -1, -1, 1, 1, -1, 1, -1, 1, -1, -1, -1, -1, -1, 1, 1, -1, -1, 1, -1, 1, -1, 1, 1, 1, 1\} \quad (42)$$

The IFFT of S gives 4 identical short symbols each of length 16 samples and the CP constitutes the 5th short symbol. The same process is repeated to generate a total of 10 short symbols, $t_1 - t_{10}$. To generate the long symbols, the IFFT of L is taken and the resulting vector is concatenated with itself forming a 128 sample segment. Then the 32 samples long CP of this segment is inserted at the beginning. Hence, due to the structure of S and L, the segments of the 802.11a frame are observed as shown in Table 9.

Table 9 – Segments constructing the OFDM frame in 802.11a

OFDM Symbol No	***Sample No***				
	-16 - -1	**0 - 15**	**16 - 31**	**32 - 47**	**48 - 63**
1	t	t	t	t	t
2	t	t	t	t	t
3	c	d	a	b	c
4	d	a	b	c	d
5	CP	Data			
6	CP	Data			
…	…	…			

Necessary mapping from the frequency domain to the time domain using the IFFT is given in Figure 56. The inverse mapping is used while transforming from time domain to frequency domain.

The data subcarriers are modulated as BPSK, QPSK, 16-QAM or 64-QAM using Gray coding. According to the modulation scheme, each subcarrier is divided by corresponding normalization factor to achieve the same average power for all mappings. The normalization factors are listed in Table 10. The pilot subcarriers are BPSK modulated according to a fixed pseudo random binary sequence to prevent the generation of spectral lines.

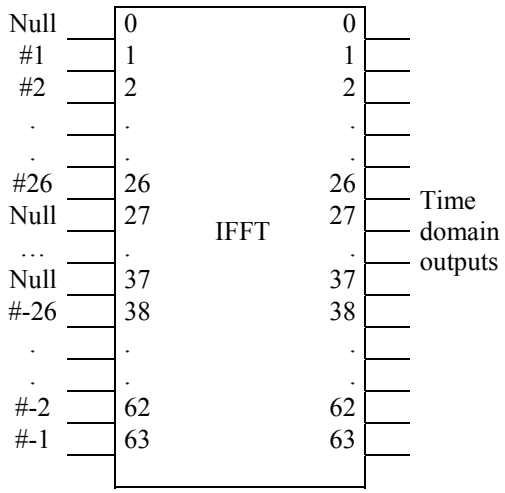

Figure 56 – Mapping from frequency domain to time domain

Table 10 – Modulation dependent normalization factor

Modulation	***Normalization factor***
BPSK	1
QPSK	$\sqrt{2}$
16-QAM	$\sqrt{10}$
64-QAM	$\sqrt{42}$

5.2 Frame Synchronization and Channel Estimation in 802.11a

In the IEEE 802.11a standard, the preamble introduced in the previous part is dedicated to various synchronization tasks. However, there is no mention in the standard how to use the preamble to achieve synchronization.

In this section, a direct approach employing the short and long symbols (hereafter referred as the SL method) of the 802.11a frame will be introduced [32]. The frame synchronization in 802.11a depends on detecting the start of the last short symbol in the preamble. A short symbol t_i is searched among the received data by means of correlating t_i (it is known at the receiver also) with the received symbols. Since the first part in the preamble has ten identical, 16-point segments, t_i, the correlation yields 10 peaks which are 16 samples apart from each other as shown in Figure 57.a. The location of the last peak is the start of the 10^{th} short symbol in the first part of the preamble.

Due to random data, some peaks may be detected at the signal part also. This affects the synchronization point and causes misalignment. To avoid this situation, received signal is correlated with a delayed version of itself. Thus, we have a boundary in which the correlation peaks are located and a candidate peak must lay inside this boundary to be used for symbol alignment. The auto-correlation is shown in Figure 57.b.

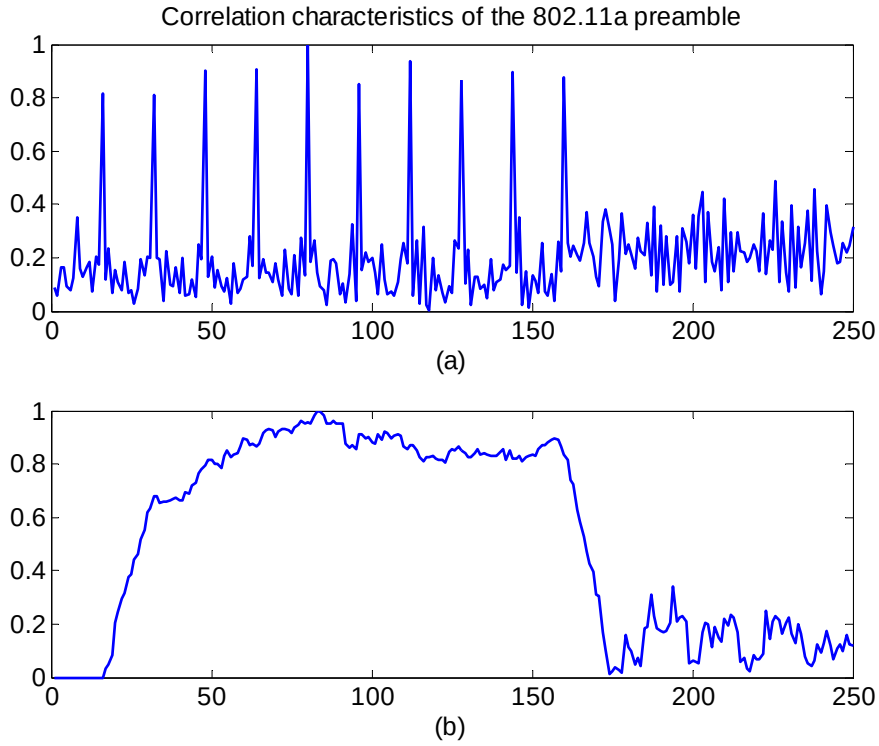

Figure 57 – Correlation characteristics of the 802.11a preamble (AWGN channel at 10 dB SNR); a) Cross correlation with the short symbol, R(t,x), b) Auto correlation of the received signal, R(x,x')

A reference for the frame start may be found by detecting the peaks in the autocorrelation boundary. The auto and cross correlation outputs may be used for coarse frame synchronization as the following:

1) Cross-correlation of a short symbol with the received signal R(t, x) is performed, where t is the short symbol known by the receiver and x is the received signal

2) Auto correlation of the received signal with its one short symbol delayed version R(x, x') is performed where x' is the delayed version of x.

3) The Hadamard product (element-wise multiplication) between R(t, x) and R(x, x') is found. Thus the erroneous peaks outside the short training symbols are eliminated.

4) The 9^{th} peak is selected to be the start of the 10^{th} short symbol in the preamble.

An alternative to this method is given in [33] that uses two autocorrelations. In [33], the first correlation is taken with the received signal and one short symbol delayed version. The second correlation is taken with the received signal and two short symbols delayed version. The position of the peak of the difference of these two correlations yields the beginning of the last short symbol.

After the coarse timing estimation given above, fine timing estimation around the coarse estimate is achieved by correlating the received samples with the known long symbols. The interval for fine synchronization may be selected such that it includes at least one short symbol.

The delayed autocorrelation is not only used for frame synchronization but also used for burst signal detection. The decision of signal existence is made by comparing the autocorrelation output to a threshold.

The channel estimation in 802.11a relies on the long symbols whose values are also known at the receiver. After the frame synchronization, the received OFDM signal is vectorized and demodulated by means of FFT. Then, the least squares estimate of the channel frequency response is obtained by dividing the received long symbols to the original long symbols ([33], [34]) as in (36).

5.3 Adaptation of ML Synchronization and Robust Synchronization to the 802.11a Frame Structure

In this section we will adopt the schemes of Van de Beek [21] (ML method) and Schmidl [15] (SC method), mentioned in Chapter 4, to the 802.11a frame structure. Considering Table 9, we see that the 802.11a preamble contains similar segments because of the short and long symbols so the ML and SC metrics must be changed and their optimization must be modified accordingly.

The ML method makes use of the cyclic nature of the OFDM symbol generated with CP. It assumes that only the samples in the CP are correlated with the data part but this is not the case in 802.11a. Since the short symbols are identical, the metric outputs a constant level instead of peaks as shown in Figure 58.a. The lengths of both the first and the second flat parts are 81 samples in the AWGN environment.

The SC method needs an OFDM symbol with two identical halves. The collection of short symbols constitutes such a symbol. However, this OFDM symbol is repeated once more, so the length of the plateau is increased to 96 samples as shown in Figure 58.b.

The ML scheme is adapted to the 802.11a frame as follows:

1) Apply the ML algorithm to the frame
2) Choose a starting point and sample the metric once in 80 samples and average the collected samples
3) Select the next sample as the starting point and repeat step 2
4) Select the position of the maximum of the new metric as the start of frame

In this way, averaging in ML metric is done and the estimator's robustness is increased against noise.

Adaptation of the SC method is finding a flat region of 96 samples and taking the first J samples as the ISI-free region where J is the length of CP minus the length of channel impulse response.

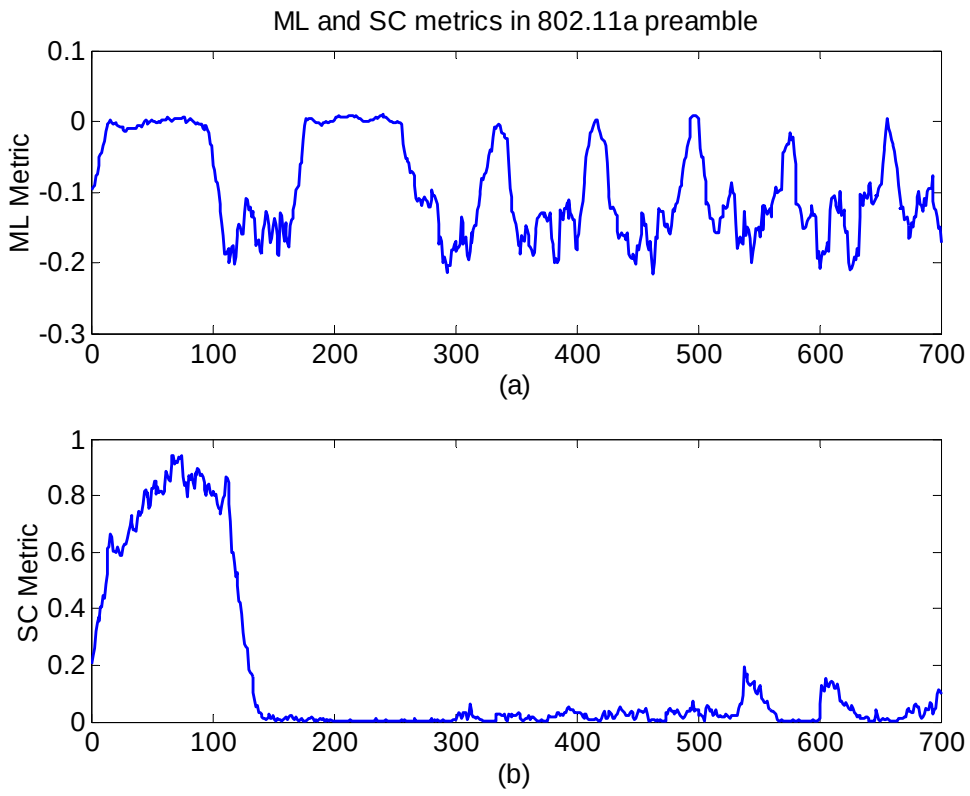

Figure 58 – The ML and SC metrics applied to an 802.11a frame; a) ML metric, b) SC Metric. Channel is AWGN with 10 dB SNR

5.4 Performance of Synchronization Algorithms in 802.11a Frame

In this section, we will compare the performance of ML synchronization and the SC method with the SL method which utilizes the short and long symbols of 802.11a. The simulations are carried out in both the AWGN and Rayleigh fading multipath channels. 802.11a frames are used but the pilot subcarriers are not employed and left as zero since they are used for fine carrier synchronization. Also, data scrambling and interleaving is not needed since the input data is already random. Error control coding is not applied also. The SIGNAL part of 802.11a frame is also fully employed for data because a fixed number of 15 OFDM symbols are sent for each frame. For each SNR value, 100 trials are performed. For each trial, the frame is leaded by a fixed number of zeros to create timing ambiguity.

5.4.1 Performance in the AWGN Channel

In Figure 59, Figure 60 and Figure 61, the distribution of the SL, ML and SC methods are shown, respectively.

As it can be seen from Figure 59, SL method estimates the frame start point in a very wide range, and even misses a symbol. However, more accurate estimates are observed as the SNR is increased. In Figure 60, we see that, even in low SNR, the ML metric performs accurate estimations. Although SL method operates on known symbols, ML method performs better since it utilizes metric averaging in every symbol transmitted. However, SL method uses special symbols for synchronization that are transmitted only at the beginning of the frame. SC method has a distribution that is narrowed in every increase in SNR as shown in Figure 61. The performance of the SC method is worse since it neither knows the symbols nor has periodicity that may help averaging the metric.

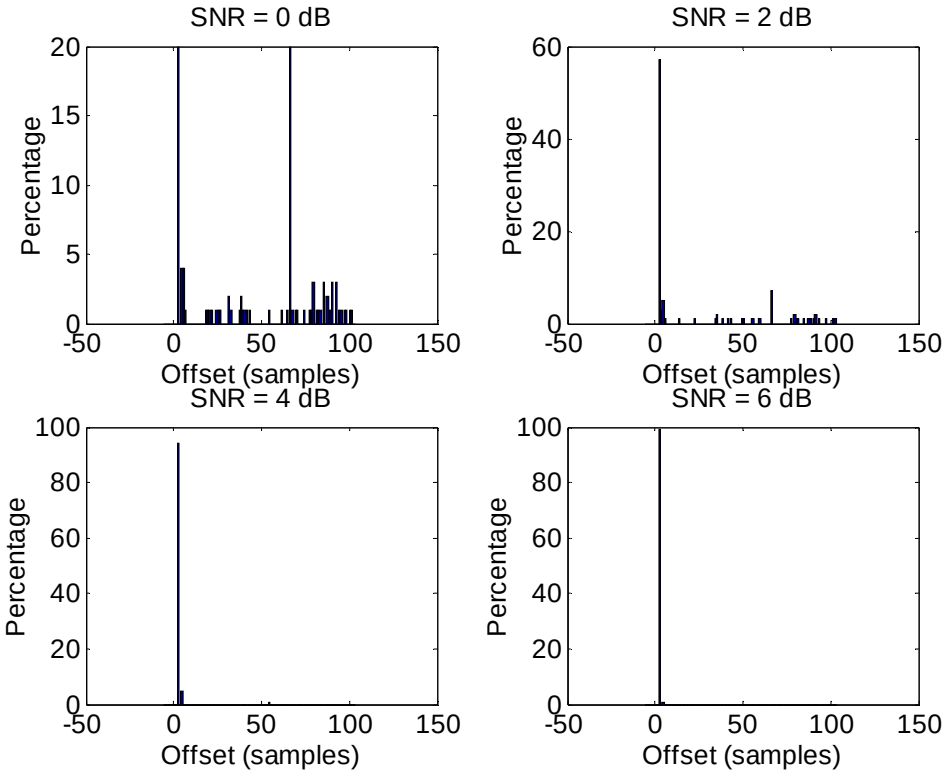

Figure 59 – Distribution of SL method in AWGN channel

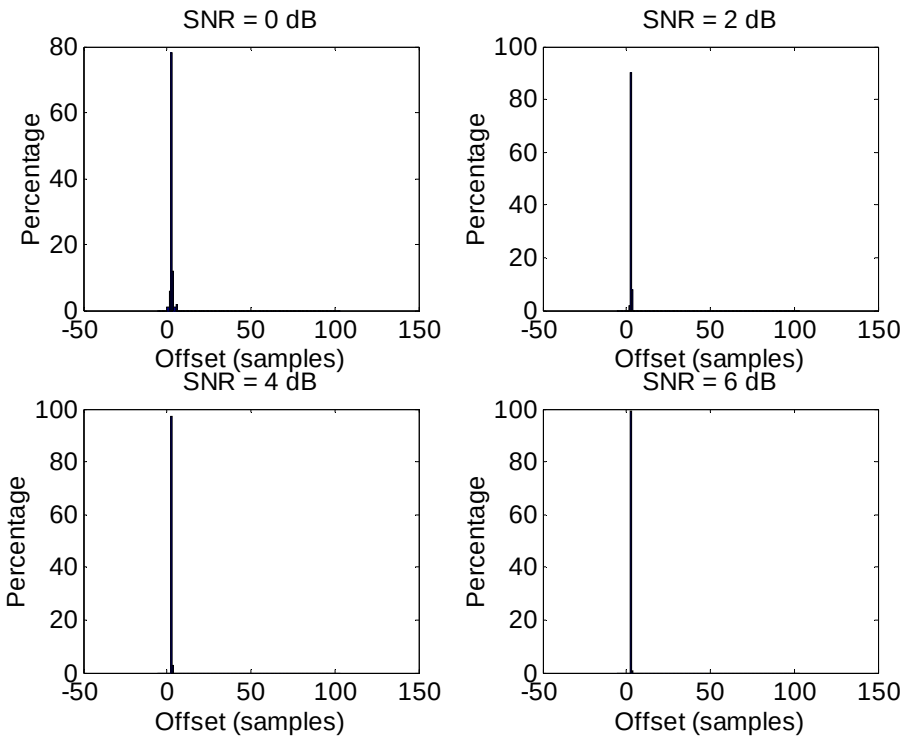

Figure 60 – Distribution of ML method in AWGN channel

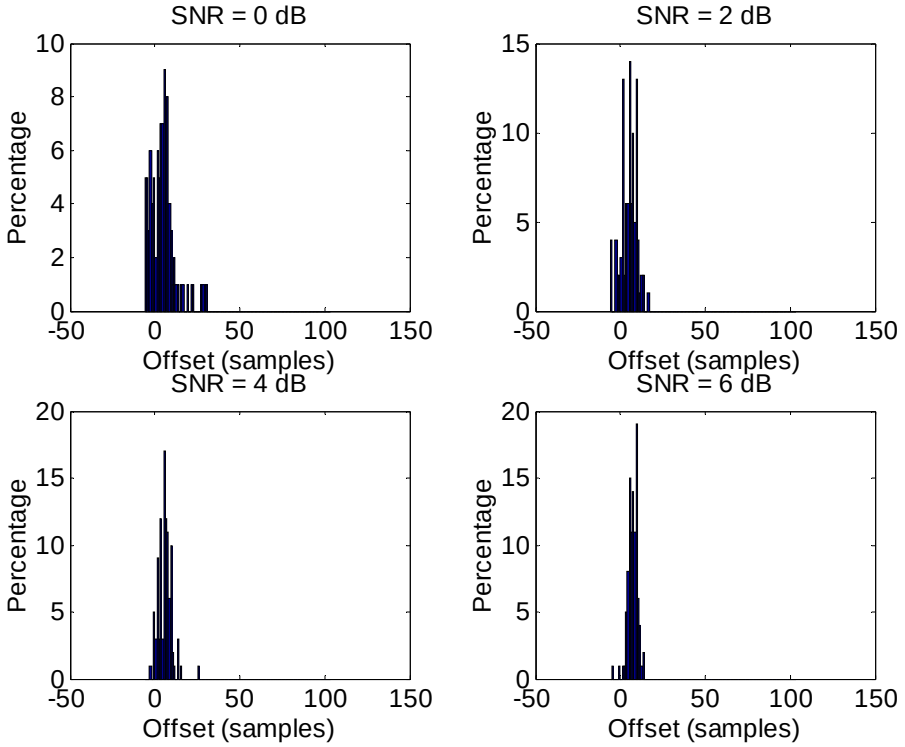

Figure 61 – Distribution of SC method in AWGN channel

For the AWGN case, the ISI-free region is the whole CP since the channel has no memory. Figure 62 shows the percentage of estimates that do not cause ISI. According to this figure, ML method estimates the frame start almost always in the ISI-free region. The SL method needs minimum 6 dB SNR whereas the limit for SC method is 8dB.

The MSE and SER performances of the SC method under AWGN case are shown in Figure 63 and Figure 64, respectively.

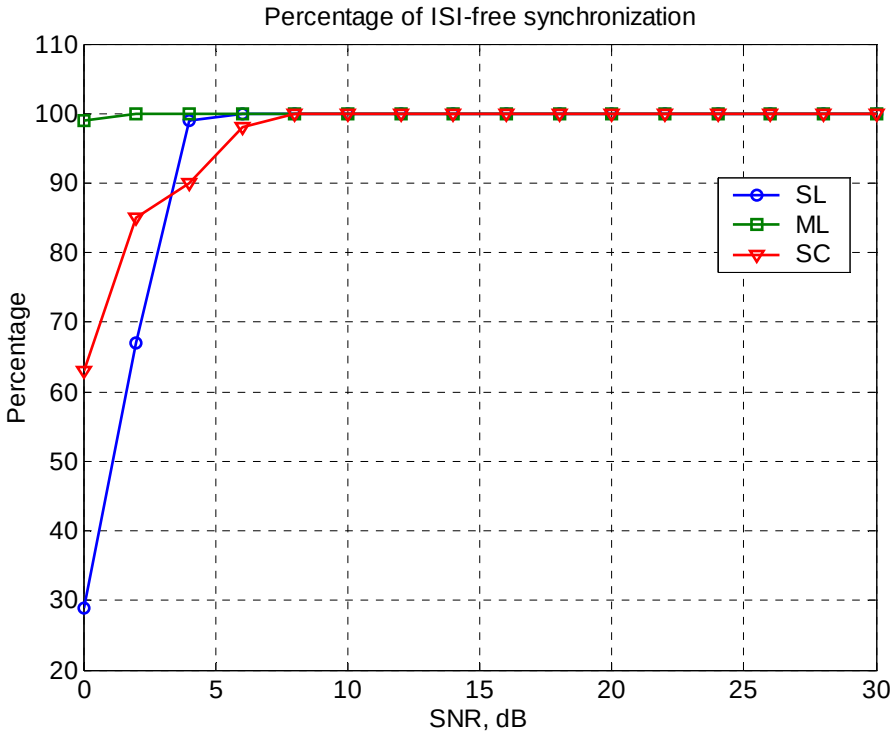

Figure 62 – Percentage of ISI-free synchronization under AWGN channel

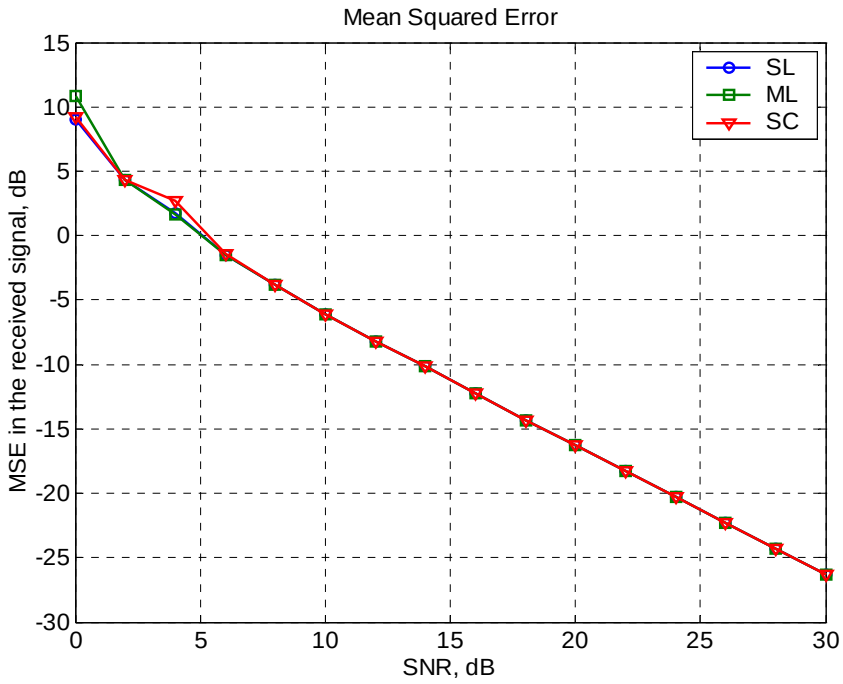

Figure 63 – Mean squared error obtained with the frame synchronization algorithms in 802.11a frame structure under AWGN channel

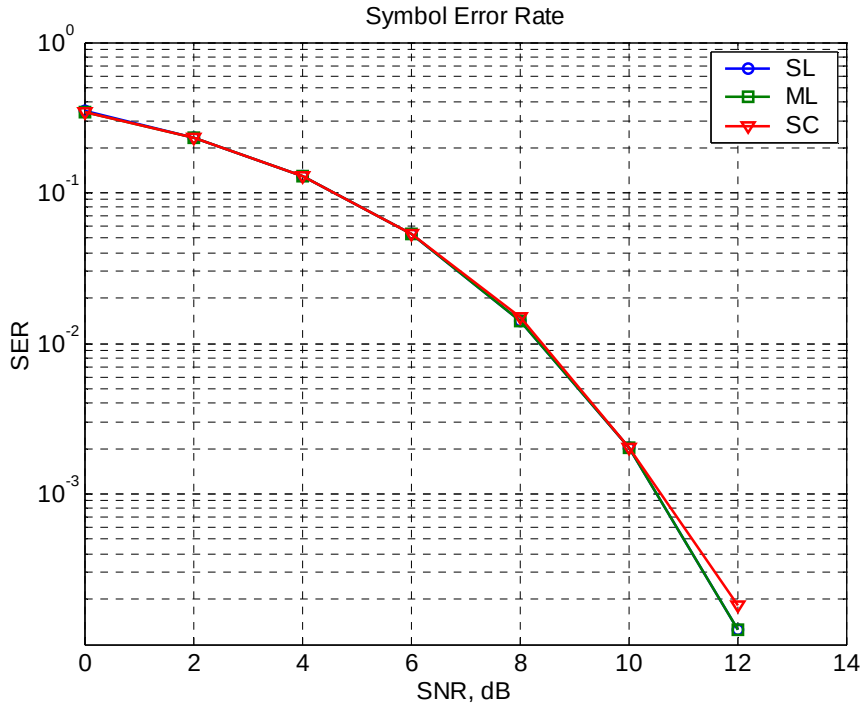

Figure 64 – Symbol error rate achieved with the synchronization algorithms in 802.11a frame structure under AWGN channel

In Figure 63 the MSE is much higher than the one given in Figure 18 because of the effect of channel estimation and rotation in received samples due to synchronization in ISI-free region, as given in (40). It is seen from Figure 64 that the symbol errors are very low after 12 dB for any synchronization method because at this SNR, the noise power is one tenth of the received signal which does not mislead the detection of symbols.

In Figure 65, the error in channel estimation is shown.

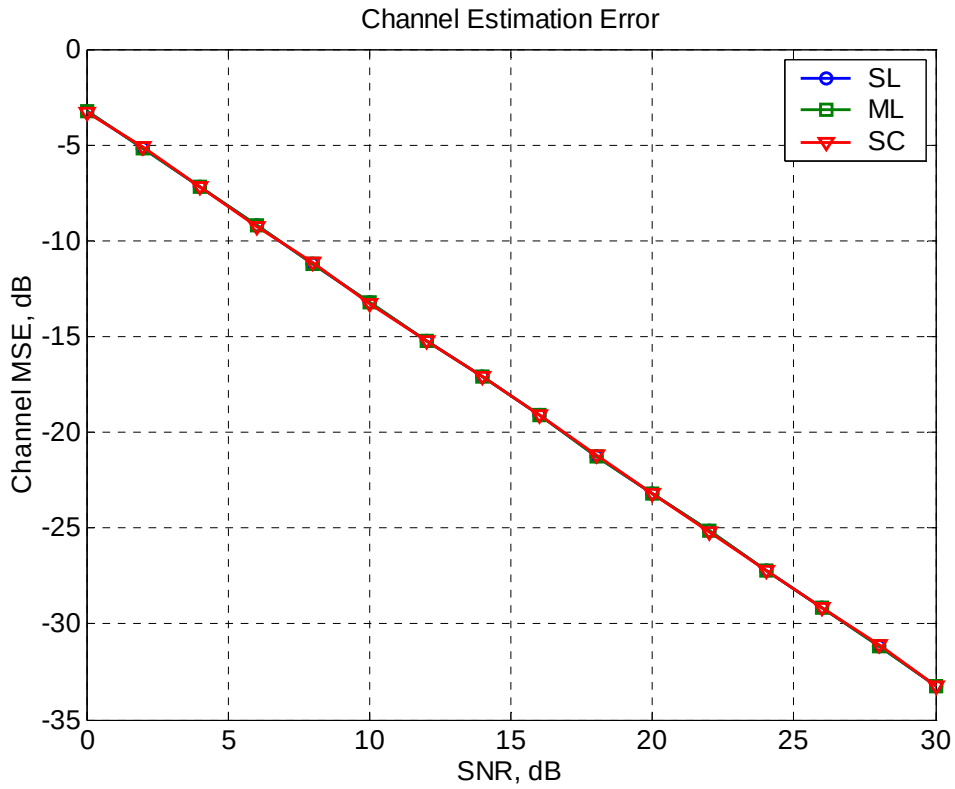

Figure 65 – Channel estimation error in AWGN channel

The channel estimation error is nearly the same with the observation error in the environment since we use +1, or -1 to estimate the channel frequency response.

The MSE, SER and channel estimation performances of three methods are the same because, detecting the ISI-free region is enough for accurate demodulation but the exact position of the frame beginning is unimportant as long as it stays in the ISI-free region.

5.4.2 Performance in the Rayleigh Fading Multipath Channel

In the following simulations, 6th order Rayleigh fading channels are used. For each trial, a different channel, signal and noise realizations are used to make a Monte-Carlo simulation. Figure 66, shows the distribution of the frame offsets of the SL method using short and long symbols. Figure 67 shows the distribution with the ML algorithm and Figure 68 is obtained with the SC method. The vertical lines enclose the ISI-free region which is 10 samples long for this case.

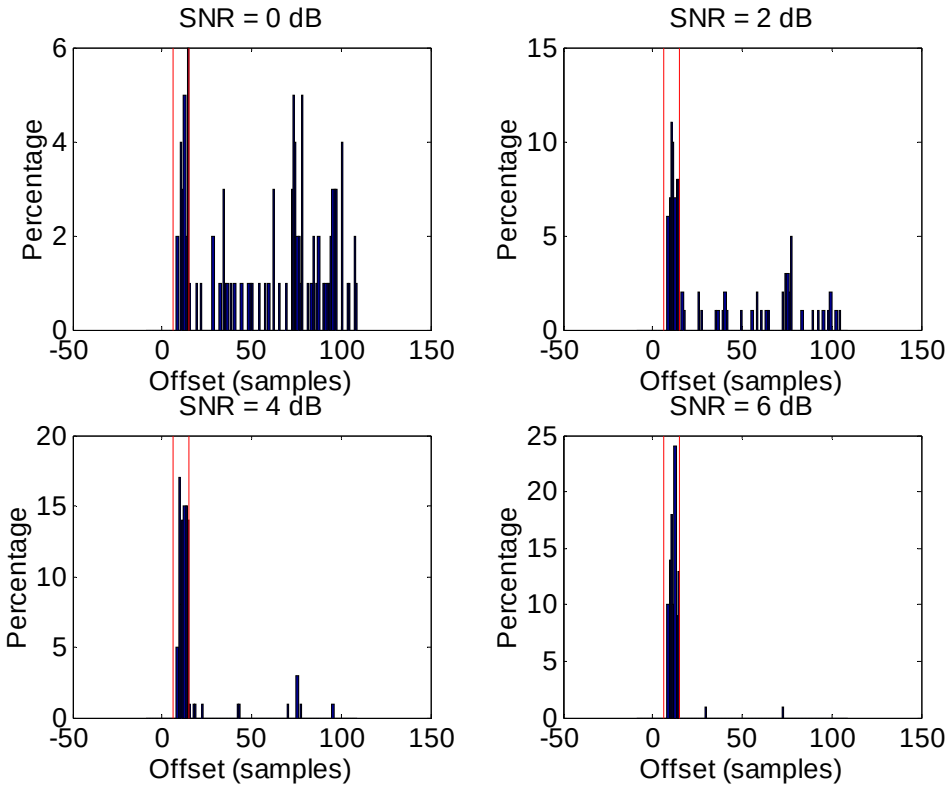

Figure 66 – Distribution of the SL method in 802.11a frame under Rayleigh fading channel

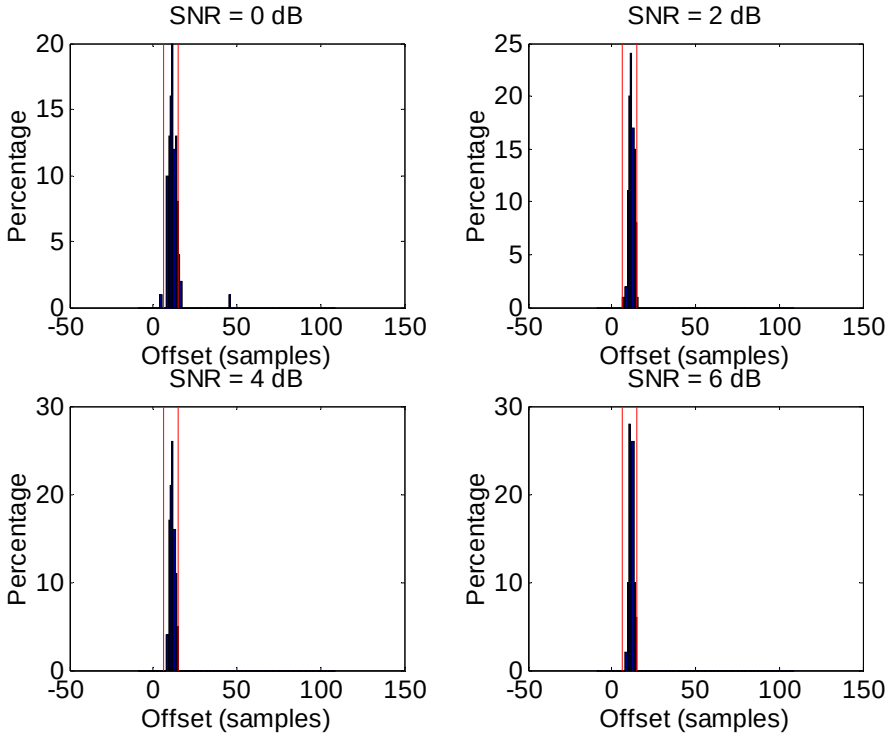

Figure 67 – Distribution of the ML metric in 802.11a frame under Rayleigh fading channel

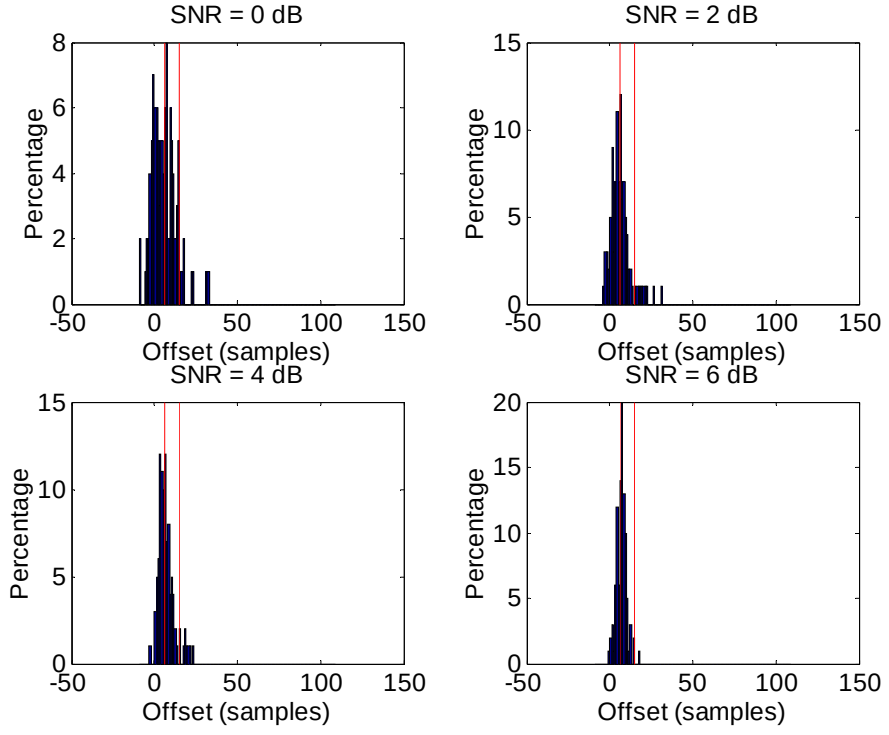

Figure 68 – Distribution of SC metric in 802.11a frame under Rayleigh fading channel.

In Figure 66, it is seen that the estimation range of the SL method is wide at 0 dB SNR but at 6 dB most of the estimates resulted in the ISI-free region. The ML estimator performs well even the noise is at the same power level with the signal. However, the performance of the SC metric is worse than that of SL and ML methods. The ISI-free synchronization performance shown in Figure 69 is worse than the performance in AWGN channel. Especially, the SC method eliminates the ISI only after 30 dB SNR. ML distribution is wider than that in the AWGN channel however; the ISI-free synchronization percentage is nearly the same. For the SL method, 10 dB SNR is needed for eliminating ISI whereas in the AWGN environment, this was 6 dB.

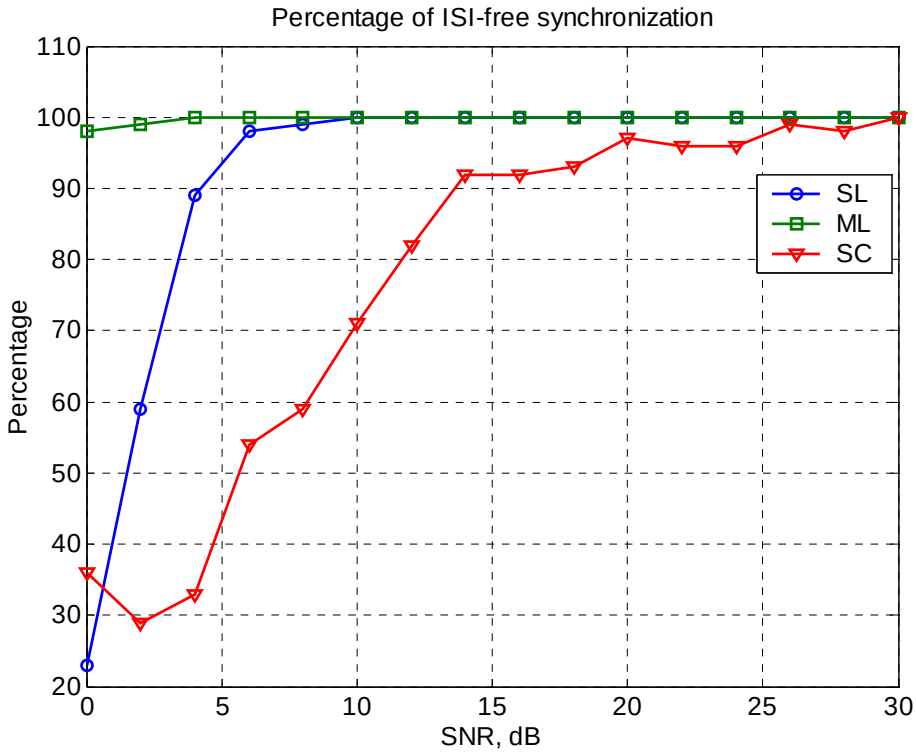

Figure 69 – Percentage of ISI-free synchronization under Rayleigh fading channel

Figure 70, shows the MSE and SER is plotted in Figure 71. Also, the error in channel estimation is shown in Figure 72.

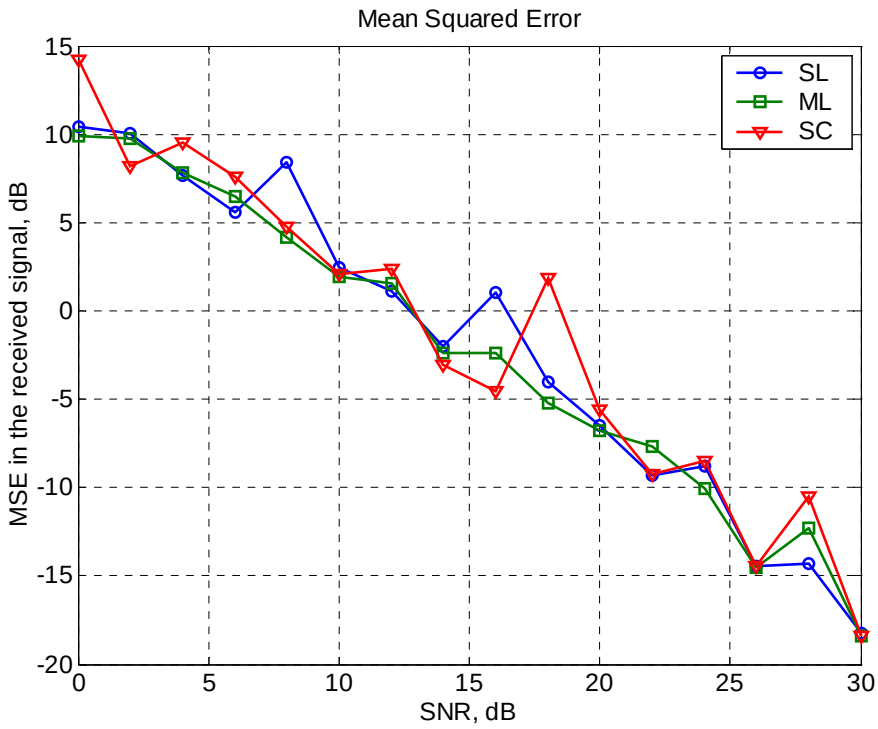

Figure 70 – Mean squared error under 6th order Rayleigh fading channel using 802.11a frame structure

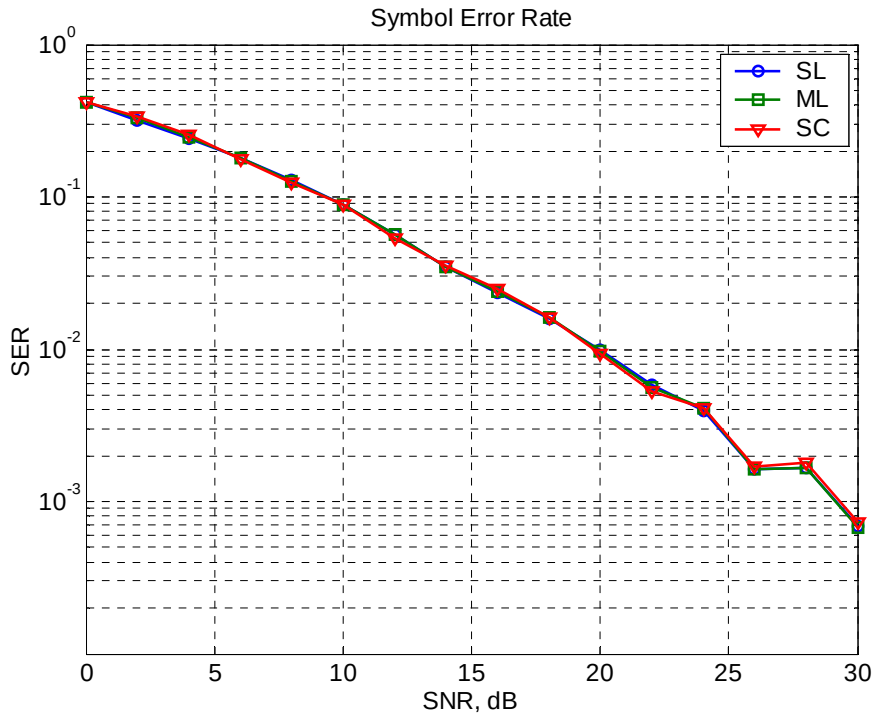

Figure 71 – Symbol error rate after synchronization under Rayleigh fading channel in 802.11a

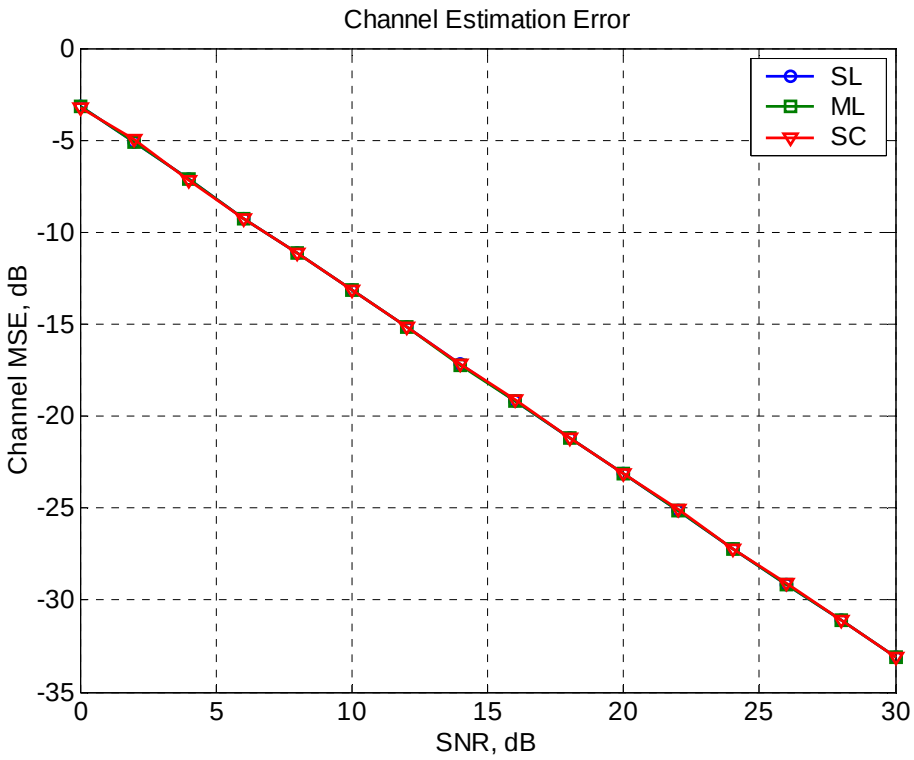

Figure 72 – Channel estimation performance after synchronization under Rayleigh fading channel.

In the trials above, random channels are used. The variations in the MSE given in Figure 70 are due to deep fades in the frequency response of the channel. Since these coefficients are small, the equalization in (16) amplifies the noise even though the channel is estimated correctly. This effect is also reflected to the SER performance in Figure 71. The error in channel estimation does not differ from the one in AWGN case, since ISI-free synchronization is enough to correctly estimate the channel.

The SL and SC methods need special training symbols whereas the ML method does not need any training symbols, thus ML is the most efficient of these three algorithms. The synchronization performance of SL and ML algorithms are similar but ML is better at low SNR. This is due to the metric averaging which is done for all symbols in the frame due to the periodicity induced by the CP. Averaging is not convenient for the SL method since there is no repeated pattern in a frame. The ML and SL methods locate a sample in the channel delay spread however

the SC method locates the ISI-free region but due to noise variations, finding a flat region is harder than finding the maxima. For this reason synchronization performance of the SC method is the worst.

CHAPTER 6

CONCLUSION

In this thesis, we have investigated the frame synchronization problem. Since this has vital importance for the OFDM systems, we focused on the OFDM symbol synchronization, inherently the frame synchronization problem.

We have first investigated the OFDM system. OFDM is a multi-carrier modulation scheme used for bandwidth efficiency, immunity to multipath effects and ISI. The main idea behind OFDM is to convert a single convolutional channel into a number of parallel, low bit-rate flat fading channels. Therefore, equalization can be done easily and only a single tap is enough for each subchannel. The parallelism is established using orthogonal subcarriers and cyclic-prefix. Orthogonal subcarriers are generated by inverse discrete Fourier transform and cyclic prefix turns the linear convolution with the channel into a cyclic convolution. Cyclic-prefix together with the orthogonality eliminates the ISI and ICI.

OFDM has also certain disadvantages. First, orthogonality must be ensured throughout the communication. Even a small offset in the carrier frequency or phase disturbs the orthogonality condition, hence introduces ICI. Second, symbol (frame) timing must be precise. The FFT window at the receiver must be free from samples of the adjacent OFDM symbols. If not, the extracted OFDM symbol is contaminated with the samples from the previous OFDM symbol because of the channel memory.

We considered the frame synchronization techniques applied in the single carrier schemes. The popular way of frame synchronization is to indicate the start of frame by a marker. The marker is selected such that its correlation must be able to indicate itself in the noisy environment. The frame is detected at the receiver by correlating the received sequence with the known marker. An alternative to marker is to use gaps between the frames. The receiver aligns the frames considering the

received signal power. Another alternative is to copy a part from the end of the frame to the start of the frame. In this case, the receiver correlates the data with itself and does not need to know a predefined sequence. However, these methods decrease the transmission efficiency since already known symbols are sent throughout the frames.

We investigated the OFDM system and analyzed the receiver structure in more detail. What we have to do at the receiver side is first to detect the start of the frame and the symbol boundaries. Secondly, frequency offset must be estimated and corrected. As the third task, the channel frequency coefficients on the subcarriers need to be estimated and equalized. The ideal detection of symbol boundaries is required to avoid ISI. However, it is pointed out that an ISI-free region in the cyclic-prefix exists and ideal synchronization is not necessary as long as the FFT window starts from a sample in the ISI-free region. The importance of finding the ISI-free region is that there is no data loss but a rotation on the carriers. Since rotation also affects the channel estimate in the same way, it can be removed during equalization after the channel is estimated provided that the channel estimation relies on the same FFT window boundary.

In our work, three synchronization methods are discussed. The first method is the ML estimator which is given in [21]. The ML estimator makes use of the periodicity introduced by the cyclic-prefix. Since the start and end of an OFDM symbol are identical due to CP, a search that matches these parts gives the symbol boundary. In the case of AWGN channels, this method can find the ideal FFT window. However, multipath channel affects the performance of synchronization and the symbol boundary is shifted according to the channel delay spread. We should note that the boundary is always found within CP which is covered also by the channel memory. Thus, as long as the length of channel impulse response is much shorter than the CP, we may shift the boundary to the ISI-free region accomplishing the minimum synchronizer requirement. In the ML estimation, since there is no need for a training symbol or sequence, the bandwidth is efficiently used. Also, since it uses the periodicity inherent in the OFDM symbol, averaging over multiple symbols increases the robustness of the estimate. Hence, ML method may be used in OFDM systems for coarse frame synchronization with any frame structure.

The second method in symbol synchronization is the SC method given in [15]. This method utilizes a special training symbol that has two identical parts in the useful data part. Since this method needs an extra symbol dedicated to time synchronization, its bandwidth efficiency is lower than the ML method. However, we do not need to know about channel delay spread since the estimated frame start is given in the ISI-free region. Thus a plateau indicating the ISI-free region is obtained as the output of the metric. Although the variation in the estimated point is high when compared to ML method, it mostly guarantees to be in the ISI-free region. Thus, SC method is considered to be a robust coarse frame synchronizer.

The third method used in this thesis is the SL method which uses known symbols in the IEEE 802.11a frame structure as markers directly for coarse and fine frame synchronization. The SL method has two stages; coarse and fine synchronization. In the coarse synchronization, the received signal is correlated with the known short symbols in the preamble and another correlation is performed with the delayed version of the received signal to detect the last short symbol [32]. In the fine synchronization long symbols of the preamble is correlated with the received signal in a window around the coarse estimate.

We have applied also the ML estimator in [21] and the SC estimator in [15] to the 802.11a frame structure. The needed adaptation to the frame structure is employed and the performances of the two metrics with that of the SL method are compared.

The ML method is a non-data-aided solution in which the periodicity induced by the cyclic prefix is used. On the other hand, SL and SC methods are data-aided algorithms in which frame synchronization is achieved by using special training symbols. The difference between SL and SC method is that in SL method both the transmitter and the receiver know the training symbols by value, however in the SC method the only thing the receiver knows is the containment of two identical halves in the first OFDM symbol. Hence, in terms of transmission efficiency, the ML method is the most efficient method. Since the SC method only restricts the form but not the value of the training symbol, data may also be sent with it, thus the SC method is more efficient than the SL method.

All these three methods perform correlations to create metrics for decision. The ML and SL methods perform the maximization of the metric whereas the SC method searches for a flat region in the metric. Due to this, the decision of ML and SL methods are easier but SC method is degraded in the noisy environment. Because of the delay spread of multipath channel response, the estimates of ML and SL methods are not ISI-free and a shift to the ISI-free region is needed. On the other hand, the flat part of the SC method is wholly ISI-free. As a result, we can say that, noise is more effective in the performance of the SC method but multipath channels influence mostly the ML and SL methods.

The performances of ML and SL methods are similar although SL is a data-aided but ML is a non-data-aided method. In the SL method, the information used for synchronization is transmitted once in a frame. Oppositely, the ML method can extract the timing information from any OFDM symbol in the frame. This means that metric averaging may be performed on consecutive OFDM symbols to improve performance against noise.

After locating the symbol boundary, the channel estimation and equalization must be done on the subcarriers. For this purpose, a symbol with known carriers is sent and the received subcarriers are compared at the receiver yielding the least squares estimates of the channel frequency response. The 802.11a frame structure supplies fixed symbols for channel estimation. However, although the channel is estimated correctly, if the channel has deep fades in its frequency response, the equalization may result with the amplification of noise.

We point out that minimum requirement for an OFDM symbol synchronizer is to locate the frame start at the ISI-free region if the channel estimation is carried out using the same alignment. The ISI-free synchronization leads to the rotation of the FFT window in each received OFDM symbol and this affects the MSE and SER performance. However, if channel estimation is performed with the same symbol boundaries, the FFT window for the dedicated symbol is also rotated. At the equalization, the rotation is compensated by simply dividing each subcarrier to the estimated channel frequency response. If the synchronization and estimation are not performed jointly, then either task should be completed free from errors. However, in

joint synchronization and estimation, we compensate for the error of the synchronizer with the channel estimator and equalizer yielding the same performance with that in the ideal case.

To eliminate the overhead needed for synchronization and channel estimation, future research in OFDM is directed towards blind algorithms for timing and frequency synchronization and channel estimation where no training or special symbols are used.

REFERENCES

[1] J. A. C. Bingham, "Multicarrier Modulation for Data Transmission: An Idea whose Time has Come", IEEE Communications Magazine, Vol. 28, No. 5, pp.5-14, May 1990

[2] "Part 11: Wireless LAN Medium Access Control (MAC) and Physical Layer (PHY) specifications High-speed Physical Layer in the 5 GHz Band", IEEE Std 802.11a-1999

[3] Broadband Radio Access Networks (BRAN); HIPERLAN Type 2; Physical (PHY) Layer, ETSI TS 101 475

[4] "Radio Broadcasting Systems; Digital Audio Broadcasting (DAB) to mobile, portable and fixed receivers", ETSI EN 300 401 v1.3.3 (2001-05), 2001

[5] "Digital Video Broadcasting (DVB); Framing structure, channel coding and modulation for digital terrestrial television", ETSI EN 300 744 v1.4.1 (2001-01), 2001.

[6] Wi-LAN Inc., "Wide-band Orthogonal Frequency Division Multiplexing (W-OFDM)", White paper, v1.0, www.wi-lan.com, September 2000

[7] B. Muquet, Z. Wang, G. Giannakis, M. Couville and P. Duhamel, "Cyclic Prefixing or Zero Padding for Wireless Multicarrier Transmissions?", IEEE Transactions on Communications, vol. 50, no. 12, December 2002.

[8] R. W. Chang, "Synthesis of Band-Limited Orthogonal Signals for Multichannel Data Transmission", Bell Syst. Tech. J., vol. 46, pp. 1775-1796, December 1966

[9] S. Zhou and G. B. Giannakis, "Finite-Alphabet Based Channel Estimation for OFDM and Related Multicarrier Systems", IEEE Transactions on Communications, vol. 49, no. 8, August 2001

[10] U. Lambratte, J. Horstmannshoff and H. Meyr, “Techniques for Frame Synchronization on Unknown Frequency Selective Channels”, IEEE Vehicular Technology Conference, 1997

[11] B. Yang, K. B. Letaief, “Timing Recovery for OFDM Transmission”, IEEE Journal on Selected Areas of Communications, vol. 18, no. 11, November 2000

[12] D. Landström, N. Petersson, Per Ödling and Per Ola Börjesson, “OFDM Frame Synchronization for Dispersive Channels”, International Symposium on Signal Processing ans its Applications (ISSPA), Kuala Lumpur, Malaysia, August 2001

[13] B. Yang, K. B. Letaief, R. S. Cheng, Z. Cao, “Burst Frame Synchronization for OFDM Transmission in Multipath Fading Links”

[14] J. L. Zhang, M. Z. Wang and W. L. Zhu, “A Novel OFDM Frame Synchronization Scheme”, IEEE International Conference on Communications, Circuits and Systems, vol. 1, pp. 119-123, 2002

[15] T. M. Schmidl and D. C. Cox, “Robust Frequency and Timing Synchronization for OFDM”, IEEE Transactions on Communications, vol. 45, no. 12, December 1997

[16] A. Palin, J. Rinne, “Enhanced Symbol Synchronization Method for OFDM System in SFN Channels”, IEEE Global Telecommunications Conference, GLOBECOM 98, vol. 5, pp. 2788-2793, 1998

[17] J. J. van de Beek, M. Sandell, M. Isaksson and Per Ola Börjesson, “Low-Complex Frame Synchronization in OFDM Systems”, Proceedings of ICUPC, pp. 982-986, Tokyo, 1995

[18] J. H. Gunther, H. Liu, A. L. Swindlehurst, “A New Approach for Symbol Frame Synchronization and Carrier Frequency Estimation in OFDM Communications”, *Proc. IEEE ICASSP*, March, 1999

[19] Meng-Han Hsieh, Che-Ho Wei, “A Low-Complexity Frame Synchronization and Frequency Offset Compensation Scheme for OFDM Systems over Fading Channels”, IEEE Transactions on Vehicular Technology, vol. 48, no. 5, September 1999

[20] M. Okada, S. Hara, S. Komaki and N. Morinaga, “Optimum Synchronization of Orthogonal Multi-Carrier Modulated Signals”, Seventh IEEE International Symposium on Personal, Indoor and Mobile Radio Communications, 1996. PIMRC'96 1996

[21] J. J. van de Beek, M. Sandell, Per Ola Börjesson, “ML Estimation of Time and Frequency Offset in OFDM Systems”, IEEE Transactions on Signal Processing, vol. 45, no. 7, July 1997

[22] R. Scholtz, “Frame Synchronization Techniques”, IEEE Transactions on Communications, vol. COM-28, no. 8, August 1980

[23] J. L. Massey, “Optimum Frame Synchronization”, IEEE Transactions on Communications, vol. COM-20, pp. 115-119, April 1972

[24] P. T. Nielsen, “Some Optimum and Suboptimum Frame Synchronizers for Binary Data in Gaussian Noise”, IEEE Transactions on Communications, vol. COM-21, pp. 770-772, June 1973

[25] H. Nogami and T. Nagashima, “A Frequency and Timing Period Acquisition Technique for OFDM Systems”, Personal, Indoor and Mobile Radio Commun. (PIRMC), pp. 1010-1015, September 1995.

[26] A. K. Ergüt, “Time Synchronization in OFDM”, M. Sc. Thesis, METU, December 2002

[27] G. H. Golub and C. F. van Loan, “Matrix Computations”, 3rd edition, Laurel Park, John Hopkins Univ. Press, 1996

[28] J. G. Proakis, “Digital Communications”, McGraw Hill Inc., Third Edition, 1995

[29] M. Speth, F. Classen and H. Meyr, “Frame Synchronization of OFDM Systems in Frequency Selective Fading Channels”, Proceedings of VTC’97, pp. 1807-1811, 1997

[30] E. P. Lawrey, “Adaptive Multiuser OFDM”, Ph.D. thesis, James Cook University, December 2001

[31] "Part 11: Wireless LAN Medium Access Control (MAC) and Physical Layer (PHY) Specifications" ANSI / IEEE Std. 802.11, 1999

[32] Y. Chiu, D. Markovic, H. Tang, N. Zhang, "OFDM Receiver Design", white paper, www.bwrc.eecs.berkeley.edu, 2000

[33] K. Wang, M. Faulkner, J. Singh and I. Tolochko, "Timing Synchronization for 802.11a WLANs under Multipath Channels", Australian Telecommunications, Networks and Applications Conference (ATNAC), 2003

[34] O. Edfors, M. Sandell, J. J. van de Beek, S. K. Wilson, P. O. Börjesson, "OFDM Channel Estimation by SVD", IEEE Transactions on Communications, vol. 46, no. 7, July 1998